AD-A129 021 DAMPER COMPONENT ANALYSIS AND INTEGRATION WITH ROTOR-DYNAMICS PROGRAM(U) MECHANICAL TECHNOLOGY INC LATHAM N Y J A TECZA ET AL. NOV 82 MTI-82TR61 1/2

UNCLASSIFIED AFWAL-TR-82-2112 F33615-79-C-2050 F/G 9/5 NL

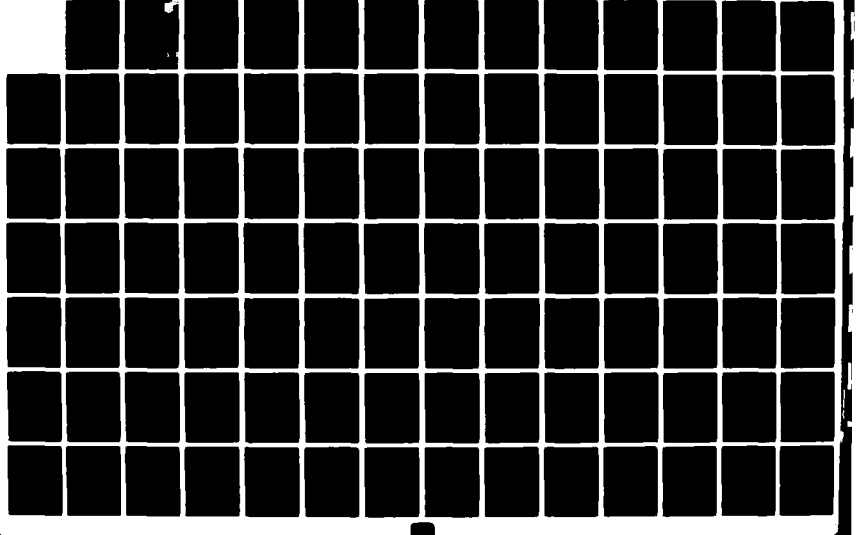

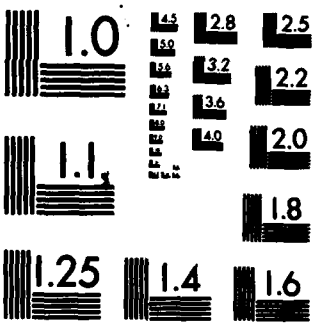

AFWAL-TR-82-2112

SQUEEZE FILM DAMPER TECHNOLOGY PROGRAM FIRST INTERIM REPORT: DAMPER COMPONENT ANALYSIS AND INTEGRATION WITH ROTOR-DYNAMICS PROGRAM

Joseph A. Tecza
Dr. Edward S. Zorzi
Mechanical Technology, Inc.
968 Albany-Shaker Road
Latham, New York 12110

W. H. Parker
Detroit Diesel Allison
P.O. Box 894
Speed Code U-29A
Indianapolis, Indiana 46206

November 1982

Interim Report for Period October 1979 - December 1981

AERO PROPULSION LABORATORY
AIR FORCE WRIGHT AERONAUTICAL LABORATORIES
AIR FORCE SYSTEMS COMMAND
WRIGHT-PATTERSON AIR FORCE BASE, OHIO 45433

NOTICE

When Government drawings, specifications, or other data are used for any purpose other than in connection with a definitely related Government procurement operation, the United States Government thereby incurs no responsibility nor any obligation whatsoever; and the fact that the government may have formulated, furnished, or in any way supplied the said drawings, specifications, or other data, is not to be regarded by implication or otherwise as in any manner licensing the holder or any other person or corporation, or conveying any rights or permission to manufacture use, or sell any patented invention that may in any way be related thereto.

This report has been reviewed by the Office of Public Affairs (ASD/PA) and is releasable to the National Technical Information Service (NTIS). At NTIS, it will be available to the general public, including foreign nations.

This technical report has been reviewed and is approved for publication.

Sandra K. Drake

SANDRA K. DRAKE
Project Engineer
Engine Assessment Branch

Robert W. Baker

ROBERT W. BAKER, Major, USAF
Chief, Engine Assessment Branch
Turbine Engine Division

FOR THE COMMANDER

James M. Shipman

JAMES M. SHIPMAN, Major, USAF
Deputy Director
Turbine Engine Division
Aero Propulsion Laboratory

"If your address has changed, if you wish to be removed from our mailing list, or if the addressee is no longer employed by your organization please notify AFWAL/POTA, W-PAFB, OH 45433 to help us maintain a current mailing list".

Copies of this report should not be returned unless return is required by security considerations, contractual obligations, or notice on a specific document.

Unclassified

SECURITY CLASSIFICATION OF THIS PAGE (When Data Entered)

REPORT DOCUMENTATION PAGE

READ INSTRUCTIONS BEFORE COMPLETING FORM

1. REPORT NUMBER: AFWAL-TR-82-2112	2. GOVT ACCESSION NO.: AD-A129 021
3. RECIPIENT'S CATALOG NUMBER:	
4. TITLE (and Subtitle): Squeeze Film Damper Technology Program First Interim Report: Damper Component Analysis and Integration with Rotor-Dynamics Program	5. TYPE OF REPORT & PERIOD COVERED: Interim Report for Period October 1979-December 1981
	6. PERFORMING ORG. REPORT NUMBER: MTI 82TR61
7. AUTHOR(s): Joseph A. Tecza, Mechanical Technology, Inc. Dr. Edward S. Zorzi, Mechanical Technology, Inc. William H. Parker, Detroit Diesel Allison	8. CONTRACT OR GRANT NUMBER(s): F33615-79-C-2050
9. PERFORMING ORGANIZATION NAME AND ADDRESS: Mechanical Technology, Inc. 968 Albany-Shaker Road Latham, New York 12110	10. PROGRAM ELEMENT, PROJECT, TASK AREA & WORK UNIT NUMBERS: 3066/12/45
11. CONTROLLING OFFICE NAME AND ADDRESS: Aero Propulsion Laboratory (AFWAL/POTA) Air Force Wright Aeronautical Laboratories/AFSC Wright-Patterson Air Force Base, Ohio 45433	12. REPORT DATE: November 1982
	13. NUMBER OF PAGES: 118
14. MONITORING AGENCY NAME & ADDRESS(if different from Controlling Office):	15. SECURITY CLASS. (of this report): Unclassified
	15a. DECLASSIFICATION/DOWNGRADING SCHEDULE

16. DISTRIBUTION STATEMENT (of this Report)

Approved for public release; distribution unlimited.

17. DISTRIBUTION STATEMENT (of the abstract entered in Block 20, if different from Report)

18. SUPPLEMENTARY NOTES

19. KEY WORDS (Continue on reverse side if necessary and identify by block number)

Damper	Computer Program
Squeeze Film	Response
Rotordynamics	Stability
Dynamics	

20. ABSTRACT (Continue on reverse side if necessary and identify by block number)

Squeeze film dampers are widely used components in modern turbomachinery, but their behavior is not well understood. This program was initiated in order to extend the squeeze film damper analytical basis, confirm predictions by means of a test program, transfer the analytical technology to a gas turbine engine manufacturer, integrate it with existing rotordynamic tools and develop and demonstrate a damper design system.

DD FORM 1 JAN 73 1473 EDITION OF 1 NOV 65 IS OBSOLETE

Unclassified

SECURITY CLASSIFICATION OF THIS PAGE (When Data Entered)

PREFACE

The work described in this report was performed under contract No. F33615-79-C2050 for the Aero Propulsion Laboratory of the Air Force Wright Aeronautical Laboratories (AFWAL/POTA), Wright-Patterson Air Force Base, Ohio. The technical monitors for AFWAL/POTA, Ms. Sandra K. Drake, and Mr. James F. Walton, who formerly served in that capacity, are recognized for their active support of this program. The authors wish to acknowledge the support of Dr. Jorgen Lund of the Technical University of Denmark for his damper analysis, Mr. John Giordano and Mrs. Frieda Gillham of MTI for their overall support and Dr. Anthony J. Smalley, formerly of MTI, for his early program management. In addition, they wish to acknowledge Mr. Richard Beck of DDA for his coupled rotor/damper implementation and Mr. Steven Klusman of DDA for development of the analysis application philosophy and log dec derivation.

TABLE OF CONTENTS

LIST OF ILLUSTRATIONS

LIST OF ILLUSTRATIONS (continued)

LIST OF TABLES

SECTION I

INTRODUCTION

With trends towards higher thrust-to-weight ratios, improved fuel consumption and increased durability in advanced gas turbine engines, conflicting design constraints have arisen. Paragraph 3.3.8.10 of MIL-E-5007D states "the engine shall be free of destructive vibration at all engine speeds and thrust, including steady-state and transient operation throughout the complete operating range of the engine". Meeting these needs while designing lighter and more flexible rotors and cases has significantly increased the requirement for analytical design capabilities that provide for the precise control of the rotor system dynamics. The overall intent of this program is to provide a better understanding of the physical phenomena that affect the design of Squeeze Film Dampers for high speed rotating machinery and to provide an integrated rotor/damper design system methodology. The integration of the squeeze film damper and rotor dynamics design tools is seen as being crucial to the development of rotor systems characterized by predictable and reliable operation.

The team of Mechanical Technology, Inc. (MTI) and Detroit Diesel Allison (DDA) is addressing this task by means of a two phase program:

Phase I - Large Squeeze Film Damper Technology

Phase II - Small Squeeze Film Damper Technology and Cavitation Effects

This first interim report documents the Phase I analysis and design systems developed under this program by both MTI and DDA. At the present, Phase I analysis tasks have been completed. Verification testing through the use of a high speed controlled orbit rig is in its final stages. Work on Phase II has just begun, in parallel with the tasks in the latter half of Phase I.

The following paragraphs outline the contents of the two phases, indicate where the program currently stands and what will be reported on in this report.

Phase I, Large Squeeze Film Damper Technology, consists of nine tasks. During the first three tasks of Phase I, MTI is to develop a squeeze-film damper component analysis tool, and then verify this capability through high speed

testing of up to five different design geometries and sealing conditions. This verified component technology is then to be assembled and documented in a form that could be directly transferred to the design systems of military gas turbine engine manufacturers. To ensure this transferability, DDA is to accept the verified, documented technology and integrate it with their rotordynamic design and analysis capability. DDA is to then develop integrated design procedures which will be applied both in application rig design and in design improvement of a current inventory Air Force engine (the TF41) which powers the single-engine LTV A7D Corsair 2. MTI, in parallel with this technology transfer and application, will oversee the design system development and provide program management and technology documentation.

Component analysis and component rig design proceeded in parallel. Initial transfer of software to DDA took place once the component analysis was complete. Component tests are to be performed and comprehensive design charts developed.

Comparisons between predictions and measurements are to be made once tests have been completed on the controlled orbit rig and the free orbit rig. Under Task IV, any needed refinements to test or analysis are to be planned and full component technology transfer to DDA can be completed and integrated fully with the DDA rotordynamics analysis capability. In parallel with the component technology transfer, MTI is to do further work in consolidating the component analysis software into the component design system for use in association with the integrated rotor/damper system design.

Utilizing the fully developed and verified damper component and rotor damper design system capability and DDA's experience in military gas turbine design, DDA is to develop, document and illustrate the procedures which should be followed to most effectively apply the damper design technology. Work will then start on a design manual. In parallel with this reporting effort, the design criteria will be applied to a current Air Force inventory engine (TF41). One or more dampers for this engine will be designed and the benefits of these design modifications will be analytically demonstrated.

Application rig work is also planned as a verification of the design procedures. Tests are to be performed on a blade-loss test rig, which will demonstrate dampers designed both for normal and for abusive unbalance. Comparisons of test results and predictions will be made. Evaluation of predictive capability will be performed as well as evaluation of the design procedures used in developing the damper components.

Phase II, Small Squeeze Film Damper Technology and Cavitation Effects, consists of six tasks which complement the Phase I effort. The investigations proposed in Phase II will lead to further state-of-the-art squeeze-film damper advancement, both in fundamentals and in applications. The main thrust of the work planned is to better understand the phenomenon of cavitation in squeeze-film dampers, to conduct parameter studies of various damper phenomena using existing software and to assess the influence of small engine size (in the 500- to 8500-lb thrust class) on engine and damper dynamics.

The first three tasks of Phase II are devoted to a detailed study of cavitation. The present analysis, while it considers cavitation, does not provide for an in-depth investigation of this phenomenon which can strongly influence damper behavior. The scope described in this effort will develop understanding and a means of handling cavitation effectively in design analysis.

The fourth task involves a series of parameter studies which have been selected to allow the full benefit of the software capabilities developed under the present Air Force program to be exercised and exploited, particularly in the nonlinear area.

The investigation of sizing effects in the fifth task is important because the present Air Force program is directed at larger engines. Although the basic technology should be extrapolatable to smaller engines, careful consideration of sizing effects, both from damper considerations and from engine dynamics considerations, is to be carefully assessed.

The overall program is outlined in the block diagram of Figure 1-1, arranged by type of effort rather than by task. The heavily outlined blocks, damper analysis and design system development are completed whereas the boxes outlined with broken lines,

- steady state verification
- transient verification
- design methods application
- cavitation analysis
- visual observation of cavitation

are currently in progress, some being nearly completed.

This first interim report covers the two completed portions of the program effort. The squeeze film damper film analysis is given in detail including the boundary conditions assumed, solution methods the computer program system and example calculations. The design system development is also covered in detail, including damper analysis/rotordynamics tools and integration philosophy and the interfacing of these tools into a system for linear and nonlinear calculations.

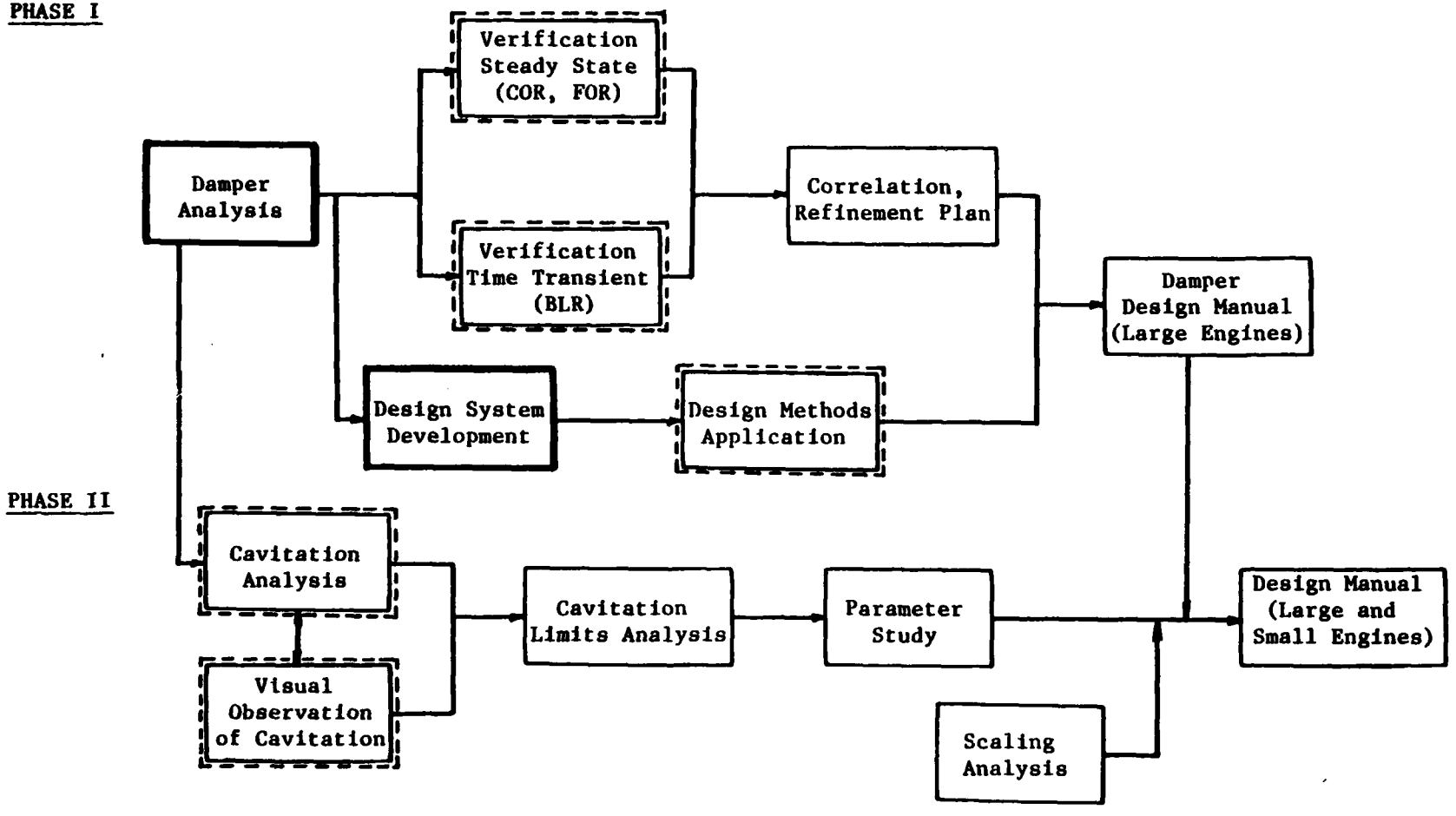

Figure 1-1 Block Diagram of Squeeze Film Damper Program Effort

SECTION II

SQUEEZE FILM DAMPER ANALYSIS

This Section describes analytical basis behind the squeeze film damper analysis computer program.

In its most general form, the computer program calculates response of the film to an imposed velocity at a particular location. Circular orbit calculations, where the velocity direction is always at 90^{o} to the eccentricity vector, are a special case of this generalized calculation. A finite difference approximation to the Reynolds equation is used which provides algebraic difference equations linking pressure values at each point of a rectangular mesh on the developed damper surface. A very mature state of the art exists for this portion of the problem. Film rupture is handled by setting computer subambient pressures to ambient (with an option for ambient pressure to be set at a nonzero value). It is noted that the choice was made to treat the zero pressure gradient boundary condition as a refinement, which could be added later if the need arose.

The specific effects which are included in the computer program are:

1. The finite length of the damper, which is handled by means of the two-dimensional finite difference solution.

2. Finite orbit size of eccentricity is an implicit part of the finite length Reynolds equation solution.

3. Finite velocity is accounted for in terms of its effect on cavitation. In combination with the supply pressure, the velocity determines the location of points in the film where the pressure changes from positive to negative. By tracking these points, finite velocity effects are accounted for. It is noted that, in the special case of zero supply pressure, the location of the boundary conditions is defined strictly by the velocity direction; therefore, in this special (though meaningful) case, fluid film forces are directly proportional to velocity magnitude; a fact to be remembered when making effective use of this computer program.

4. Damper clearance and diameter are implicit in the physics of the problem represented by the Reynolds equation.

5. Fluid viscous effects are also implicit in the Reynolds equation.

6. Fluid inertia effects are accounted for by a perturbation solution based upon the Reynolds number (λ). The approach used is that described by Lund in Reference 1. The result of the fluid inertia effects calculation is a linear correction to the predicted pressure and viscous damping results.

7. Fluid film rupture is handled normally by the π or half-film type approach where any computed subambient pressures are set to ambient pressure and ambient pressure can be set as an input parameter.

8. Fluid supply conditions are treated by specifying pressure to be equal to inlet pressure over the region of the supply groove or hole. Flow boundary conditions and inlet and outlet will be handled by satisfying either the local or global relationships between flow and pressure drop. Satisfying global boundary conditions affects the steady pressure level, about which the dynamic motion of the damper causes a perturbation. Satisfaction of local boundary conditions influence the dynamic pressure response by influencing the local dynamic continuity.

9. Frequency is accounted for in a similar manner to that already described for finite velocity. Indeed, whether one is concerned about the effect of finite velocity or finite frequency is dependent upon whether the general impedance analysis is being performed or the more specialized circular orbit analysis. In the case of the circular orbit analysis, the orbit frequency sets the velocity. For use in rotordynamics calculation, the frequency is the most convenient parameter to talk about. For fluid film computation, the implicit finite velocity is accounted for and, in combination with supply conditions, dictates the location of the zero pressure boundaries, and thereby, the extent of the cavitated region.

10. The direct result of the Reynolds equation solution are pressures. These are integrated numerically to give forces. The relationship of force to velocity or displacement gives coefficients as needed.

11. Flow is calculated by integrating around the boundary of interest. The local flow is determined from the computed pressure gradient, film thickness, and viscosity.

The following is a description of the damper film analysis, along with descriptions of the solution scheme, the mobility method application and jump analysis.

2.1 Reynolds' Equation Without Inertia Effects

The squeeze film damper is a cylindrical bearing which supports a non-rotating bushing or journal. Figure 2-1 shows the fixed coordinate system and quantities used to describe the damper geometry.

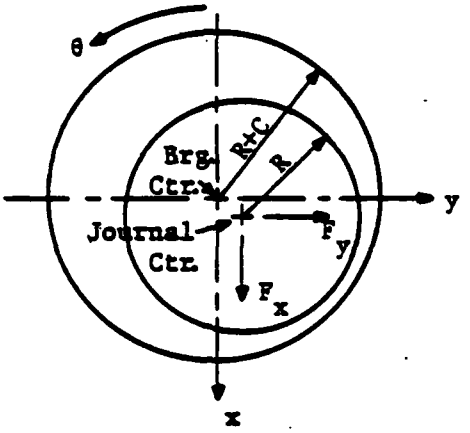

Figure 2-1 Squeeze Film Damper Geometry

The bearing dimensions and lubricant properties are:

D = bearing diameter, (m)

R = 1/2D = bearing radius, (m)

L = bearing length, (m)

C = radial clearance, (m)

μ = lubricant viscosity, (N-sec/m^2)

ρ = lubricant density, (kg/m^3)

x, y = bushing center coordinates, (m)

θ = circumferential coordinate angle, measured from negative x-axis (radians)

z = axial coordinate, (m)

$h = C + x\cos\theta + y\sin\theta$ = local film thickness, (in) (2-1)

t = time, (sec)

q_k = flow from k'th feeding hole, (m^3/sec)

f = reference frequency, (Hz)

$\omega = 2\pi f$ = reference angular frequency, (radians/sec)

p = film pressure, (N/m^2)

By ignoring inertia effects, the pressure p in the lubricant film derives from Reynold's equation in the form:

$$\frac{\partial}{R\partial\theta}\left(\frac{h^3}{12\mu}\frac{\partial p}{R\partial\theta}\right)+\frac{\partial}{\partial z}\left(\frac{h^3}{12\mu}\frac{\partial p}{\partial z}\right)=\frac{\partial h}{\partial t}-\frac{1}{R}\sum_k q_k\,\delta(\theta-\theta_k)\,\delta(z-z_k) \qquad (2\text{-}2)$$

where $\delta(\theta - \theta_k)$ and $\delta(z - z_k)$ are unit delta-functions, and θ_k and z_k give the coordinates of the k'th feeding hole. Furthermore:

$$\frac{\partial h}{\partial t}=\frac{dx}{dt}\cos\theta+\frac{dy}{dt}\sin\theta \qquad (2\text{-}3)$$

With z measured from the centerplane of the bearing the boundary conditions for eq. 2-2 are:

at $z = 1/2L$:

with sealed end groove: $$\int_0^{2\pi}\left(-\frac{h^3}{12\mu}\frac{\partial p}{\partial z}\right)_{1/2L} R\,d\theta = C_G\,p(1/2L) \qquad (2\text{-}4)$$

with end seal (no groove): $$\left(-\frac{h^3}{12\mu}\frac{\partial p}{\partial z}\right)_{1/2L} = C_L\,p(1/2L) \qquad (2\text{-}5)$$

with no end sealing: $$p(1/2L) = 0 \qquad (2\text{-}6)$$

where C_G and C_L are flow coefficients for the seals.* When the bearing is not symmetric with respect to the centerplane, these boundary conditions also apply at $z = -\frac{1}{2}L$. When there is symmetry around the centerplane, only half the film needs to be considered, and the boundary conditions at $z = 0$ become:

at $z = 0$: with circumferential feeding groove: $p(0) = p_s$ (2-7)

without circumferential feeding groove: $\left(\frac{\partial p}{\partial z}\right)_0 = 0$ (2-8)

where p_s is the supply pressure in the groove.

---

* Flow coefficients for a resistance relate flow through the resistance to pressure drop across the resistance units are (m^5/N·sec) for C_{G_1} (m^4/N·sec) for C_L.

The pressure, p_k, at the k'th feeding hole is related to the feeder hole supply pressure, p_{sk}, and the flow, q_k, by:

$$\text{at } z = z_k,\ \theta = \theta_k: \quad p_k = p_{sk} - \alpha_k\, q_k \tag{2-9}$$

where α_k represents the resistance of the feeder hole.

In order to generalize the results the equations are solved in dimensionless form. The variables are made dimensionless by:

$$\zeta = \frac{z}{R} \tag{2-10}$$

$$\tau = \omega t \tag{2-11}$$

$$\bar{p} = p/12\mu\omega\left(\frac{R}{C}\right)^2 \tag{2-12}$$

$$\bar{q}_k = q_k/\omega C R^2 \tag{2-13}$$

$$\bar{x},\ \bar{y} = x/C,\ y/C \tag{2-14}$$

$$\bar{h} = h/C = 1 + \bar{x}\cos\theta + \bar{y}\sin\theta \tag{2-15}$$

Thereby eq. (2-2) is transformed into:

$$\frac{\partial}{\partial\theta}\left(\bar{h}^3\frac{\partial\bar{p}}{\partial\theta}\right) + \frac{\partial}{\partial\zeta}\left(\bar{h}^3\frac{\partial\bar{p}}{\partial\zeta}\right) = \dot{\bar{x}}\cos\theta + \dot{\bar{y}}\sin\theta - \sum_k \bar{q}_k\,\delta(\theta - \theta_k)\,\delta(\zeta - \zeta_k) \tag{2-16}$$

where

$$\dot{\bar{x}},\ \dot{\bar{y}} = \frac{\partial\bar{x}}{\partial\tau},\ \frac{\partial\bar{y}}{\partial\tau} = \frac{1}{C\omega}\frac{dx}{dt},\ \frac{1}{C\omega}\frac{dy}{dt} \tag{2-17}$$

ω (radians/sec) is a representative angular frequency. Its precise value is not important to the dimensionless form of the equation as it only serves as a scaling factor, but typically it should be selected such that $\dot{x}$, $\dot{y}$ are of the order of 1.

$$\text{at } \zeta = \frac{L}{D}\ \left(z = \frac{1}{2}L\right):$$

$$\text{with sealed end groove:} \quad \int_0^{2\pi}\left(-\bar{h}^3\frac{\partial\bar{p}}{\partial\zeta}\right)_{L/D} d\theta = \bar{C}_G\,\bar{p}(\zeta = L/D) \tag{2-18}$$

with end seal (no groove): $(-\bar{h}^3 \frac{\partial \bar{p}}{\partial \zeta})_{L/D} = \bar{C}_L \bar{p}(\zeta = \frac{L}{D})$ (2-19)

with no end sealing: $\bar{p}(\zeta = L/D) = 0$ (2-20)

The dimensionless seal flow coefficients are defined as:

$$\bar{C}_G = \frac{12\mu}{C^3} C_G \quad \text{(sealed end groove)} \tag{2-21}$$

$$\bar{C}_L = \frac{12\mu R}{C^3} C_L \quad \text{(end seal, no groove)} \tag{2-22}$$

As an example, the seal may be represented as a ring of width W with a leakage gap of height S, as shown in Figure 2-2.

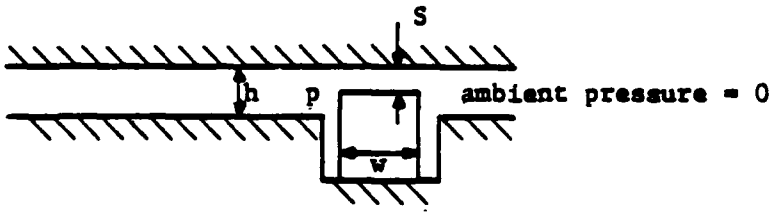

Figure 2-2 Representation of Sealing Ring in Groove

The flow through the seal gap is:

for sealed end groove: $2\pi R \frac{S^3}{12\mu} \frac{p(1/2L)}{W} = C_G\, p(1/2L)$ (see Eq. (2-4))

for end seal, no groove: $\frac{S^3}{12\mu} \frac{p(1/2L)}{W} = C_L\, p(1/2L)$ (see Eq. (2-5))

With this seal model the dimensionless seal coefficients become:

$$\bar{C}_G = 2\pi \left(\frac{R}{W}\right) \left(\frac{S}{C}\right)^3 \tag{2-23}$$

$$\bar{C}_L = \left(\frac{R}{W}\right) \left(\frac{S}{C}\right)^3 \tag{2-24}$$

When there is symmetry around the centerplane, the boundary conditions at $\zeta = 0$ are:

at $\zeta = 0$:

with circumferential feeding groove: $\bar{p}(0) = \bar{p}_s$ (2-25)

without circumferential feeding groove: $(\frac{\partial \bar{p}}{\partial \zeta})_o = 0$ (2-26)

where $\bar{p}_s$ is the dimensionless supply pressure:

$$\bar{p}_s = \frac{p_s}{12\mu\omega(\frac{R}{C})^2} \tag{2-27}$$

At the feeder holes, Eq. (2-9) applies:

at $\zeta = \zeta_k$, $\theta = \theta_k$: $\bar{p}_k = \bar{p}_{sk} - \bar{\alpha}_k \bar{q}_k$ (2-28)

where $\bar{\alpha}_k$ is the dimensionless feeder hole resistance:

$$\bar{\alpha}_k = \frac{C^3}{12\mu} \alpha_k \tag{2-29}$$

As an example, the feeder hole may be represented as a capillary for which the flow is given by:

$$q_k = \frac{2\pi d^4}{\mu \ell} (p_{sk} - p_k) \tag{2-30}$$

where d is the tube diameter and ℓ is the length. Hence, the resistance is:

$$\bar{\alpha}_k = \frac{\mu \ell}{2\pi d^4}$$

and the dimensionless resistance becomes:

$$\bar{\alpha}_k = \frac{1}{24\pi} (\frac{\ell}{d}) (\frac{C}{d})^3$$

With the given boundary conditions Eq. (2-16) may be solved numerically as discussed later.

By integrating the film pressures the damper film forces are computed as (see Fig. 2-1):

$$\left.\begin{matrix} F_x \\ F_y \end{matrix}\right\} = \int_{-\frac{1}{2}L}^{\frac{1}{2}L} \int_0^{2\pi} p \left\{\begin{matrix} \cos\theta \\ \sin\theta \end{matrix}\right\} R\, d\theta\, dz \qquad (2\text{-}31)$$

or, in dimensionless form:

$$\left.\begin{matrix} \bar{F}_x = \dfrac{Fx}{\mu\omega LR(\frac{R}{C})^2} \\ \bar{F}_y = \dfrac{Fy}{\mu\omega LR(\frac{R}{C})^2} \end{matrix}\right\} = \frac{6}{L/D} \int_{-\frac{L}{D}}^{\frac{L}{D}} \int_0^{2\pi} \bar{p} \left\{\begin{matrix} \cos\theta \\ \sin\theta \end{matrix}\right\} d\theta\, d\zeta \qquad (2\text{-}32)$$

The flow out of the film at the end is:

$$\text{at } z = \tfrac{1}{2}L: \quad Q_{out} = \int_0^{2\pi} \left(-\frac{h^3}{12\mu} \frac{\partial p}{\partial z}\right)_{\frac{1}{2}L} R d\theta \qquad (2\text{-}33)$$

which in dimensionless form becomes:

$$\text{at } \zeta = \frac{L}{D}: \quad \bar{Q}_{out} = \frac{Q_{out}}{\omega CR^2} = \int_0^{2\pi} \left(-\bar{h}^3 \frac{\partial \bar{p}}{\partial \zeta}\right)_{L/D} d\theta \qquad (2\text{-}34)$$

An analogous expression holds for the end at $\zeta = -\frac{L}{D}$ and for the flow in from a circumferential groove. The inflow from any feeder holes is the sum of the calculated $\bar{q}_k$ values.

2.2 Inertia Effects in Reynold's Equation

Under the conventional assumption of lubrication theory where the lubricant film is assumed thin ($C/R \ll 1$), the Navier-Stokes equations reduce to:

$$\begin{aligned} \rho\left(\frac{\partial u}{\partial t} + u \frac{\partial u}{R\partial\theta} + v \frac{\partial u}{\partial y} + w \frac{\partial u}{\partial z}\right) &= -\frac{\partial p}{R\partial\theta} + \mu \frac{\partial^2 u}{\partial y^2} \\ \rho\left(\frac{\partial w}{\partial t} + u \frac{\partial w}{R\partial\theta} + v \frac{\partial w}{\partial y} + w \frac{\partial w}{\partial z}\right) &= -\frac{\partial p}{\partial z} + \mu \frac{\partial^2 w}{\partial y^2} \end{aligned} \qquad (2\text{-}35)$$

where y is the coordinate across the film, u, v and w are the fluid velocity components in the θ, y and z directions, respectively, and ρ is the fluid mass density. The terms on the left hand side of the equations represent the inertia forces, and they are normally ignored as being small in most cases. To assess their magnitude, the equations are made dimensionless by:

$$\bar{u} = \frac{u}{R\omega} \qquad \bar{w} = \frac{w}{R\omega} \qquad \bar{v} = \frac{v}{C\omega} \qquad \eta = \frac{y}{C}$$

while the remaining variables are made dimensionless in accordance with eqs. (2-10), (2-11), (2-12) and (2-15). The dimensionless equations become:

$$\lambda\left(\frac{\partial \bar{u}}{\partial \tau} + \bar{u}\frac{\partial \bar{u}}{\partial \theta} + \bar{v}\frac{\partial \bar{u}}{\partial \eta} + \bar{w}\frac{\partial \bar{u}}{\partial \zeta}\right) = -12\frac{\partial \bar{p}}{\partial \theta} + \frac{\partial^2 \bar{u}}{\partial \eta^2} \tag{2-36}$$

$$\lambda\left(\frac{\partial \bar{w}}{\partial \tau} + \bar{u}\frac{\partial \bar{w}}{\partial \theta} + \bar{v}\frac{\partial \bar{w}}{\partial \eta} + \bar{w}\frac{\partial \bar{w}}{\partial \zeta}\right) = -12\frac{\partial \bar{p}}{\partial \zeta} + \frac{\partial^2 \bar{w}}{\partial \eta^2}$$

where

$$\lambda = \left(\frac{C}{R}\right) R_e \tag{2-37}$$

and R_e is the Reynold's number:

$$R_e = \frac{\rho\omega RC}{\mu} \tag{2-38}$$

Thus, only when λ is of the order of unity are the inertia terms important. To include them, a perturbation solution is employed, setting:

$$\bar{p} = \bar{p}_o + \lambda\,\bar{p}_1 + \cdots$$

$$\bar{u} = \bar{u}_o + \lambda\,\bar{u}_1 + \cdots \tag{2-39}$$

and similarly for $\bar{v}$ and $\bar{w}$. By substituting into Eqs. (2-36) and collecting terms of like power in λ, the following equations result:

$$\frac{\partial^2 \bar{u}_o}{\partial \eta^2} = 12\frac{\partial \bar{p}_o}{\partial \theta} \tag{2-40}$$

$$\frac{\partial^2 \bar{w}_o}{\partial \eta^2} = 12 \frac{\partial \bar{p}_o}{\partial \zeta} \tag{2-41}$$

$$\frac{\partial^2 \bar{u}_1}{\partial \eta^2} = 12 \frac{\partial \bar{p}_1}{\partial \theta} + \frac{\partial \bar{u}_o}{\partial \tau} + \bar{u}_o \frac{\partial \bar{u}_o}{\partial \theta} + \bar{v}_o \frac{\partial \bar{u}_o}{\partial \eta} + \bar{w}_o \frac{\partial \bar{u}_o}{\partial \zeta} \tag{2-42}$$

$$\frac{\partial^2 \bar{w}_1}{\partial \eta^2} = 12 \frac{\partial \bar{p}_1}{\partial \zeta} + \frac{\partial \bar{w}_o}{\partial \tau} + \bar{u}_o \frac{\partial \bar{w}_o}{\partial \theta} + \bar{v}_o \frac{\partial \bar{w}_o}{\partial \eta} + \bar{w}_o \frac{\partial \bar{w}_o}{\partial \zeta} \tag{2-43}$$

(the equations for higher order terms are ignored).

As the pressure is independent of y, $\bar{p}_o$ and $\bar{p}_1$ do not depend on η, and eqs. (2-40) and (2-41) may be integrated twice to give:

$$\begin{aligned} \bar{u}_o &= -6 \frac{\partial \bar{p}_o}{\partial \theta} \eta(\bar{h} - \eta) \\ \bar{w}_o &= -6 \frac{\partial \bar{p}_o}{\partial \zeta} \eta(\bar{h} - \eta) \end{aligned} \tag{2-44}$$

which satisfy the boundary conditions that u and w are zero at the two film surfaces (y = 0 and y = h). The continuity equation is

$$\frac{\partial \bar{u}}{\partial \theta} + \frac{\partial \bar{v}}{\partial \eta} + \frac{\partial \bar{w}}{\partial \zeta} = 0 \tag{2-45}$$

Thus:

$$\frac{\partial \bar{v}_o}{\partial \eta} = -\frac{\partial \bar{u}_o}{\partial \theta} - \frac{\partial \bar{w}_o}{\partial \zeta} = 6 \frac{\partial^2 \bar{p}_o}{\partial \theta^2} \eta(\bar{h} - \eta) + 6 \frac{\partial \bar{p}_o}{\partial \theta} \frac{\partial \bar{h}}{\partial \theta} + 6 \frac{\partial^2 \bar{p}_o}{\partial \zeta^2} \eta(\bar{h} - \eta)$$

and upon integration:

$$\bar{v}_o = \eta^2(3\bar{h} - 2\eta) \frac{\partial^2 \bar{p}_o}{\partial \theta^2} + 3\eta^2 \frac{\partial \bar{h}}{\partial \theta} + \eta^2(3\bar{h} - 2\eta) \frac{\partial^2 \bar{p}_o}{\partial \zeta^2} \tag{2-46}$$

(boundary condition: $\bar{v} = o$ at $\eta = o$).

At $\eta = \bar{h}$, $\bar{v}_o$ equals the squeeze velocity $\frac{\partial \bar{h}}{\partial \tau}$ such that Eq. (2-46) yields:

$$\frac{\partial}{\partial \theta}\left(\bar{h}^3 \frac{\partial \bar{p}_o}{\partial \theta}\right) + \frac{\partial}{\partial \zeta}\left(\bar{h}^3 \frac{\partial \bar{p}_o}{\partial \zeta}\right) = \frac{\partial \bar{h}}{\partial \tau} = \dot{\bar{x}} \cos\theta + \dot{\bar{y}} \sin\theta \qquad (2\text{-}47)$$

which is Reynold's equation without inertia effects as previously given in Eq. (2-16). By substituting into Eq. (2-46), $\bar{v}_o$ may also be expressed as:

$$\bar{v}_o = \frac{\eta^2(3\bar{h} - 2\eta)}{\bar{h}^3} \frac{d\bar{h}}{d\tau} - \frac{6\eta^2(\bar{h} - \eta)}{\bar{h}} \frac{\partial \bar{h}}{\partial \theta} \frac{\partial \bar{p}_o}{\partial \theta} \qquad (2\text{-}48)$$

With $\bar{u}_o$, $\bar{w}_o$ and $\bar{v}_o$ determined, Eqs. (2-41) and (2-42) can be integrated twice to yield:

$$\bar{u}_1 = -6\eta(\bar{h} - \eta) \frac{\partial \bar{p}_1}{\partial \theta} + \frac{1}{2}(\eta\bar{h}^3 - 2\bar{h}\eta^3 + \eta^4) \frac{\partial^2 \bar{p}_o}{\partial \theta \partial \tau} + \eta(\bar{h}^2 - \eta^2) \frac{\partial \bar{h}}{\partial \tau} \frac{\partial \bar{p}_o}{\partial \theta}$$
$$+ \iint (\bar{u}_o \frac{\partial \bar{u}_o}{\partial \theta} + \bar{v}_o \frac{\partial \bar{u}_o}{\partial \eta} + \bar{w}_o \frac{\partial \bar{u}_o}{\partial \zeta}) d\eta d\eta \qquad (2\text{-}49)$$

$$\bar{w}_1 = -6\eta(\bar{h} - \eta) \frac{\partial \bar{p}_1}{\partial \zeta} + \frac{1}{2}(\eta\bar{h}^3 - 2\bar{h}\eta^3 + \eta^4) \frac{\partial^2 \bar{p}_o}{\partial \zeta \partial \tau} + \eta(\bar{h}^2 - \eta^2) \frac{\partial \bar{h}}{\partial \tau} \frac{\partial \bar{p}_o}{\partial \zeta}$$
$$+ \iint (\bar{u}_o \frac{\partial \bar{w}_o}{\partial \theta} + \bar{v}_o \frac{\partial \bar{w}_o}{\partial \eta} + \bar{w}_o \frac{\partial \bar{w}_o}{\partial \zeta}) d\eta d\eta \qquad (2\text{-}50)$$

By restricting the analysis to the terms which involve the squeeze acceleration $\frac{d^2\bar{h}}{d\tau^2} = \ddot{\bar{x}} \cos\theta + \ddot{\bar{y}} \sin\theta$, only the two first terms on the right hand side of the equations are retained, after which $\bar{u}_1$ and $\bar{v}_1$ are substituted into the continuity equation:

$$\frac{\partial \bar{v}_1}{\partial \eta} = -\frac{\partial \bar{u}_1}{\partial \theta} - \frac{\partial \bar{w}_1}{\partial \zeta}$$

such that:

$$\frac{\partial \bar{v}_1}{\partial \eta} = 6\eta(\bar{h} - \eta)\frac{\partial^2 \bar{p}_1}{\partial \theta^2} + 6\eta\frac{\partial \bar{h}}{\partial \theta}\frac{\partial \bar{p}_1}{\partial \theta} - \frac{1}{2}(\eta\bar{h}^3 - 2\bar{h}\eta^3 + \eta^4)\frac{\partial^3 \bar{p}_o}{\partial \theta^2 \partial \tau}$$
$$- \frac{1}{2}(3\eta\bar{h}^2 - 2\eta^3)\frac{\partial \bar{h}}{\partial \theta}\frac{\partial^2 \bar{p}_o}{\partial \theta \partial \tau} + 6\eta(\bar{h} - \eta)\frac{\partial^2 \bar{p}_1}{\partial \zeta^2}$$
$$- \frac{1}{2}(\eta\bar{h}^3 - 2\bar{h}\eta^3 + \eta^4)\frac{\partial^3 \bar{p}_o}{\partial \zeta^2 \partial \tau}$$

This equation may be integrated with respect to η, applying the boundary conditions of $\bar{v}_1 = 0$ at $\eta = 0$ and $\eta = \bar{h}$. By making use of Eq. (2-47) and retaining only acceleration terms, the final result is:

$$\frac{\partial}{\partial \theta}(\bar{h}^3\frac{\partial \bar{p}_1}{\partial \theta}) + \frac{\partial}{\partial \zeta}(\bar{h}^3\frac{\partial \bar{p}_1}{\partial \zeta}) = \frac{\bar{h}^2}{10}\frac{\partial^2 \bar{h}}{\partial \tau^2} + \frac{\bar{h}^4}{5}\frac{\partial \bar{h}}{\partial \theta}\frac{\partial^2 \bar{p}_o}{\partial \tau \partial \theta} \qquad (2\text{-}51)$$

From Eqs. (2-47) and the boundary conditions it is seen that $\bar{p}_o$ may be written as the sum of 3 terms:

$$\bar{p}_o = \bar{p}_{\dot{x}}\,\dot{\bar{x}} + \bar{p}_{\dot{y}}\,\dot{\bar{y}} + \bar{p}_b\,\bar{p}_s \qquad (2\text{-}52)$$

Similarly $\bar{p}_1$ may be written as:

$$\bar{p}_1 = \bar{p}_{\ddot{x}}\,\ddot{\bar{x}} + \bar{p}_{\ddot{y}}\,\ddot{\bar{y}} \qquad (2\text{-}53)$$

By substitution into Eq. (2-51) two equations are obtained:

$$\frac{\partial}{\partial \theta}(\bar{h}^3\frac{\partial \bar{p}_{\ddot{x}}}{\partial \theta}) + \frac{\partial}{\partial \zeta}(\bar{h}^3\frac{\partial \bar{p}_{\ddot{x}}}{\partial \zeta}) = \frac{\bar{h}^2}{10}\cos\theta + \frac{\bar{h}^4}{5}\frac{\partial \bar{h}}{\partial \theta}\frac{\partial \bar{p}_{\dot{x}}}{\partial \theta}$$
$$\qquad (2\text{-}54)$$
$$\frac{\partial}{\partial \theta}(\bar{h}^3\frac{\partial \bar{p}_{\ddot{y}}}{\partial \theta}) + \frac{\partial}{\partial \zeta}(\bar{h}^3\frac{\partial \bar{p}_{\ddot{y}}}{\partial \zeta}) = \frac{\bar{h}^2}{10}\sin\theta + \frac{\bar{h}^4}{5}\frac{\partial \bar{h}}{\partial \theta}\frac{\partial \bar{p}_{\dot{y}}}{\partial \theta}$$

2.3 Solution of Reynold's Equation

The solution of Eqs. (2-47) and (2-16) is obtained in the form:

$$\bar{p}_o = \bar{p}'_{\dot{x}}\dot{\bar{x}} + \bar{p}'_{\dot{y}}\dot{\bar{y}} + \sum_m \bar{p}'_m \bar{q}_m + \bar{p}'_b \bar{p}_s \tag{2-55}$$

where the variables are solutions of:

$$\left\{\frac{\partial}{\partial\theta}(\bar{h}^3\frac{\partial}{\partial\theta}) + \frac{\partial}{\partial\zeta}(h^{-3}\frac{\partial}{\partial\zeta})\right\}\begin{Bmatrix}\bar{p}'_{\dot{x}}\\ \bar{p}'_{\dot{y}}\\ \bar{p}'_m\\ \bar{p}'_b\end{Bmatrix} = \begin{Bmatrix}\cos\theta & (a)\\ \sin\theta & (b)\\ -\delta(\theta-\theta_m)\ \delta(\zeta-\zeta_m) & (c)\\ 0 & (d)\end{Bmatrix} \tag{2-56}$$

The equation is solved as a finite difference equation as discussed later.

The boundary conditions are as follows: if there is end seal, but not in a groove, Eq. (2-19) applies such that:

$$\text{at } \zeta = \frac{L}{D}: \qquad (-\bar{h}^3\frac{d\bar{p}'_{\dot{x}}}{d\zeta})_{L/D} = \bar{C}_L(\bar{p}'_{\dot{x}})_{L/D} \tag{2-57}$$

and similarly for $\bar{p}'_{\dot{y}}$, $\bar{p}'_m$ and $\bar{p}'_b$. The solution for $\bar{p}'_b$, however, is only needed when there is a circumferential feeding groove. If the bearing is not symmetric around the centerplane, Eq. (2-57) also applies at $\zeta = L/D$. If there is symmetry, the boundary conditions at the centerplane are:

$$\text{at } \zeta = 0: \qquad \begin{array}{l}\text{with circumferential feeding groove:}\\ \qquad \bar{p}'_{\dot{x}} = \bar{p}'_{\dot{y}} = \bar{p}'_m = 0,\ \bar{p}'_b = 1\\ \text{no circumferential feeding groove:}\\ \qquad \dfrac{d\bar{p}'_{\dot{x}}}{d\zeta} = \dfrac{d\bar{p}'_{\dot{y}}}{d\zeta} = \dfrac{d\bar{p}'_m}{d\zeta} = 0\end{array} \tag{2-58}$$

If, instead, the end seal is in a groove, the boundary condition at the end is given by Eq. (2-18). The groove pressure may be expressed as:

$$\bar{p}_o(\zeta = \frac{L}{D}) = \bar{p}_o^{(+)} = \bar{p}_{\dot{x}}^{(+)}\dot{\bar{x}} + \bar{p}_{\dot{y}}^{(+)}\dot{\bar{y}} + \sum_m \bar{p}_m^{(+)}\bar{q}_m + \bar{p}_b^{(+)}\bar{p}_s \qquad (2\text{-}59)$$

If the bearing is not symmetric around the centerplane, the groove pressure at the other end is: $\bar{p}_o(\zeta = \frac{L}{D}) = \bar{p}_o^{(-)}$ which may be expressed analogously.

The pressure field set up by the groove pressure and/or the pressure in the circumferential feeding groove is:

$$\bar{p}_b'' = \begin{cases} (1 - \frac{\zeta}{L/D})\ \bar{p}_s + \frac{\zeta}{L/D}\ \bar{p}_o^{(+)} & \text{(with circ. feed groove, symmetric bearing)} \\ \bar{p}_o^{(+)} & \text{(without circ. feed groove, symmetric bearing)} \\ \frac{1}{2}(1 - \frac{\zeta}{L/D})\ \bar{p}_o^{(-)} + \frac{1}{2}(1 + \frac{\zeta}{L/D})\ \bar{p}_o^{(+)} & \text{(not symmetric bearing)} \end{cases} \qquad (2\text{-}60)$$

which replaces the term: $\bar{p}'_b\bar{p}_s$ in Eq. (2-55) when the end seals are in a groove.

By substitution into Eq. (2-18), the boundary conditions at $\zeta = L/D$ becomes:

$$\dot{\bar{x}} \int_0^{2\pi} (-\bar{h}^3 \frac{\partial \bar{p}'_{\dot{x}}}{\partial \zeta})\, d\theta + \dot{\bar{y}} \int_0^{2\pi} (-\bar{h}^3 \frac{\partial \bar{p}'_{\dot{y}}}{\partial \zeta})\, d\theta + \sum_m \bar{q}_m \int_0^{2\pi} (-\bar{h}^3 \frac{\partial \bar{p}'_m}{\partial \zeta})\, d\theta + \int_0^{2\pi} (-\bar{h}^3 \frac{\partial \bar{p}''_b}{\partial \zeta})\, d\theta = \bar{C}_G\, \bar{p}_o^{(+)} \qquad (2\text{-}61)$$

When the film is fed from a circumferential groove, and not from feeder holes such that the $\bar{q}_m$ term does not apply, the equation can be solved directly for $\bar{p}_o^{(+)}$ to get the pressure parameters in Eq. (2-64).

On the other hand, when there are feeder holes and no circumferential feeder groove, Eq. (2-61) must be solved simultaneously with the feeder hole flow equations. They are obtained from Eq. (2-28) with substitution from Eqs. (2-55) and (2-60):

$$\text{at } \zeta = \zeta_k,\ \theta = \theta_k: \quad \bar{\alpha}_k \bar{q}_k + \sum_m \bar{p}'_m \bar{q}_m + \bar{p}''_b \quad -\bar{p}'_{\dot{x}} \dot{\bar{x}} - \bar{p}_{\dot{y}} \dot{\bar{y}} + \bar{p}_{sk} \tag{2-62}$$

These equations can be solved together with Eq. (2-61) to give $\bar{q}_k$ and $\bar{p}_o^{(+)}$ (and $\bar{p}_o^{(-)}$) in the form:

$$\bar{q}_k = \bar{q}_{k\dot{x}} \dot{\bar{x}} + \bar{q}_{k\dot{y}} \dot{\bar{y}} + \bar{q}_{ks} \bar{p}_s \tag{2-63}$$

$$\bar{p}_o^{(+)} = \bar{p}_{o\dot{x}}^{(+)} \dot{\bar{x}} + \bar{p}_{o\dot{y}}^{(+)} \dot{\bar{y}} + \bar{p}_{os}^{(+)} \bar{p}_s \tag{2-64}$$

By substituting these equations into Eqs. (2-55) and (2-60), the pressure distribution, $\bar{p}_o$, can be expressed as given in Eq. (2-52). By integrating $\bar{p}_o$ in accordance with Eq. (2-32), the dimensionless film forces are obtained in the form:

$$\begin{aligned} \bar{F}_x &= -\bar{B}_{xx} \dot{\bar{x}} - \bar{B}_{xy} \dot{\bar{y}} + \bar{F}_{xs} \\ \bar{F}_y &= -\bar{B}_{yx} \dot{\bar{x}} - \bar{B}_{yy} \dot{\bar{y}} + \bar{F}_{ys} \end{aligned} \tag{2-65}$$

where:

$$\left.\begin{matrix} \bar{B}_{xx} \\ \bar{B}_{yx} \end{matrix}\right\} = -\frac{6}{L/D} \int_{-\frac{L}{D}}^{\frac{L}{D}} \int_0^{2\pi} \bar{p}_{\dot{x}} \left\{\begin{matrix} \cos\theta \\ \sin\theta \end{matrix}\right\} d\theta d\zeta \tag{2-66}$$

$$\left.\begin{matrix} \bar{B}_{xy} \\ \bar{B}_{yy} \end{matrix}\right\} = -\frac{6}{L/D} \int_{-\frac{L}{D}}^{\frac{L}{D}} \int_0^{2\pi} \bar{p}_{\dot{y}} \left\{\begin{matrix} \cos\theta \\ \sin\theta \end{matrix}\right\} d\theta d\zeta \tag{2-67}$$

$$\left.\begin{matrix}\bar{F}_{xs}\\ \bar{F}_{ys}\end{matrix}\right\} = \bar{p}_s \frac{6}{L/D} \int_{-\frac{L}{D}}^{\frac{L}{D}} \int_{0}^{2\pi} \bar{p}_b \left\{\begin{matrix}\cos\theta\\ \sin\theta\end{matrix}\right\} d\theta d\zeta \qquad (2\text{-}68)$$

$\bar{B}_{xx}$, $\bar{B}_{xy}$, $\bar{B}_{yx}$ and $\bar{B}_{yy}$ are the dimensionless damping coefficients in the form:

$$\bar{B}_{xx} = \frac{B_{xx}}{\mu L (\frac{R}{C})^3} \qquad (2\text{-}69)$$

and similarly for the other coefficients.

Once $\bar{p}_{\dot{x}}$ and $\bar{p}_{\dot{y}}$ are determined, Eq. (2-54) can be solved for $\bar{p}_{\ddot{x}}$ and $\bar{p}_{\ddot{y}}$ which can be integrated in accordance with Eq. (2-32) where $\bar{p}$ is replaced by $\lambda\bar{p}_1 = \lambda(\bar{p}_{\ddot{x}}\ddot{\bar{x}} + \bar{p}_{\ddot{y}}\ddot{\bar{y}})$ (see Eqs. (2-39) and (2-53)):

$$\begin{aligned}\bar{F}_{x1} &= -\lambda(\bar{C}_{xx}\ddot{\bar{x}} + \bar{C}_{xy}\ddot{\bar{y}})\\ \bar{F}_{y1} &= -\lambda(\bar{C}_{yx}\ddot{\bar{x}} + \bar{C}_{yy}\ddot{\bar{y}})\end{aligned} \qquad (2\text{-}70)$$

where:

$$\left.\begin{matrix}\bar{C}_{xx}\\ \bar{C}_{yx}\end{matrix}\right\} = -\frac{6}{L/D} \int_{-\frac{L}{D}}^{\frac{L}{D}} \int_{0}^{2\pi} \bar{p}_{\ddot{x}} \left\{\begin{matrix}\cos\theta\\ \sin\theta\end{matrix}\right\} d\theta d\zeta \qquad (2\text{-}71)$$

$$\left.\begin{matrix}\bar{C}_{xy}\\ \bar{C}_{yy}\end{matrix}\right\} = -\frac{6}{L/D} \int_{-\frac{L}{D}}^{\frac{L}{D}} \int_{0}^{2\pi} \bar{p}_{\ddot{y}} \left\{\begin{matrix}\cos\theta\\ \sin\theta\end{matrix}\right\} d\theta d\zeta \qquad (2\text{-}72)$$

$\bar{C}_{xx}$, $\bar{C}_{xy}$, $\bar{C}_{y\,x}$ and $\bar{C}_{yy}$ are the dimensionless inertia coefficients in the form:

$$\bar{C}_{xx} = \frac{C_{xx}}{\rho_L R^2 (\frac{R}{C})} \qquad (2\text{-}73)$$

and similarly for the other coefficients. The actual coefficients have the unit of mass.

2.4 Numerical Solution

Reynolds' equation is solved as a finite difference equation. A finite difference grid shown in Figure 2-3, is introduced with a j-axis in the circumferential direction (θ-direction) and an i-axis in the axial direction (z-direction):

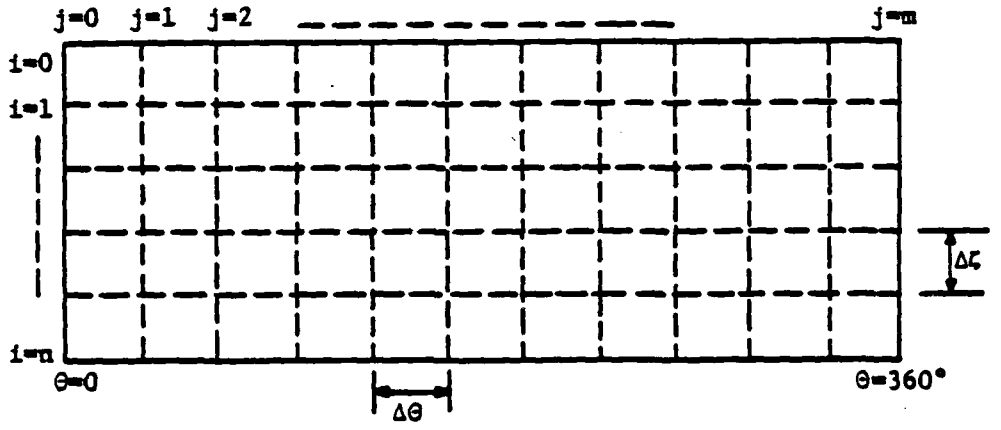

Figure 2-3 Finite Difference Grid for Damper Film

When the bearing end is a sealed groove, or there is no seal, the end is at i = 0. When the seal has no groove, the end is at i = 1. For a symmetric bearing where only one half of the film needs to be considered, the center-plane is at i = n. For a full bearing, i = n gives the other end of the film.

The finite difference increments are:

$$\Delta\theta = \frac{2\pi}{m} \qquad (2\text{-}74)$$

$$\Delta\zeta = \frac{L/D}{n'}$$

where n' is adjusted according to whether the film is half or full, and to the sealing conditions.

In finite difference form, the dimensionless Reynold's equation (Eqs. (2-56) and (2-54)) may be written as:

$$b_{ij}\,\bar{p}_{i,j-1} + b_{i,j+1}\,\bar{p}_{i,j+1} + a'_{ij}\,\bar{p}_{i-1,j} + a_{ij}\,\bar{p}_{ij} + a''_{ij}\,\bar{p}_{i+1,j} = f_{ij} \tag{2-75}$$

where $\bar{p}_{ij}$ represents any of the six pressure variables in Eqs. (2-56) and (2-54), and where:

$$b_{ij} = \frac{1}{\Delta\theta^2}\,\bar{h}^3_{i,j-1/2} \qquad b_{i,j+1} = \frac{1}{\Delta\theta^2}\,\bar{h}^3_{i,j+1/2} \tag{2-76}$$

$$a'_{ij} = \frac{1}{\Delta\zeta^2}\,\bar{h}^3_{i-1/2,j} \qquad a''_{ij} = \frac{1}{\Delta\zeta^2}\,\bar{h}^3_{i+1/2,j} \tag{2-77}$$

$$a_{ij} = -\,(a'_{ij} + a''_{ij} + b_{ij} + b_{i,j+1}) \tag{2-78}$$

f_{ij} = right hand side of Eqs. (2-56) and (2-54), evaluated at

$\theta = \theta_j\,,\ \zeta = \zeta_i$

For the special case of Eq. (2-56c), f_{ij} is given by

$$f_{ij} = \begin{cases} 0 \text{ when } \theta_j \neq \theta_m \text{ or } \zeta_i \neq \zeta_m \\ -\,\frac{1}{\Delta\theta\Delta\zeta} \text{ when } \theta_j = \theta_m,\ \zeta_i = \zeta_m \end{cases} \tag{2-79}$$

When the bearing end has a sealed groove, or there is no seal, then:

$$\bar{p}_{oj} = 0 \tag{2-80}$$

When the bearing end has a seal which is not in a groove, Eq. (2-19) yields:

$$\frac{\bar{h}^3_{1j}}{\Delta\zeta}\left(-\,\frac{3}{2}\,\bar{p}_{1j} + 2\,\bar{p}_{2j} - \frac{1}{2}\,\bar{p}_{3j}\right) = \bar{C}_L\,\bar{p}_{1j} \tag{2-81}$$

where the gradient: $-\frac{d\bar{p}}{d\zeta}$ is derived on the basis of a second order polynomial. By comparing with Eq. (2-75) it is found that in this case:

$$\underline{i = 1}: \qquad b_{ij} = b_{i,j+1} = f_{ij} = 0$$

$$(\bar{C}_L + \frac{3}{2}\frac{\bar{h}_{ij}^3}{\Delta\zeta})\,\bar{p}_{1j} - 2\frac{\bar{h}_{1j}^3}{\Delta\zeta}\,\bar{p}_{2j} + \frac{1}{2}\frac{\bar{h}_{1j}^3}{\Delta\zeta}\,\bar{p}_{3j} = 0 \qquad (2\text{-}82)$$

For a full length film, the boundary conditions at the opposite end (i = n) are analogous to Eqs. (2-80) and (2-82). For a symmetric film, i = n gives the centerplane where the boundary conditions are given by Eqs. (2-25) and (2-26):

$$\underline{\text{at } i = n}: \quad \text{with circumferential feeding groove: } \bar{p}_{nj} = 0 \qquad (2\text{-}83)$$

$$\text{without circumferential feeding groove: } \bar{p}_{n+1,j} = \bar{p}_{n-1,j}$$

The pressures along any j-grid line may be arranged in a column vector:

$$\bar{p}_j = \begin{Bmatrix} \bar{p}_{1j} \\ \vdots \\ \bar{p}_{ij} \\ \vdots \\ \bar{p}_{nj} \end{Bmatrix} \qquad (2\text{-}84)$$

whereby Eq. (2-75) can be written as a matrix equation:

$$\underline{A}_j\,\bar{p}_j + \underline{B}_j\,\bar{p}_{j-1} + \underline{B}_{j+1}\,\bar{p}_{j+1} = F_j \qquad (2\text{-}85)$$

where F_j is the column vector:

$$F_j = \begin{Bmatrix} f_{1j} \\ \vdots \\ f_{ij} \\ \vdots \\ f_{nj} \end{Bmatrix} \qquad (2\text{-}86$$

$\underline{B}_j$ and $\underline{B}_{j+1}$ are diagonal matrices:

$$\underline{B}_j = \text{diag}\left\{b_{ij}\right\} \qquad \underline{B}_{j+1} = \text{diag}\left\{b_{i,j+1}\right\} \tag{2-87}$$

and $\underline{A}_j$ is a tri-diagonal matrix:

$$A_j = \left\{ \begin{array}{ccccc} a_{1j} & & a'_{1j} & & a''_{1j} \\ & a_{ij} & & a'_{ij} & \\ a'_{nj} & & a_{nj} & & \end{array} \right\} \tag{2-88}$$

It should be noted that the boundary conditions of eqs. (2-80), (2-82) and (2-83) are built in $\underline{A}_j$, $\underline{B}_j$ and $\underline{B}_{j+1}$. Eq. (2-85) is solved in the form:

$$\bar{P}_{j-1} = \underline{D}_{j-1}\, \bar{P}_j + \underline{G}_{j-1}\, \bar{P}_m + E_{j-1} \tag{2-89}$$

where $\underline{D}_j$ and $\underline{G}_j$ are matrices while E_j is a column vector. By substitution into Eq. (85) it is found that:

$$\begin{aligned} \underline{D}_j &= -\,\underline{H}_j\, \underline{B}_{j+1} \\ \underline{G}_j &= -\,\underline{H}_j\, \underline{B}_j\, \underline{G}_{j-1} \\ E_j &= \underline{H}_j (F_j - \underline{B}_j\, E_{j-1}) \end{aligned} \tag{2-90}$$

where

$$\underline{H}_j = (\underline{A}_j + \underline{B}_j\, \underline{D}_{j-1})^{-1} \tag{2-91}$$

As the pressure at $\theta = 0$ has to be equal to the pressure at $\theta = 2\pi$, circumferential continuity requires that:

$$\bar{P}_o = \bar{P}_m \tag{2-92}$$

Hence, it is seen from Eq. (2-89) that:

$$\underline{D}_o = \underline{0} \qquad E_o = 0 \qquad \underline{G}_o = \underline{I} \tag{2-93}$$

where $\underline{I}$ is the identity matrix. Hence, Eqs. (2-90) and (2-91) may be used for j going from 1 to m. For j = m+1, eq. (2-89) yields:

$$\bar{P}_m = \underline{D}_m \bar{P}_{m+1} + \underline{G}_m \underline{P}_m + E_m$$

With $\bar{P}_{m+1} = \bar{P}_1$ this equation may be solved:

$$\bar{P}_m = \bar{p}_o = (\underline{I} - \underline{G}_m)^{-1} (\underline{D}_m P_1 + E_m) \tag{2-94}$$

With $\bar{P}_1$ still unknown, set:

$$\bar{P}_j = \underline{S}_j \bar{P}_1 + T_j \tag{2-95}$$

where $\underline{S}_j$ is a matrix and T_j is a column vector. It is seen from Eq. (2-94) that:

$$\underline{S}_m = (\underline{I} - \underline{G}_m)^{-1} \underline{D}_m$$

$$T_m = (\underline{I} - G_m)^{-1} E_m \tag{2-96}$$

By substituting Eq. (2-95) into Eq. (2-89) it is found that:

$$\underline{S}_{j-1} = \underline{D}_{j-1} \underline{S}_j + \underline{G}_{j-1} \underline{S}_m$$

$$T_{j-1} = \underline{D}_{j-1} T_j + \underline{G}_{j-1} T_m + E_{j-1} \tag{2-97}$$

With $\underline{S}_m$ and T_m given by Eq. (2-96), Eq. (2-97) may be used for j going from j = m to j = 2 after which Eq. (2-95) yields:

$$\bar{P}_1 = \underline{S}_1 \bar{P}_1 + T_1 \tag{2-98}$$

This equation may be solved for $\bar{P}_1$:

$$\bar{P}_1 = (\underline{I} - \underline{S}_1)^{-1} T_1 \qquad (2\text{-}99)$$

after which Eq. (2-95) can be used to compute $\bar{P}_j$ for j going from j-2 to j=m whereby the complete pressure distribution is determined.

The advantage of this method is that the most time consuming part of the calculation, namely the calculation of $\underline{H}_j$ (Eq. (2-81)) for j going from j=1 to j=m, needs only to be done once in any given case. Thus, Eqs. (2-90), (2-91), (2-96) and (2-97) may be employed to compute and store $\underline{H}_j$, $\underline{G}_j$ and $\underline{S}_j$ (and also $(\underline{I} - \underline{G}_m)^{-1}$ and $(\underline{I} - \underline{S}_1)^{-1}$, see Eqs. (2-96) and (2-99)). With $\underline{B}_j$ stored during the calculations, Eqs. (2-90), (2-96), (2-97) and (2-99) and, finally, Eq. (2-98), may be used to obtain the solution for any of the six pressure variables in Eqs. (2-56) and (2-54) by simple matrix multiplication. The stored matrices represent the operator on the left hand side of Eqs. (2-56) and (2-54) together with the associated boundary conditions which means that they apply at a given journal center position, a specified seal leakage coefficient for an end seal without a groove, and whether the bearing is symmetric or of full length. To make calculations for any number and combinations of feeder holes, or sealed end grooves with difference leakage coefficient, requires little computation time. The boundary conditions to satisfy are those of Eqs. (2-67) and/or Eq. (2-62).

The calculations end up with five pressure distributions, namely $\bar{p}_{\dot{x}}$, $\bar{p}_{\dot{y}}$ and $\bar{p}_b$ (see Eq. (2-52)), and $\bar{p}_{\ddot{x}}$ and $\bar{p}_{\ddot{y}}$ (see Eq. (2-53)). They are integrated according to Eqs. (2-66), (2-67), (2-68), (2-71) and (2-72) to yield the four damping coefficients and the four inertia coefficients. The integrals are evaluated numerically as:

$$\frac{6}{L/D}\int_{-\frac{L}{D}}^{\frac{L}{D}}\int_{0}^{2\pi} \bar{p}\begin{Bmatrix}\cos\theta\\ \\ \sin\theta\end{Bmatrix} d\theta d\zeta = \frac{6}{L/D}\sum_{i=1}^{n}\sum_{j=1}^{m} \bar{P}_{ij}\begin{Bmatrix}\cos\theta_j\\ \\ \sin\theta_j\end{Bmatrix}\Delta\theta\Delta\zeta \qquad (2\text{-}100)$$

(The result is multiplied by two when only half of the film has been computed. Also, any point at the end or at the centerplane only contributes by half its pressure value).

The integration is performed for given values of the squeeze velocity ($\hat{\dot{x}}$ and $\hat{\dot{y}}$) and of the supply pressure, $\bar{p}_s$. Hence, the pressure, $\bar{p}_{oj}$ can be computed at any selected point from Eq. (2-52). If the thus calculated value is less than a specified cavitation pressure, the pressure at the point is set equal to the cavitation pressure, and the point does not contribute to the damping coefficients or the inertia coefficients. This means that only the pressures in the non-cavitating domain of the film are included in the integration, and as the domain changes with the magnitude and direction of the squeeze velocity, so do the film forces and coefficients change. This also means, that the calculated damping coefficients are not exactly equal to the partial derivatives of the film forces.

2.5 Comments on the Mobility Method

The external forces acting on the damper journal are W_x and W_y, shown in Figure 2-4, which are functions of time.

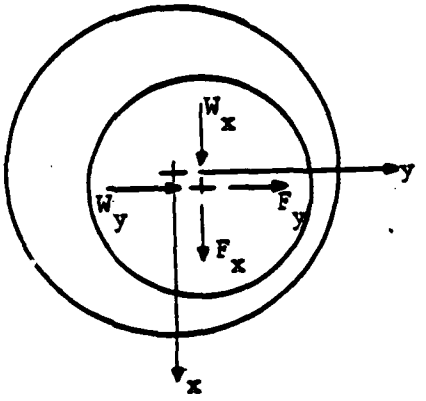

Figure 2-4 Forces Acting on the Journal

The forces from the film are F_x and F_y which are function of the journal center coordinates, x and y, and the corresponding velocities $\dot{x}$ and $\dot{y}$. Let the journal at time t be at the position x(t), y(t). A force balance requires:

$$W_x + F_x = 0 \qquad W_y + F_y = 0 \tag{2-101}$$

These equations are satisfied by determining those values at $\dot{x}$ and $\dot{y}$ which will make the expressions zero. Thus, with guessed values at $\dot{x}$ and $\dot{y}$ an expansion yields:

$$W_x + F_{xo} + \left(\frac{\partial F_x}{\partial \dot{x}}\right)_o \Delta\dot{x} + \left(\frac{\partial F_x}{\partial \dot{y}}\right)_o \Delta\dot{y} = 0 \tag{2-102}$$

and similarly for the y direction. F_{xo}, F_{yo} and the derivatives are evaluated for the given values at x(t), y(t), $\dot{x}$ and $\dot{y}$. Set:

$$B_{xx} = -\left(\frac{\partial F_x}{\partial \dot{x}}\right)_o \qquad B_{xy} = -\left(\frac{\partial F_x}{\partial \dot{y}}\right)_o$$
$$B_{yx} = -\left(\frac{\partial F_y}{\partial \dot{x}}\right)_o \qquad B_{yy} = -\left(\frac{\partial F_y}{\partial \dot{y}}\right)_o \tag{2-103}$$

such that eq. (2-102) may be written:

$$\begin{Bmatrix} B_{xx} & B_{xy} \\ B_{yx} & B_{yy} \end{Bmatrix} \begin{Bmatrix} \Delta\dot{x} \\ \Delta\dot{y} \end{Bmatrix} = \begin{Bmatrix} W_x + F_{xo} \\ W_y + F_{yo} \end{Bmatrix} \tag{2-104}$$

This equation is readily solved for $\Delta\dot{x}$ and $\Delta\dot{y}$. Because B_{xx}, B_{xy}, B_{yx} and B_{yy} in themselves are functions of velocity, due to the change in cavitation boundary, it is necessary to iterate a number of times until the right hand side becomes sufficiently small and thereby satisfies eq. (2-101).

With $\dot{x}$ and $\dot{y}$ determined at time t, the next journal center position is:

$$x(t+\Delta t) = x(t) + \Delta t \cdot \dot{x}(t) \qquad y(t+\Delta t) = y(t) + \Delta t \cdot \dot{y}(t) \tag{2-105}$$

after which the procedure is repeated.

F_x, F_y and the four damping coefficients are computed by interpolation from stored pressure field data. These data assume that the bearing geometry is axisymmetric such that the only parameter is the eccentricity e as illustrated in Figure 2-5.

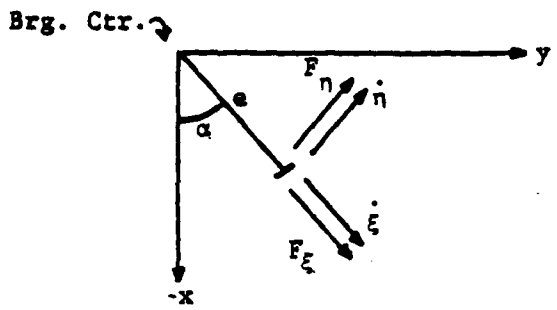

Figure 2-5 Forces in ξη Coordinate System

Hence, the stored data refers to the ξη coordinate system, and can be used to compute F_ξ, F_η and the 4 associated damping coefficients $B_{\xi\xi}$, $B_{\xi\eta}$, $B_{\eta\xi}$ and $B_{\eta\eta}$. To transform back into the fixed x-y-system it is seen that:

$$e = \sqrt{x^2 + y^2} \qquad \cos\alpha = \frac{x}{e} \qquad \sin\alpha = \frac{y}{e} \tag{2-106}$$

and:

$$\begin{aligned} F_x &= F_\xi \cos\alpha - F_\eta \sin\alpha & \dot{F}_y &= F_\xi \sin\alpha + F_\eta \cos\alpha \\ \dot{\xi} &= \dot{x}\cos\alpha + \dot{y}\sin\alpha & \dot{\eta} &= -\dot{x}\sin\alpha + \dot{y}\cos\alpha \end{aligned} \tag{2-107}$$

while the coefficients transform as:

$$\begin{aligned} B_{xx} &= B_{\xi\xi}\cos^2\alpha + B_{\eta\eta}\sin^2\alpha - (B_{\xi\eta} + B_{\eta\xi})\cos\alpha\cdot\sin\alpha \\ B_{xy} &= B_{\xi\eta}\cos^2\alpha - B_{\eta\xi}\sin^2\alpha + (B_{\xi\xi} - B_{\eta\eta})\cos\alpha\cdot\sin\alpha \\ B_{yx} &= B_{\eta\xi}\cos^2\alpha - B_{\xi\eta}\sin^2\alpha + (B_{\xi\xi} - B_{\eta\eta})\cos\alpha\cdot\sin\alpha \\ B_{yy} &= B_{\eta\eta}\cos^2\alpha + B_{\xi\xi}\sin^2\alpha + (B_{\xi\eta} + B_{\eta\xi})\cos\alpha\cdot\sin\alpha \end{aligned} \tag{2-108}$$

2.6 Static Jump

2.6.1 Analysis Using Short Bearing Approximation, Rigid Rotor

Static jump is a condition wherein, for a given set of conditions, a damper journal may have more than one stable orbit. In fact as many as three possible orbits may exist: a "whirl orbit" with large eccentricity, an "inverted orbit" with small eccentricity, or an intermediate orbit which is not stable and degenerates into one or the other of the first two. The shift from one steady-state orbit to the other is discontinuous, hence the use of the term "static jump" to describe the change between states. White, in Reference (2) performed an analysis of static jump in which he used the "short bearing" approximation for the squeeze film and certain force relationships to derive charts or jump "maps". The procedure described below is similar to White's but extends the analysis to finite length dampers with parallel springs and rotor flexibility.

The first problem to be addressed is to develop the conditions for equilibrium (i.e., a stable orbit) for a whirling damper executing a circular orbit to support a rigid rotor whose mass center is eccentric from the geometric center of the damper by a distance αc, where c is the damper radial clearance and α is a nondimensional unbalance parameter. Figure 2-6 shows the various quantities involved in the analysis and in particular 3 points: the center of the damper clearance circle, the damper geometric center and the mass center of the rotor. The distance between the mass center and the geometric center of the damper is defined by the unbalance parameter α and remains fixed for a particular equilibrium analysis. If the angular velocity of the rotor is ω, a synchronous whirl orbit, also with frequency ω, will be developed.

As shown by Figure 2-6 two distances define the orbit which is developed. The first is the distance from the center of the clearance circle to the geometric center of the damper. This distance is expressed as the product

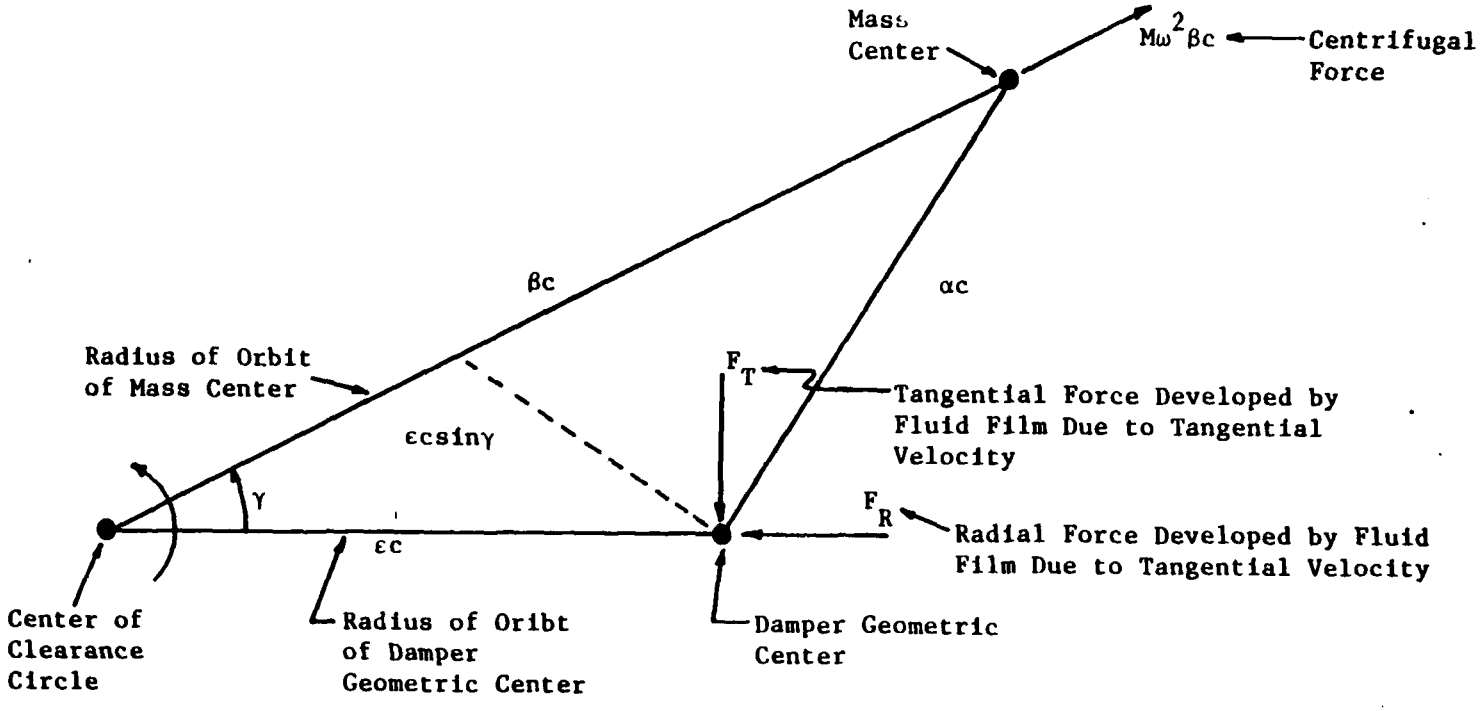

Figure 2-6 Equilibrium Geometry for Whirling Damper Supporting a Rigid Rotor with Mass Center Eccentric from Geometric Center by Distance αc

of ε and c, where ε is a nondimensional orbit circle radius and c is the radial clearance of the damper. The second is the distance from the center of the clearance circle to the center of mass. This distance is expressed as the product of β and c, where β is a nondimensional mass center orbit radius.

To quantify the severity of whirling vibration exhibited by this unbalanced rotor in a particular squeeze film damper, the problem, mathematically, is to find ε for a specified value of the mass M and the mass eccentricity αc. To keep the development as general as possible, nondimensional parameters will be used. These are:

- The nondimensional unbalance parameter α
- A nondimensional speed or mass parameter $\sigma = M\omega c^3/(\mu RL^3)$

The significance of these parameters will become clearer as analysis is developed. Ideally we will develop charts from which ε can be directly read when values of α and σ are specified. Unfortunately, because of the nature of the equations involved, the equilibrium analysis cannot proceed directly. Specifically, to avoid any need for iteration, it is necessary to seek, from the equations, values of σ which correspond to given values of α and ε. Of course, once a table of matching values of α, ε and σ is established it matters little how the values were arrived at, and the desired charts can be directly created from the tables.

In this analysis, equilibrium requires that the centrifugal force $M\omega^2\beta c$ acting on the rotor mass is equal to the fluid film force F acting on the damper:

$$M\omega^2\beta c = F \tag{2-109}$$

So recalling the definition of σ,

$$\sigma = \frac{Fc^2}{\omega\mu RL^3} \cdot \frac{1}{\beta}, \tag{2-110}$$

and if, given α and ε, we find β and F, the problem is solved. The total fluid-film force F is related to its components as follows:

$$F = \sqrt{F_R^2 + F_T^2} \tag{2-111}$$

and, the fluid-film analysis based on short bearing assumptions and the π or half-film treatment of film rupture gives the following expressions for F_R and F_T in terms of ε and the damper geometry parameters and frequency (for circular orbit whirl):

$$\frac{F_R C^2}{\mu R L^3 \omega} = 2\varepsilon^2/(1-\varepsilon^2)^2 \tag{2-112}$$

$$\frac{F_T C^2}{\mu R L^3 \omega} = \pi \varepsilon/(2(1-\varepsilon^2)^{3/2}) \tag{2-113}$$

An inspection of the geometry of equilibrium shown in Figure 2-6 gives relationships between fluid film components and the load angle γ:

$$\frac{F_T}{F_R} = \tan \gamma \tag{2-114}$$

and the triangle whose sides are αc, βc and εc gives the quadratic relationship for β:

$$\beta = \varepsilon \cos \gamma \pm (\alpha^2 - \varepsilon^2 \sin^2 \gamma)^{1/2} \tag{2-115}$$

With the above equations, the mass parameter σ can be calculated from given values of eccentricity ratio ε or unbalance parameter α using the following scheme:

Step Number	Value Assumed or Resulting from Previous Step	Calculate	Using Equation
1	ε	$(F_T, F_r)\ \frac{C^2}{\mu R L^3 \omega}$	(2-112) and (2-113)
2	(F_T, F_R)	δ	(2-114)
3	(F_T, F_R)	$\frac{Fc^2}{\mu R L^3 \omega}$	(2-111)
4	$(\varepsilon, \alpha, \gamma)$	β	(2-115)
5	$(\beta, \frac{Fc^2}{\mu R L^3 \omega})$	σ	(2-110)

As intended, this procedure yields sets of values of α, σ and ε from which charts can be prepared. It should be noted that, for certain combinations of the mass or speed parameter σ, and the unbalance parameter α, more than one equilibrium value of orbit radius ε exists and, in fact, as many as three can exist, as explained at the beginning of this section.

2.6.2 Coupling to the Finite Length Damper Program, Including Shaft Flexibility and Parallel Springs

The squeeze film damper analysis program calculates and stores tables of direct ($\bar{B}_{xx}$) and cross coupled ($\bar{B}_{xy}$) circular orbit damping coefficients as functions of eccentricity ratio. The coefficients are in nondimensional form, specifically:

$$\bar{B}_{xx} = \frac{B_{xx}}{\mu R(L/c)^3} \tag{2-116a}$$

$$\bar{B}_{xy} = \frac{B_{xy}}{\mu R(L/c)^3} \tag{2-116b}$$

The interfacing to the program is done by interpolating in the tables for the $\bar{B}_{xx}$ and $\bar{B}_{xy}$ values corresponding to the eccentricity value of interest. Nondimensional forces are then calculated using the equations:

$$f_t(\varepsilon) = \bar{B}_{xx}\varepsilon \tag{2-117a}$$

$$f_r(\varepsilon) = \bar{B}_{xy}\varepsilon \tag{2-117b}$$

The forces can now be used in an equilibrium analysis which incorporates shaft (or bearing) flexibility in series with the squeeze film. The flexible element is assumed to be light and can be envisioned as a bearing which carries a rigid rotor or a simple, Jeffcott-type rotor on stiff bearings. Figure 2-7 is an equilibrium diagram showing the modification to the mass center location caused by a flexible element of stiffness K_s in series with the damper. If we define f from Equation (2-117) to be

$$f(\varepsilon) = \sqrt{f_r^2 + f_t^2} \tag{2-118}$$

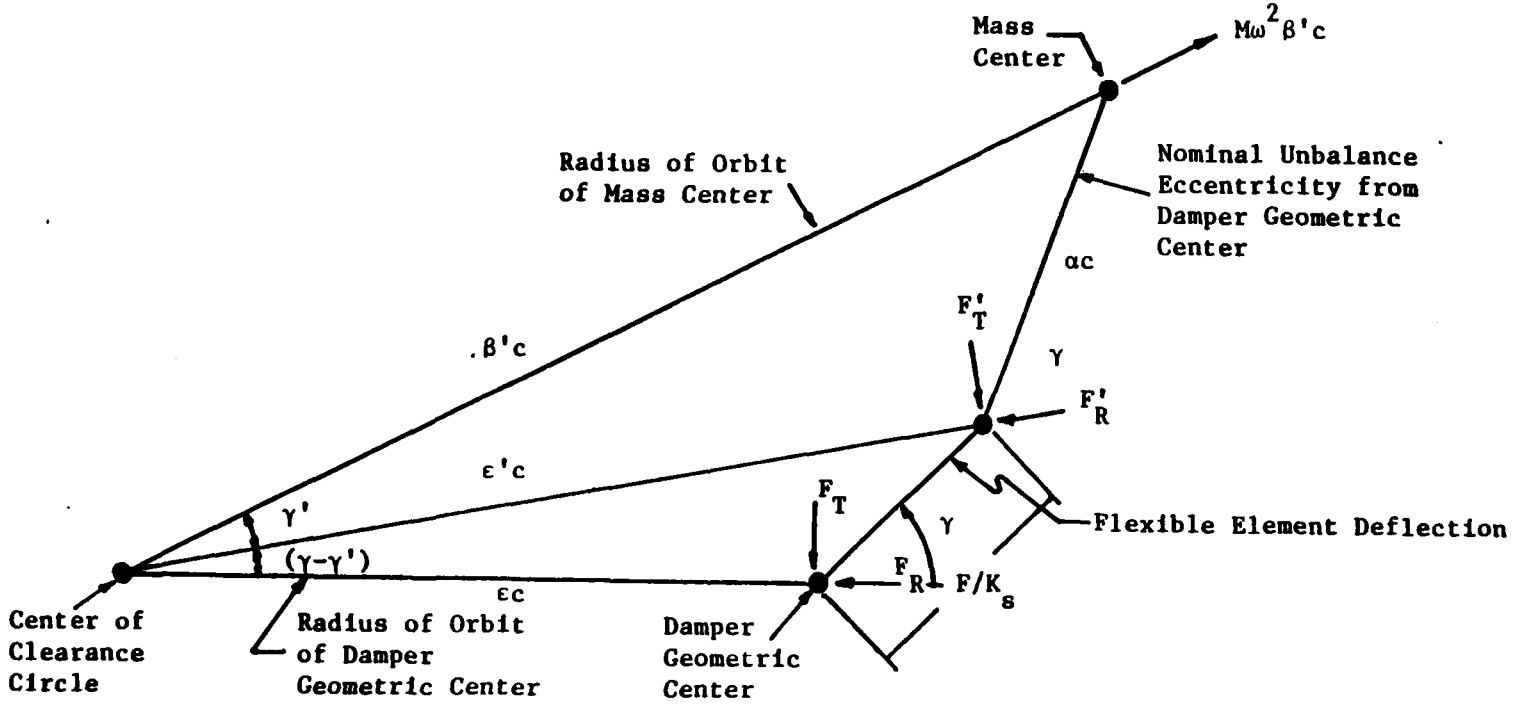

Figure 2-7 Damper Rotor Equilibrium for Case of a Flexible Element in Series with the Damper

then forces F_R, F_T and F are:

$$F_T = f_t(\varepsilon)\ \omega\mu RL^3/C^2 \tag{2-119a}$$

$$F_R = f_r(\varepsilon)\ \omega\mu RL^3/C^2 \tag{2-119b}$$

$$F = f(\varepsilon)\ \omega\mu RL^3/C^2 \tag{2-119c}$$

From geometry (cosine rule) we get,

$$(\varepsilon')^2 = \varepsilon^2 + \left(\frac{F}{K_s C}\right)^2 + 2\,\frac{\varepsilon F}{K_s C}\cos\gamma \tag{2-120}$$

and from the sine rule we have:

$$\sin\gamma' = \frac{\varepsilon \sin\gamma}{\varepsilon'} \tag{2-121}$$

From equation (2-119c) we get

$$\frac{F}{CK_s} = \frac{f\omega\mu RL^3}{C^2}\,\frac{1}{CK_s} \tag{2-122}$$

and a parameter Ψ_s for shaft flexibility can be defined as

$$\Psi_s = \frac{\omega\mu R}{K_s}\left(\frac{L}{C}\right)^3 \tag{2-123}$$

therefore

$$\frac{F}{CK_s} = f\ \Psi_s \tag{2-124}$$

The effect of springs, such as flexures, in parallel with the damper film can also be modelled by defining a parallel spring flexibility parameter similar to Equation (2-123):

$$\Psi_f = \frac{\omega\mu R}{K_f}\left(\frac{L}{C}\right)^3 \tag{2-124}$$

where K_f is the parallel spring stiffness. The radial force f_r must then be modified to account for this additional force

$$f_r = f_r + \frac{\varepsilon}{\Psi_f} \tag{2-117c}$$

The equilibrium computation then proceeds as follows: a value of ε is assumed and values of γ, f_r, f_t and f are calculated using

$$\gamma = \tan^{-1}\left(\frac{f_t}{f_r}\right) \tag{2-125}$$

and Equations (2-117) and (2-118). The modified eccentricity ratio ε' is found from Equation (2-120), γ' is calculated from Equation (2-121), rewritten as

$$\gamma' = \sin^{-1}\left(\frac{\varepsilon \sin\gamma}{\varepsilon'}\right) \tag{2-121a}$$

and force components F_R and F_T are extracted from Equation (2-119). Now the inertia force applied to the mass must equal the fluid film force (as modified by series and/or parallel stiffnesses):

$$F_T' = F_T \cos(\gamma-\gamma') - F_R \sin(\gamma-\gamma') \tag{2-126a}$$

$$F_R' = F_R \cos(\gamma-\gamma') + F_T \sin(\gamma-\gamma') \tag{2-126b}$$

and similarly

$$f_t' = f_t \cos(\gamma-\gamma') - f_r \sin(\gamma-\gamma') \tag{2-127a}$$

$$f_r' = f_r \cos(\gamma-\gamma') + f_t \sin(\gamma-\gamma') \tag{2-127b}$$

$$f' = \left[(f_r)^2 + (f_t)^2\right]^{1/2} \tag{2-127c}$$

From Equation (2-115), 2 values of β (β_1 and β_2) can be found to be:

$$\beta'_{1,2} = \varepsilon' \cos\gamma' \pm \left[(\alpha)^2 - (\varepsilon' \sin\gamma')^2\right]^{1/2} \tag{2-128}$$

The new equilibrium requires that inertial and fluid film forces balance, so that:

$$M\omega^2 c\beta' = F' \tag{2-129}$$

or

$$F' = \frac{\sigma'\omega\mu RL^3\beta'_{1,2}}{c^2} \tag{2-130}$$

so that the condition is

$$\sigma' \beta' = f' \tag{2-131}$$

We therefore get two values for the nondimensional speed or mass parameter σ:

$$\sigma_1 = \frac{f'}{\beta_1'} \tag{2-132a}$$

$$\sigma_2 = \frac{f'}{\beta_2'} \tag{2-132b}$$

Therefore for given values of the displacement parameter (or eccentricity ratio) ε and mass eccentricity parameter α we can find equilibrium solutions, if they exist, for the speed/mass parameter σ. These values can be plotted to generate a "jump map" of the type shown in Figure (2-8), which is an example using short bearing analysis, where it was assumed that the shaft was infinitely flexible ($\Psi_s = 0$) and the flexures were infinitely rigid ($\Psi_f = \infty$).

The above equations have been programmed and samples of the input and output are given in Section III of this report. An additional quantity calculated by the program is transmissibility

$$T = \frac{f}{\sigma\alpha} \tag{2-133}$$

which is often of interest, especially when force transmitted to pedestals is of concern.

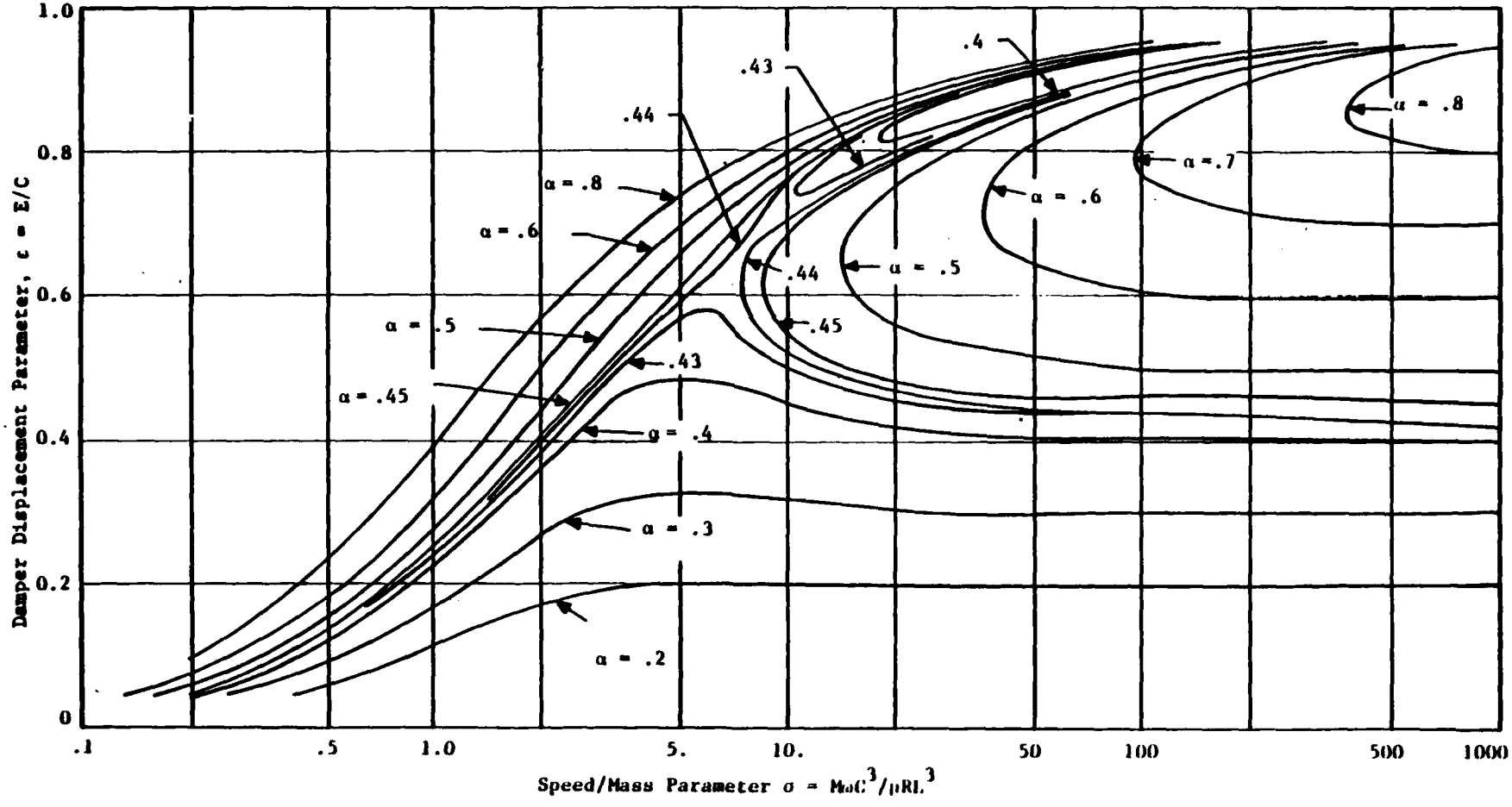

Figure 2-8 Map of Displacement Parameter Versus Speed/Mass Parameter for Different Values of Mass Eccentricity Parameter (α)

791766

SECTION III

DAMPER ANALYSIS COMPUTER PROGRAMS

The squeeze film damper analysis described in Section II of this report has been implemented in the form of a series of computer programs. These programs are linked by data files to form an interlocking set of tools for generation and display of damper performance data, and to provide an interface with rotordynamics system analysis programs.

In this section, the individual programs will be described as they would be used in the context of a damper component design analysis system. In addition, examples of program input and output will be presented which exercise major program options.

Program Descriptions

A total of eight computer programs have been written to generate and process squeeze film damper data. These programs are listed in Table 3-1.

Table 3-1

Squeeze Film Damper Analysis Programs

1. SQZDMP
2. JUMP
3. DIMOUT
4. INTERP
5. CIRCULAR ORBIT GRAPHICS
6. POST
7. NON-CIRCULAR ORBIT GRAPHICS
8. INTERFACE

Figure 3-1 illustrates the interaction and flow of data between programs. Program SQZDMP joins the analytical base and must be run initially in all cases to generate the appropriate data file(s) through the solution of the Reynolds equation. The files generated can then be accessed as shown in Figure 3-1 by any of the seven post processing routines. Each individual

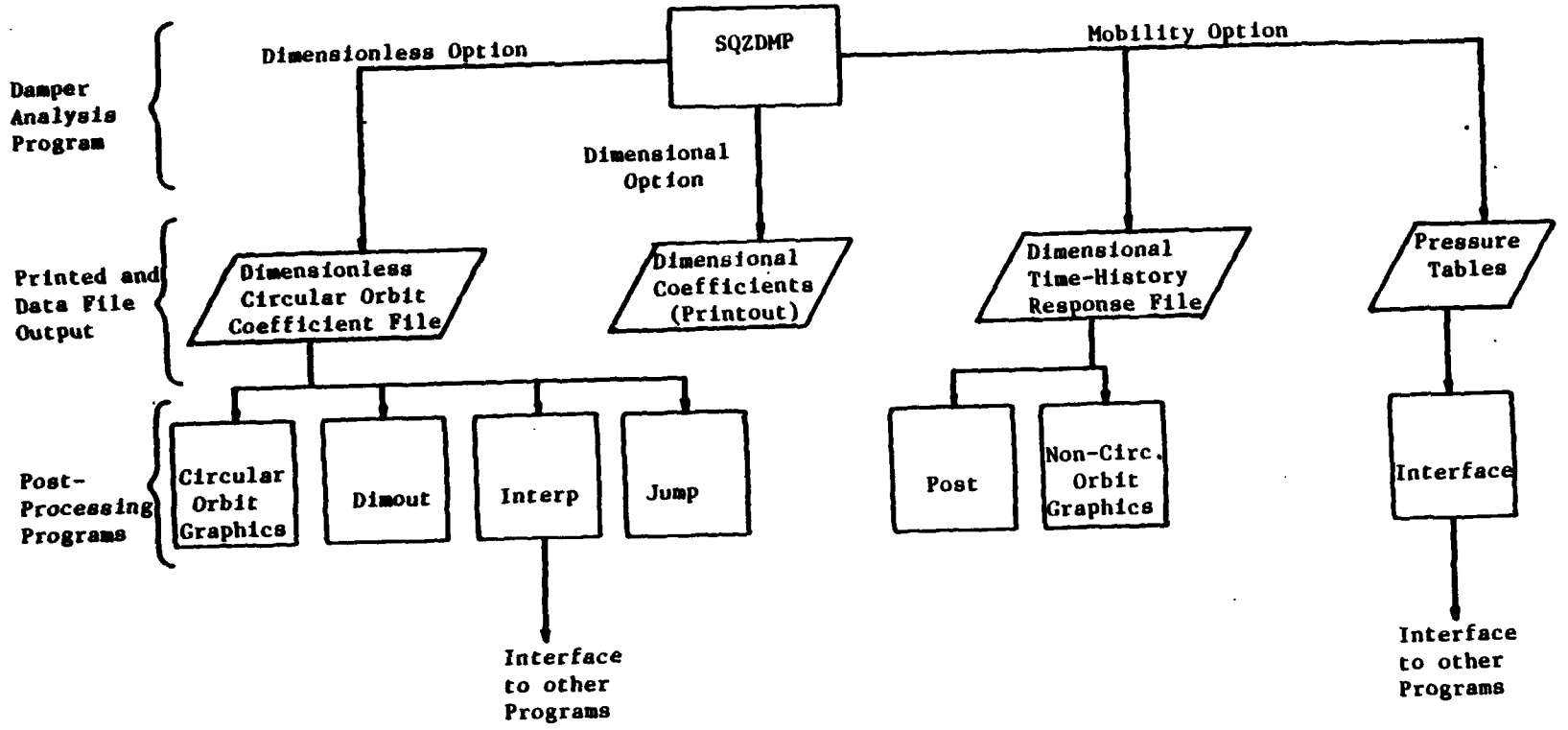

Figure 3-1 Squeeze Film Damper Analysis Program

program will now be described in functional grouping according to the SQZDMP option chosen, either dimensionless, dimensional, or mobility.

a. Dimensionless Circular Orbit Calculations

This option involves the exercise of as many as five programs and is intended for use as a design tool wherein the effects on performance of a variety of damper parameters can be conveniently determined. The damper is assumed to be executing a centered, circular orbit at a user-specified range of eccentricities.

It is important to note that by performing the initial calculations in dimensionless form, basic damper trends may be examined. For example, damper clearance, oil viscosity and/or supply pressure may be varied conveniently to determine their effects on damper performance for a given damper geometry without having to repeat the damper fluid-film solution sequence for every such variation. Dimensionless files also provide an efficient way to supply data for programs performing dynamics calculations (such as nonlinear steady-state damped response).

SQZDMP, regardless of the option chosen, requires as input a definition of damper geometry, which consists of the feeding and sealing arrangement and the finite difference mesh used for calculations, the leakage and flow coefficients and the necessary program control parameters. The dimensionless circular orbit option in particular requires the L/D ratio, nondimensional supply and cavitation pressures and a series (up to 12) of values for journal center eccentricity and angular location with respect to the coordinate axes (in order, for example, to locate the journal center with respect to a feed or drain hole). The result of the calculation is a table of dimensionless circular orbit coefficients which is also suitable for use in a design chart. This information includes:

- dimensionless damping
- dimensionless inertia
- dimensionless flow in/out

- dimensionless pressure distribution (optional)

and is put out in the form of printed tables or a data file to be accessed automatically by other programs.

CIRCULAR ORBIT GRAPHICS generates plots of the nondimensional SQZDMP - generated damping and inertia coefficients as functions of eccentricity ratio. This allows for convenient checking of the calculations and for their use as design charts. Input quantities are the tables of dimensionless coefficients produced by SQZDMP and the appropriate plotting control variables. Program output consists of plots of damping or inertia coefficients (direct or cross-coupled) as functions of eccentricity ratio.

DIMOUT uses as input the nondimensional circular orbit coefficient tables generated by SQZDMP and dimensionalizes them using a set of user-input damper dimensions. Thus a single nondimensional file may be used to represent a range of dampers (of similar configuration but different sizes, etc.) during a design exercise without having to rerun the analysis program repeatedly.

INTERP accepts the dimensionless data generated by SQZDMP along with supply pressures or eccentricity ratios and provides as output dimensionless circular orbit coefficient tables. The program uses an interpolation scheme so that coefficient values may be provided which are in between those in the input tables. INTERP can also be used to couple a damper model with a rotordynamics computer program. For example, a nonlinear steady-state response program can extract successive values of damping coefficients as it iterates on response amplitude by using INTERP to access the appropriate nondimensional data files and interpolate to find the correct coefficients for a given damper circular orbit eccentricity.

JUMP uses as input a dimensionless circular orbit coefficient file produced by SQZDMP along with parameters which describe damper displacement, mass eccentricity and shaft flexibility and parallel spring stiffness if present. The program output is a series of tables which relate the damper orbit circle radius and mass eccentricity with a third parameter representing

nondimensional speed or mass. These results are plotted manually to form "jump maps" which reveal regions where the damper may be bistable, that is have two possible orbit radii at which stable operation is possible.

b. Dimensional Calculations

Calculations for a squeeze film damper can also be performed based on a specific set of user supplied damper dimensions and operating conditions. Data file output is not provided for this option since it is designed for evaluations of individual dampers rather than to study variations of a design. With this calculation the damper journal position and velocity are specified for each eccentricity by the user. Therefore circular orbit conditions can be simulated as well as individual points on an arbitrary noncircular orbit, for which instantaneous values of damping and inertia coefficients (valid for those points only) are provided.

SQZDMP (Dimensional Option) is the only program which is run under this option. In addition to the standard set of input data described previously, it requires the damper dimensions, a reference operating frequency, viscosity and density of the damper fluid, dimensional supply and cavitation pressures and the location and velocity of the damper journal. The output includes instantaneous values of force and local damping coefficient, circular orbit damping and inertia coefficients, power loss and pressure distributions and is available, as noted above, as a printout only.

c. Mobility Calculations

Up to this point, calculations have been described which are either steady-state (circular orbit) or quasi-static (calculations for a given journal position and velocity vector). However, it is also necessary to be able to calculate damper behavior in response to an arbitrary load history. This must be a time-transient calculation since the forces on the damper can include both steady and time-varying components and the inherent nonlinearity of the damper causes it's response to depend heavily on the damper journal's

position and velocity vector. To increase the efficiency of the calculation the mobility method, described in Section 2.5, is used. This method avoids the necessity of re-solving the Reynolds equations for every time step by basing damper response on nondimensional pressure tables which have been precalculated by SQZDMP. Thus, a laborious equation solution scheme has been replaced by a much simpler table - lookup procedure.

A total of four programs may be exercised under this option. Post-processing involves both damper response analysis and also linkup of the pressure tables to an external rotordynamics program (user-supplied) for system time-transient calculations.

SQZDMP (Mobility Option), which performs dimensional calculations only, requires the same input quantities as the dimensional program option, except that the journal center coordinates are read in as a set (12 maximum) to produce the pressure tables corresponding the journal eccentricity points for unit X and Y velocities. The pressure tables may be used in two ways. First, they can be used in the calculation of damper force during time transient analyses using a rotordynamics program, and secondly they can be used for rigid-rotor time transient analysis using a built-in mobility-based calculation scheme. For the latter calculation, a load history must be specified along with a convergence error and maximum iteration number. The program will then use the mobility method to compute, in printed table and data file form, a response time history consisting of force, displacement and velocity as functions of time, based on the pressure tables generated, and input parameters describing the applied load.

POST calculates the following:

1. Effective stiffness and damping based on the time-transient, noncircular orbit calculation results.

2. Frequency spectra of relevant quantities (e.g. displacement) to determine synchronous and non-synchronous content.

Results are presented in tabular form.

NON-CIRCULAR ORBIT GRAPHICS displays plots of the time-transient mobility method calculation. It can display:

- hysteresis loops
- displacement or force as a function of time
- journal orbits (X vs Y amplitude)
- frequency spectra of calculated waveforms.

INTERFACE couples the pressure tables generated by the mobility option of SQZDMP with an external rotordynamics program (e.g. a time-transient analysis program). Journal velocity and displacement information is given to INTERFACE, which then returns the corresponding damping and inertia coefficients.

2. Sample Input/Output

Figure 3-2 is an expanded version of Figure 3-1 and shows in more detail the interaction of the damper analysis programs and their individual input requirements and output quantities. The programs themselves are shown in heavily outlined boxes, required input quantities in lightly outlined boxes and program output quantities are shown in parallelograms. Solid lines denote data flow through a given program and broken lines show data transfer by file.

To illustrate program input/output, an example case for an end groove feed/end groove drain damper was prepared. This damper geometry is shown schematically in Figure 3-3 along with the relevant dimensions and operating parameters. The balance of Section 3.2 shows calculations made for this damper using dimensionless, dimensional and mobility options.

a. Dimensional Calculations

The damper configuration described in Figure 3-3 was first analyzed using the dimensional input option to SQZDMP. This is highlighted in Figure 3-4, which has been extracted from Figure 3-2 and illustrates the flow of information for this option.

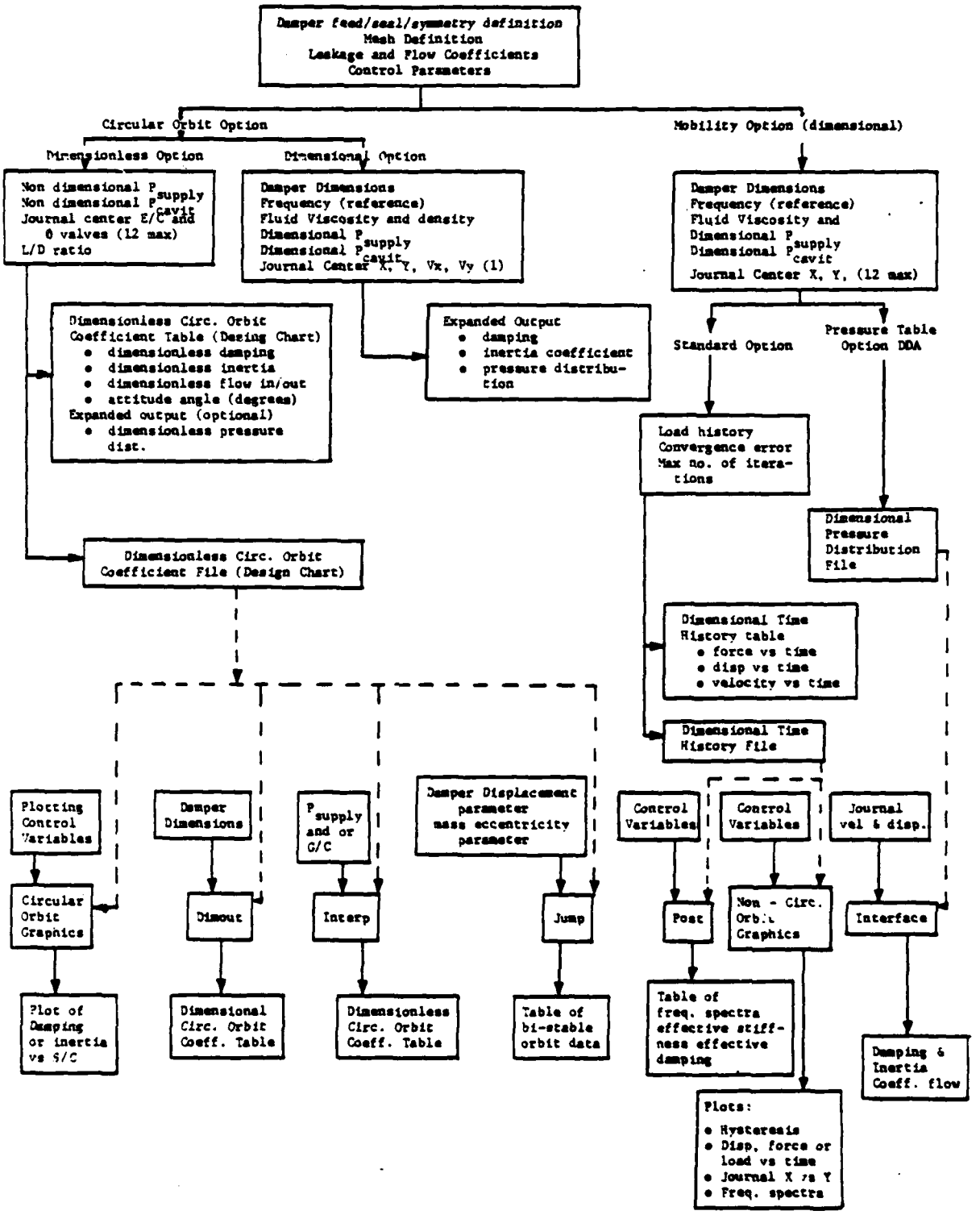

Figure 3-2 Damper Analysis and Post-Processing Program Interaction

END GROOVE FEED/DRAIN DAMPER

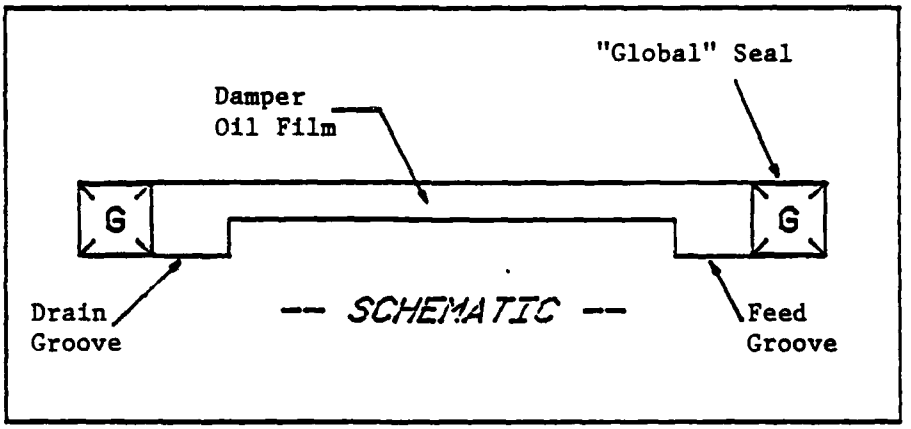

PARAMETERS

Length	=	1.0 in
Diameter	=	5.0 in
Radial Clearance	=	.008 in
Fluid Viscosity	=	1.0×10^{-6} lbs-sec/in^2
Fluid Density	=	7.9×10^{-5} lbs-sec^2/in^4
Frequency	=	133.33 Hz (8,000 RPM)
Feed Groove Pressure	=	20 psig
Cavitation Pressure	=	14.7 psig
Journal Coordinates	=	X = 0.004 in Y = 0
Journal Velocities	=	V_x = 0 V_y = 3.35 in/sec
Seal Flow Coefficient	=	2.0

Figure 3-3 Sample Problem for Exercising Damper Software

SQZDMP

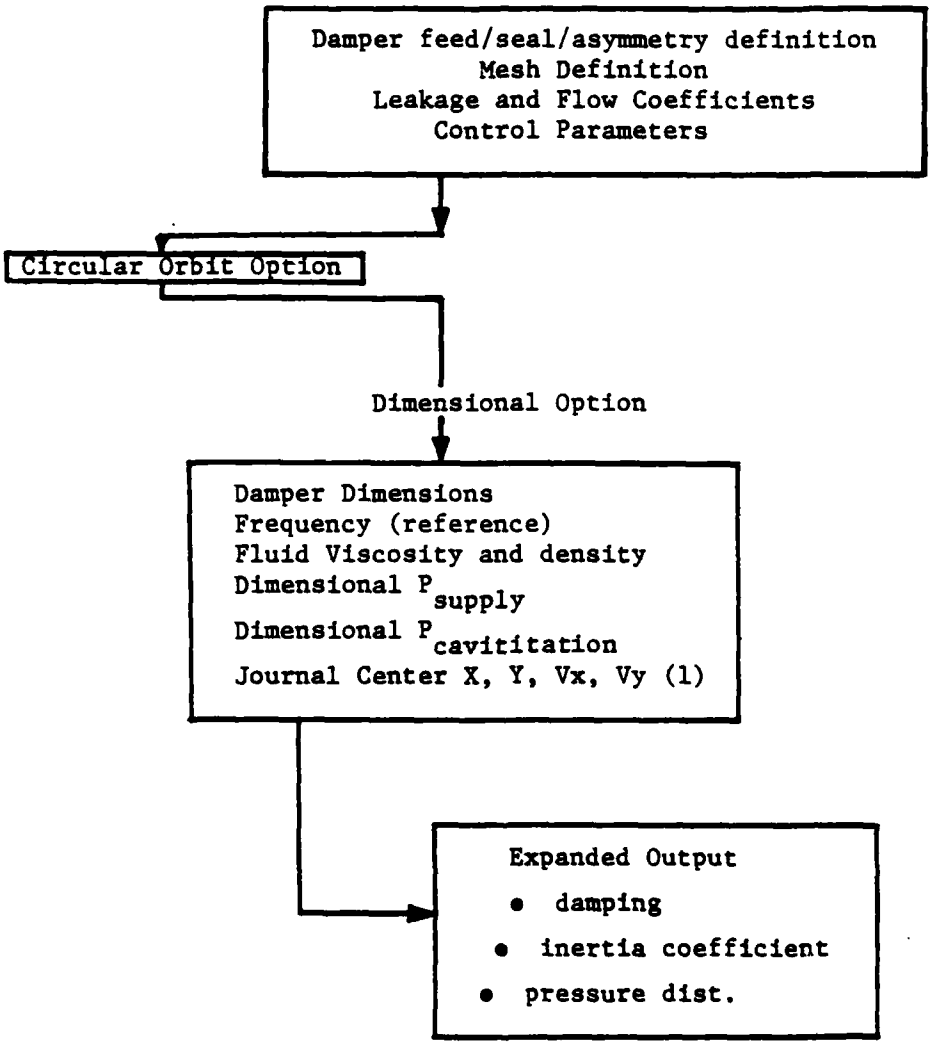

Figure 3-4 Dimensional Calculation Flowchart

Output from the dimensional calculation includes:

- Damper forces
- Instantaneous damping coefficients (for the specified journal position and velocity)
- Instantaneous power loss
- Tondl coefficients
- Circular orbit damping coefficients
- Circular orbit inertia coefficients
- Flows into/out of damper
- Pressure distribution.

Table 3-2 shows the complete input and output for a dimensional calculation using the damper geometry and operating parameters from Figure 3-3 as input quantities.

b. Dimensionless Calculations

The next analysis to be performed exercises the dimensionless option of SQZDMP and key post-processing programs. The flow of information for this option is shown in Figure 3-5 (again, a subset of Figure 3-2). The damper to be analyzed is, as before, that described in Figure 3-3 but because of the nature of the calculations nondimensionalization of some input parameters was required and a series of eccentricity ratios was specified (as opposed to a single eccentricity for the dimensional case). The new parameters are:

L/D ratio	=	0.2
Supply pressure	=	0.02122
Cavitation pressure	=	-0.0156
Journal center coordinates (12 values)	X =	.00001,.1,.2,.3,.4,.5,.6,.7,.8,.9,.95,.99
	Y =	0.0 (all values)

From this input data, SQZDMP generates an "echo print" of the input data, a series of 12 tables (one for each eccentricity) of nondimensional pressure distributions and a summary table of dimensionless circular orbit coefficients. Table 3-3a shows the input data printout and a representative

```
INPUT DATA LISTING
PROGRAM   PN812                    01/07/82  13:33:29


 USE THIS FORM IF (NXY.GT.0) *** BEARING HAS END-SEALS WITHOUT GROOVES
**********************************************************************
 CARD1                          TITLE
 CASE 1 - SEALED DAMPER : DIMENSIONAL OPTION  1/7/82  F.GILLHAM
----------------------------------------------------------------------
 CARD2      INTEGER CONTROLS
  M N   NDIM  INERT  NXY   INP  IUNITS  ICIRC  MCONST
   24  9  0    1      1     1     0       0      1
----------------------------------------------------------------------
 CARD3B       BEARING DIMENSIONS                    *SUBMIT IF NDIM.GE.0*
  DIAM  BLG  CLRC  VISC  DENS  FREQ
  5.0  1.0  .008 1.0000E-6 7.90E-5  133.33
----------------------------------------------------------------------
 CARD4        BEARING DESCRIPTION  OPTIONS
  MSL MFD MHF MFS
   1   0   1   1
----------------------------------------------------------------------
 CARD6A  X-COORDINATES OF JOURNAL CENTER
TXZ  VALUES      (IF ICIRC =1, SUBMIT ECCENTRICITY RATIOS)
.004
----------------------------------------------------------------------
 CARD6B  Y-COORDINATE OF JOURNAL CENTER
TYZ  VALUES       (IF ICIRC =1, SUBMIT ATTITUDE ANGLE IN DEGREES)
 0.0
----------------------------------------------------------------------
  CARD7                          (SUBMIT IF MSL=1)
  MFD       MVL
   0         1


----------------------------------------------------------------------
  CARD 9
  CGL1    CGL2
  2.00    2.00


----------------------------------------------------------------------
 CARD12   VELOCITY AND PRESSURE VALUES
      XV       YV       PSP       PCV
   0.  3.35     20.00      -14.7
----------------------------------------------------------------------
```

Table 3-2a

Input Data Listing for Dimensional SQZDMP Run

CASE 1 - SEALED DAMPER : DIMENSIONAL OPTION 1/7/82 F.GILLHAM 01/07/82

********** INTEGER CONTROLS **********

NUMBER OF FINITE DIFFERENCE INCREMENTS IN THE CIRCUMFERENTIAL DIRECTION , (M)	24
NUMBER OF FINITE DIFFERENCE INCREMENTS IN THE AXIAL DIRECTION , (N)	9
INPUT AND OUTPUT DATA ARE IN TRUE CONSISTENT UNITS , (NDIM)	0
INERTIA COEFFICIENTS WILL BE COMPUTED , (INERT)	1
PARAMETRIC STUDY OF THE SQUEEZE FILM DAMPER WILL BE PERFORMED , NUMBER OF ECCENTRICITIES ,(NXY)	1
ONE OR MORE COMPLETE SETS OF INPUT WILL BE SUBMITTED; PROGRAM WILL TERMINATE WITH END OF FILE ,(INP)	1
PRINTED OUTPUT WILL BE LABELLED IN ENGLISH UNITS , (IUNITS)	0
CIRCULAR ORBIT OPTION; COORDINATES OF THE JOURNAL CENTER WILL BE SUBMITTED , (ICIRC)	0
MESH SIZE WILL BE HELD CONSTANT; THE VALUE OF M WILL NOT BE ADJUSTED INTERNALLY , (MCONST)	1

******** BEARING DIMENSIONS *********

DIAMETER (INCH)	LENGTH (INCH)	RAD.CLEARANCE (INCH)	VISCOSITY (LBF-SEC/IN**2)	DENSITY (LBF-SEC**2/IN**4)	FREQUENCY (HZ)
5.0000000D+00	1.0000000D+00	8.0000000D-03	1.0000000D-06	7.9000000D-05	1.3333000D+02

BEARING DESCRIPTION	OPTIONS MSL	MFD	MHF
THE BEARING HAS SEALED GROOVE AT ONE END; AND FEEDING GROOVE AT THE OTHER END.	1	0	1

Table 3-2b

Program Control Parameters for Dimensional SQZDMP Run

```
COORDINATES OF JOURNAL CENTER (INCH)= (  4.0000D-03,  0.0        )
        BEARING IS ASYMMETRIC                    END SEAL WITH GROOVE

     CIRCUMFERENTIAL GROOVE,PRESSURE= 2.0000000D+01 LBF/IN**2

  GROOVE AT I= 0     FLOW COEFF.= 2.000000D+00     GROOVE PRESSURE= 1.830497D+01 LBF/IN**2
```

JOURNAL CENTER COORDINATES X (INCH)	Y (INCH)	VELOCITIES V-X (IN/SEC)	V-Y (IN/SEC)	FORCES F-X (LBF)	F-Y (LBF)	INSTANTANEOUS DAMPING COEFFICIENTS AT SPECIFIED JOURNAL POSITION BXX (LB-SEC/IN)	BXY (LB-SEC/IN)	BYX (LB-SEC/IN)	BYY (LB-SEC/IN)	CAVITATION PRESSURE (GAUGE PRESSURE) P (LB-IN**2)
4.00D-03	0.0	0.0	3.350D+00	8.511D-10	-7.551D+01	4.489D+01	3.751D-12	3.815D-12	2.254D+01	-1.470D+01

FTOTAL = 7.5512D+01

```
*** INSTANTANEOUS POWER LOSS IN DAMPER ***
     (LB-IN/SEC)              (HP)
       2.530D+02            3.833D-02
```

```
*** TONDL COEFFICIENTS ****
(LB-SEC)      (LB-SEC/IN)     (LB-SEC)      (LB-SEC/IN)
 TOC(1)        TOC(2)          TOC(3)        TOC(4)
7.0942D-11    UNDEFINED     6.2945D+00    UNDEFINED
```

```
**** DAMPING COEFFICIENTS ****
CIRCULAR ORBIT COEFF.,BXX=BYY(LB-SEC/IN)=  2.254104D+01    BXY=-BYX(LB-SEC/IN)=   -2.540494D-10
```

```
**** INERTIA COEFFICIENTS ****
          CXX                CXY                CYX                CYY
(LB-SEC**2/IN) (LB-SEC**2/IN) (LB-SEC**2/IN) (LB-SEC**2/IN)
     9.3512536D-03  4.2764578D-15  4.2951404D-15  8.1819734D-03
    CIRCULAR ORBIT INERTIA COEFFICIENTS,CXXP=CYYP(LB-SEC**2/IN)= 9.3512540-03
 CXYP=CYXP(LB-SEC**2/IN)=    4.2951400-15
```

```
**********  FLOWS  **********    ****** PRESSURES **********

 FLOW IN        FLOW OUT       SEAL FLOW      PRESS.I=0      PRESS.I=N
 (IN**3/SEC)    (IN**3/SEC)    (IN**3/SEC)    (LBF/IN**2     (LBF/IN**2)

 1.5620244D+00  1.5620244D+00  1.5620244D+00  1.8304973D+01  0.0
```

Table 3-2c

Program Output for Dimensional SQZDMP Run

TITLE: CASE 1 - SEALED DAMPER : DIMENSIONAL OPTION 1/7/82 F.GILLHAM DATE: 01/07/82

PRESSURE DISTRIBUTION

PRESSURES ARE IN UNITS OF LBF/IN**2

THETA (DEG.)	AXIAL DIVISION NUMBER 1	2	3	4	5	6	7	8	9
15.	1.830D+01	1.818D+01	1.814D+01	1.817D+01	1.828D+01	1.847D+01	1.873D+01	1.908D+01	1.950D+01
30.	1.830D+01	1.783D+01	1.751D+01	1.737D+01	1.739D+01	1.758D+01	1.793D+01	1.845D+01	1.914D+01
45.	1.830D+01	1.738D+01	1.672D+01	1.635D+01	1.626D+01	1.645D+01	1.692D+01	1.767D+01	1.869D+01
60.	1.830D+01	1.676D+01	1.565D+01	1.497D+01	1.473D+01	1.491D+01	1.554D+01	1.659D+01	1.808D+01
75.	1.830D+01	1.589D+01	1.412D+01	1.301D+01	1.255D+01	1.273D+01	1.357D+01	1.506D+01	1.721D+01
90.	1.830D+01	1.464D+01	1.194D+01	1.020D+01	9.428D+00	9.617D+00	1.077D+01	1.288D+01	1.596D+01
105.	1.830D+01	1.291D+01	8.922D+00	6.332D+00	5.132D+00	5.321D+00	6.897D+00	9.864D+00	1.423D+01
120.	1.830D+01	1.077D+01	5.203D+00	1.564D+00	-1.572D-01	3.109D-02	2.129D+00	6.144D+00	1.209D+01
135.	1.830D+01	8.818D+00	1.804D+00	-2.782D+00	-4.974D+00	-4.786D+00	-2.217D+00	2.746D+00	1.014D+01
150.	1.830D+01	8.527D+00	1.318D+00	-3.389D+00	-5.637D+00	-5.449D+00	-2.824D+00	2.260D+00	9.845D+00
165.	1.830D+01	1.178D+01	6.996D+00	3.899D+00	2.453D+00	2.641D+00	4.464D+00	7.937D+00	1.310D+01
180.	1.830D+01	1.849D+01	1.868D+01	1.887D+01	1.906D+01	1.925D+01	1.943D+01	1.962D+01	1.981D+01
195.	1.830D+01	2.521D+01	3.037D+01	3.384D+01	3.566D+01	3.585D+01	3.441D+01	3.131D+01	2.653D+01
210.	1.830D+01	2.846D+01	3.605D+01	4.113D+01	4.375D+01	4.394D+01	4.169D+01	3.699D+01	2.978D+01
225.	1.830D+01	2.817D+01	3.556D+01	4.052D+01	4.309D+01	4.328D+01	4.109D+01	3.650D+01	2.949D+01
240.	1.830D+01	2.621D+01	3.216D+01	3.618D+01	3.827D+01	3.846D+01	3.674D+01	3.310D+01	2.753D+01
255.	1.830D+01	2.408D+01	2.844D+01	3.141D+01	3.298D+01	3.317D+01	3.197D+01	2.938D+01	2.539D+01
270.	1.830D+01	2.235D+01	2.543D+01	2.754D+01	2.869D+01	2.888D+01	2.810D+01	2.637D+01	2.367D+01
285.	1.830D+01	2.110D+01	2.324D+01	2.473D+01	2.557D+01	2.576D+01	2.530D+01	2.418D+01	2.242D+01
300.	1.830D+01	2.022D+01	2.171D+01	2.277D+01	2.339D+01	2.358D+01	2.333D+01	2.266D+01	2.154D+01
315.	1.830D+01	1.961D+01	2.064D+01	2.139D+01	2.186D+01	2.204D+01	2.195D+01	2.158D+01	2.093D+01
330.	1.830D+01	1.916D+01	1.985D+01	2.037D+01	2.073D+01	2.092D+01	2.094D+01	2.079D+01	2.048D+01
345.	1.830D+01	1.881D+01	1.923D+01	1.957D+01	1.984D+01	2.003D+01	2.014D+01	2.017D+01	2.012D+01
360.	1.830D+01	1.849D+01	1.868D+01	1.887D+01	1.906D+01	1.925D+01	1.943D+01	1.962D+01	1.981D+01

** ELAPSED TIME FROM START TO BEGINNING OF TIME HISTORY **
4.4001D+00 CP SECONDS

** ELAPSED TIME FROM BEGINNING OF TIME HISTORY ***
7.5500D-03 CP SECONDS

Table 3-2d

Pressure Distribution for Dimensional SQZDMP Run

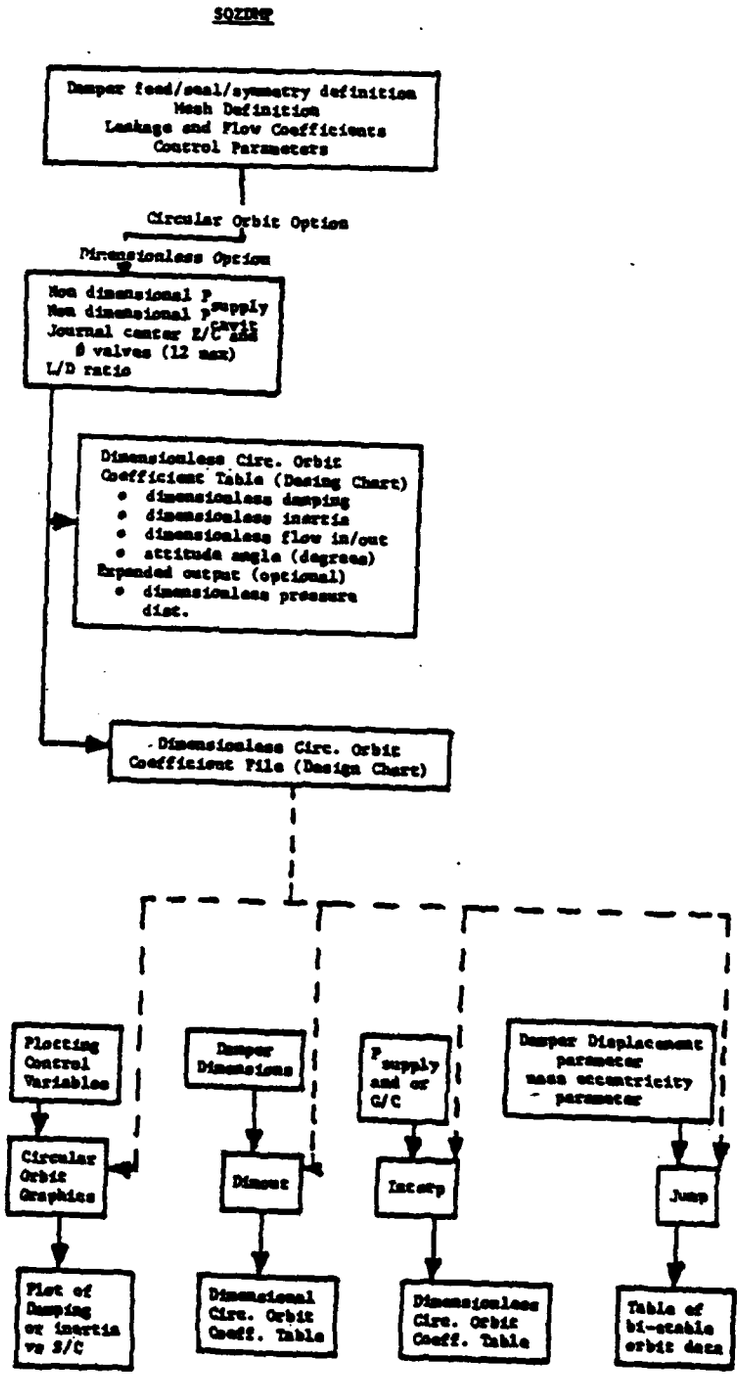

Figure 3-5 Dimensionless Calculation Flowchart

```
INPUT DATA LISTING
PROGRAM   PN812                    01/07/82  14:17:45


USE THIS FORM FOR DESIGN CHARTS OR PARAMETER STUDIES (NXY.GT.0)
**********************************************************************
CARD1                          TITLE
 CASE 2 - SEALED DAMPER - DIMENSIONLESS OPTION  1/7/82  F.GILLHAM   .
----------------------------------------------------------------------
CARD2      INTEGER CONTROLS
 M N   NDIM  INERT  NXY   INP  IUNITS  ICIRC  NCONST
 24 9    1     1    12     1     1       1      1
----------------------------------------------------------------------
CARD3A      BEARING DIMENSIONS: (LENGTH/DIAMETER)
 BLD
 .20
----------------------------------------------------------------------
CARD4       BEARING DESCRIPTION  OPTIONS
 NSL NFD NNF NFS
  1   0   1   1


----------------------------------------------------------------------
 CARD6A  X-COORDINATES OF JOURNAL CENTER
TXZ  VALUES      (IF ICIRC =1, SUBMIT ECCENTRICITY RATIOS)
.00001  .1  .2  .3  .4  .5  .6  .7  .8  .9  .95  .99
----------------------------------------------------------------------
 CARD6B  Y-COORDINATE OF JOURNAL CENTER
TYZ  VALUES      (IF ICIRC =1, SUBMIT ATTITUDE ANGLE IN DEGREES)
0.  0.  0.  0.  0.  0.  0.  0.  0.  0.  0.  0.
----------------------------------------------------------------------
 CARD7
 NFD      NVL
  0        1
----------------------------------------------------------------------
 CARD 9
 CGL1   CGL2
 2.00   2.00
----------------------------------------------------------------------
 CARD 12          (SUBMIT NVL CARDS)
 XV      YV      PSP      PCV
 0.      0.    .02122     -.0156


----------------------------------------------------------------------
```

Table 3-3a

Input Data Listing for Dimensionless SQZDMP Run

pressure distribution (for an eccentricity ratio of 0.5) is shown in Table 3-3b, while Table 3-3c gives the summary of circular orbit coefficients for this case.

Plots of dimensionless damping and inertia are available through the use of the CIRCULAR ORBIT GRAPHICS program. Figures 3-6a and 3-6b are plots of direct and cross-coupled damping coefficients for the output printed in Table 3-3c.

The dimensionaless data generated by SQZDMP can also be dimensionalized using program DIMOUT. Table 3-4 shows a typical DIMOUT summary table for the example damper.

The results of running the JUMP program, for a bi-stable orbit or "jump" analysis, are given in Table 3-5. For this case both shaft and flexure flexibility were assumed to be zero and the resulting output gives values for the speed/mass parameter "SIGMA" in terms of the displacement parameter (or eccentricity ratio) "EPS" and the mass eccentricity parameter "ALPHA" along with intermediate results and the transmissibility "T".

c. Mobility Calculations

The final analysis to be performed uses the Mobility option to SQZDMP and its key post processing programs as described in Figure 3-7. Since the Mobility calculation is dimensional, the damper test case described in Figure 3-3 was run for a new set of journal center coordinates (to generate the required pressure tables) of:

Journal center eccentricity	X =	.00001, .001, .004, .006, .0079 in
	Y =	0.0, 0.0, 0.0, 0.0, 0.0

For the mobility calculation, the journal was set initially at X = .0001 in., y = -.002 in. (i.e. slightly off-center). A steady state force of 25 lbs. was applied in the X direction and a rotating unbalance of 8.5×10^{-5} lbs-sec^2 at 260^{o} was also applied. Table 3-6a shows the input data for this calculation and Table 3-6b is the first page of the calculation output showing the stepwise time integration.

TITLE: CASE 2 - SEALED DAMPER - DIMENSIONLESS OPTION 1/7/82 F.GILLHAM . DATE: 01/07/82

PRESSURE DISTRIBUTION

MESH SIZE 9 X 24
PRESSURES ARE NORMALIZED AS (P)/(12*MU*(R/C)**2)

THETA (DEG.)	AXIAL DIVISION NUMBER 1	2	3	4	5	6	7	8	9
15.	1.942D-02	1.930D-02	1.926D-02	1.930D-02	1.942D-02	1.962D-02	1.990D-02	2.026D-02	2.070D-02
30.	1.942D-02	1.894D-02	1.863D-02	1.849D-02	1.852D-02	1.872D-02	1.909D-02	1.963D-02	2.034D-02
45.	1.942D-02	1.848D-02	1.783D-02	1.746D-02	1.737D-02	1.757D-02	1.806D-02	1.883D-02	1.988D-02
60.	1.942D-02	1.786D-02	1.673D-02	1.605D-02	1.581D-02	1.601D-02	1.665D-02	1.773D-02	1.926D-02
75.	1.942D-02	1.697D-02	1.518D-02	1.405D-02	1.358D-02	1.378D-02	1.465D-02	1.618D-02	1.837D-02
90.	1.942D-02	1.569D-02	1.295D-02	1.119D-02	1.041D-02	1.061D-02	1.179D-02	1.395D-02	1.709D-02
105.	1.942D-02	1.393D-02	9.878D-03	7.246D-03	6.032D-03	6.231D-03	7.845D-03	1.088D-02	1.533D-02
120.	1.942D-02	1.176D-02	6.087D-03	2.388D-03	6.420D-04	8.419D-04	2.987D-03	7.087D-03	1.316D-02
135.	1.942D-02	9.763D-03	2.625D-03	-2.041D-03	-4.266D-03	-4.066D-03	-1.441D-03	3.624D-03	1.116D-02
150.	1.942D-02	9.467D-03	2.129D-03	-2.659D-03	-4.942D-03	-4.742D-03	-2.059D-03	3.128D-03	1.087D-02
165.	1.942D-02	1.278D-02	7.914D-03	4.767D-03	3.302D-03	3.501D-03	5.366D-03	8.913D-03	1.418D-02
180.	1.942D-02	1.962D-02	1.982D-02	2.002D-02	2.022D-02	2.042D-02	2.062D-02	2.082D-02	2.102D-02
195.	1.942D-02	2.646D-02	3.173D-02	3.528D-02	3.714D-02	3.734D-02	3.588D-02	3.273D-02	2.786D-02
210.	1.942D-02	2.978D-02	3.751D-02	4.270D-02	4.538D-02	4.558D-02	4.330D-02	3.851D-02	3.117D-02
225.	1.942D-02	2.948D-02	3.702D-02	4.208D-02	4.471D-02	4.491D-02	4.268D-02	3.802D-02	3.088D-02
240.	1.942D-02	2.749D-02	3.356D-02	3.765D-02	3.980D-02	4.000D-02	3.825D-02	3.455D-02	2.888D-02
255.	1.942D-02	2.531D-02	2.976D-02	3.280D-02	3.441D-02	3.461D-02	3.340D-02	3.076D-02	2.671D-02
270.	1.942D-02	2.355D-02	2.669D-02	2.885D-02	3.003D-02	3.023D-02	2.945D-02	2.769D-02	2.495D-02
285.	1.942D-02	2.228D-02	2.447D-02	2.599D-02	2.686D-02	2.706D-02	2.659D-02	2.547D-02	2.367D-02
300.	1.942D-02	2.139D-02	2.291D-02	2.399D-02	2.464D-02	2.484D-02	2.459D-02	2.391D-02	2.278D-02
315.	1.942D-02	2.076D-02	2.182D-02	2.259D-02	2.307D-02	2.327D-02	2.319D-02	2.281D-02	2.216D-02
330.	1.942D-02	2.030D-02	2.101D-02	2.155D-02	2.192D-02	2.212D-02	2.215D-02	2.201D-02	2.170D-02
345.	1.942D-02	1.994D-02	2.038D-02	2.074D-02	2.102D-02	2.122D-02	2.134D-02	2.138D-02	2.134D-02
360.	1.942D-02	1.962D-02	1.982D-02	2.002D-02	2.022D-02	2.042D-02	2.062D-02	2.082D-02	2.102D-02

Table 3-3b

Pressure Distribution for Dimensionless SQZDMP Run
(Eccentricity Ratio = 0.5)

```
**********************************************
* SQUEEZE FILM DAMPER PERFORMANCE TABLE *     **********
*          CIRCULAR ORBIT DATA          *     *01/07/82*
*      MTI PROGRAM  SQZDAMP  (PN812)    *     **********
**********************************************
```

CASE 2 - SEALED DAMPER - DIMENSIONLESS OPTION 1/7/82 F.GILLHAM .

******* NON-DIMENSIONAL DATA ********

L/D RATIO	0.2000
SUPPLY PRESSURE PARAMETER (PSP/(12W*MU*(R/C)**2))	2.1220D-02
CAVITATION PARAMETER (PCV/(12W*MU*(R/C)**2))	-1.5600D-02
LOCAL SEAL PARAMETER 1 (CL1*12MU*R/C**3)	0.0
LOCAL SEAL PARAMETER 2 (CL2*12MU*R/C**3)	0.0
OIL SUPPLY	CIRCUMFERENTIAL GROOVE
DAMPER IS	ASYMMETRIC

********** CIRCULAR ORBIT COEFFICIENTS *********

ORBIT RADIUS/C	***** DAMPING ***** B/(MU*L*(R/C)**3) DIRECT (BXX=BYY)	X-COUPLED (BXY=-BYX)	***** INERTIA ***** INERT./(RHO*L*R**3/C) DIRECT (CXX=CYY)	X-COUPLED (CXY=-CYX)	**** FLOW *** Q/(W*C*R**2) (SEE NOTE 1) IN	OUT
0.000010	4.886D-01	-4.334D-07	4.886D-02	4.153D-14	3.8D-02	3.8D-02
0.100000	4.957D-01	-4.306D-11	4.923D-02	3.780D-14	3.8D-02	3.8D-02
0.200000	5.182D-01	-2.149D-11	5.038D-02	3.470D-14	3.8D-02	3.8D-02
0.300000	5.597D-01	-1.435D-11	5.244D-02	3.206D-14	3.8D-02	3.8D-02
0.400000	6.280D-01	-1.080D-11	5.568D-02	2.980D-14	3.8D-02	3.8D-02
0.500000	7.386D-01	-8.674D-12	6.061D-02	2.784D-14	3.9D-02	3.9D-02
0.600000	9.084D-01	2.680D-02	5.884D-02	5.475D-03	3.9D-02	3.9D-02
0.700000	1.103D+00	3.174D-01	5.633D-02	1.337D-02	5.0D-02	2.9D-02
0.800000	1.482D+00	1.184D+00	7.015D-02	1.908D-02	2.9D-02	5.2D-02
0.900000	2.863D+00	4.852D+00	1.111D-01	3.079D-02	1.3D-02	6.9D-02
0.950000	5.844D+00	1.413D+01	1.862D-01	4.936D-02	-5.0D-03	8.7D-02
0.990000	1.737D+01	5.389D+01	8.295D-01	1.632D-01	-1.8D-02	9.9D-02

NOTE 1: DUE TO CAVITATION CONDITION ASSUMPTIONS,
PREDICTED FLOW IN DOES NOT NECESSARILY EQUAL FLOW OUT

ABBREVIATION KEY : W = ROTATIONAL SPEED R = DAMPER RADIUS
MU = FLUID VISCOSITY C = DAMPER CLEARANCE
RHO = MASS DENSITY L = DAMPER LENGTH

Table 3-3c

Summary Output for Dimensionless SQZDMP Run

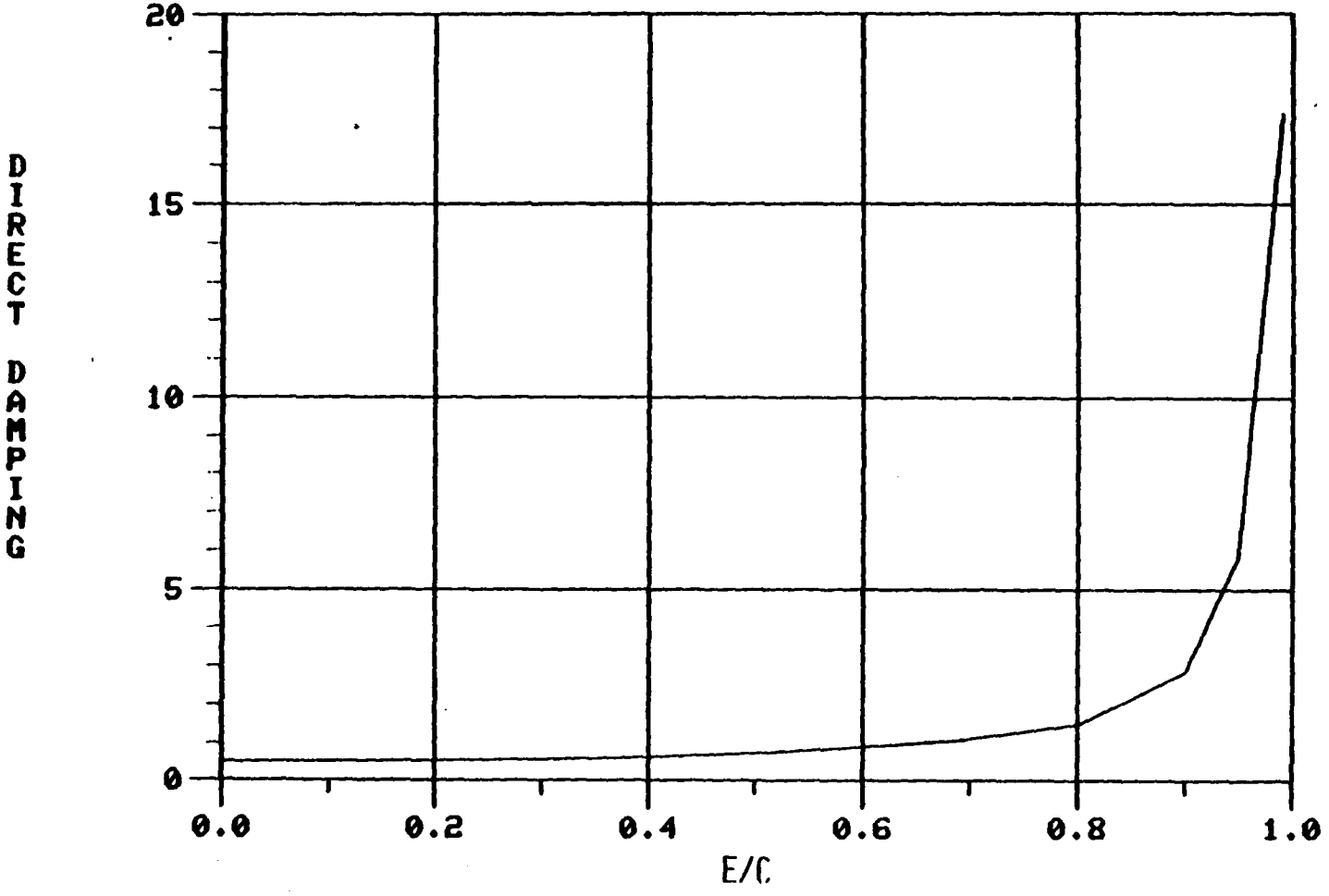

Figure 3-6a Direct Damping Coefficient as a Function of Eccentricity Ratio

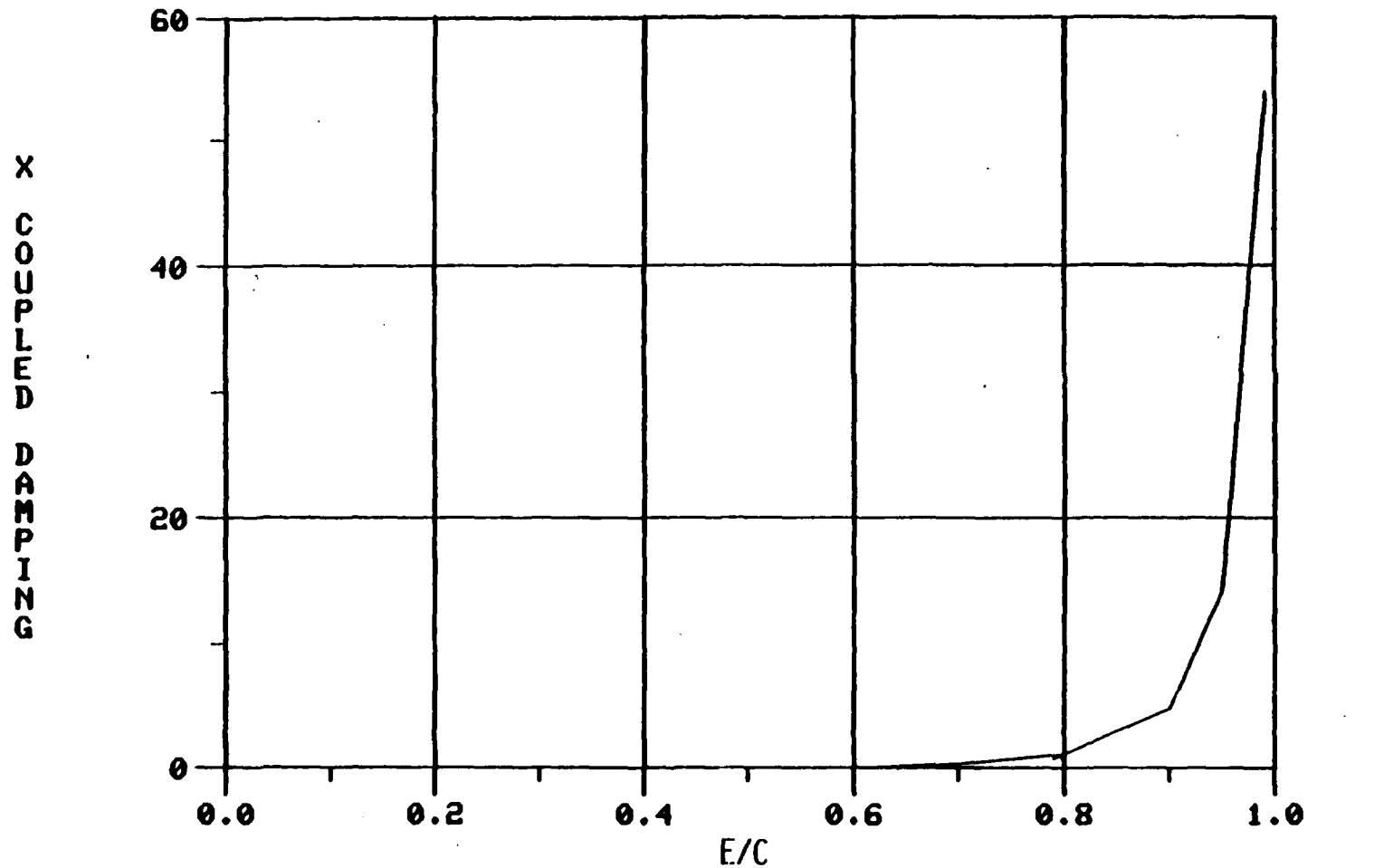

Figure 3-6b Cross-Coupled Damping Coefficient as a Function of Eccentricity Ratio

```
**********************************************************
*  DIMENSIONAL OUTPUT FOR SQUEEZE FILM DAMPER PERFORMANCE  *
*            CIRCULAR     ORBIT     DATA                  *
**********************************************************

CASE 2 - SEALED DAMPER - DIMENSIONLESS OPTION  1/7/82  F.GILLHAM
         01/07/82

  DIAMETER      LENGTH      CLEARANCE   VISCOSITY    FREQUENCY    DENSITY
   (INCH)       (INCH)        (INCH)    (LBF-SEC     (HERTZ)   (LBF-SEC**2
                                         /IN**2)                  /IN**4)
  5.0000E+00  1.0000E+00  8.0000E-03  1.0000E-06  1.3333E+02  7.9000E-05

 L/D RATIO ..................................................  0.2000
 SUPPLY PRESSURE          (LBF/IN**2)      ..... 2.0833E+01
 CAVITATION PRESSURE      (LBF/IN**2)      .....-1.5315E+01
 GLOBAL SEAL PARAMETER 1 (IN**3/SEC/PSI) ..... 8.5333E-02
 GLOBAL SEAL PARAMETER 2 (IN**3/SEC/PSI) ..... 8.5333E-02
 LOCAL SEAL PARAMETER 1 (IN**3/SEC/(PSI-IN))..... 0.0
 LOCAL SEAL PARAMETER 2 (IN**3/SEC/(PSI-IN))..... 0.0

 OIL SUPPLY.....................................CIRCUMFERENTIAL GROOVE
 DAMPER IS .....................................ASYMMETRIC

          ***** CIRCULAR ORBIT COEFFICIENTS *****

 ORBIT    DIRECT     X-COUPLED    DIRECT     X-COUPLED     FLOW        FLOW     PSI
 RADIUS   DAMPING    DAMPING      INERTIA    INERTIA       IN          OUT
 INCH     LBF-SEC    LBF-SEC      LBF-SEC**2 LBF-SEC**2    IN**3       IN**3    DEG
           /IN        /IN          /IN        /IN          /SEC        /SEC

0.0       1.491E+01 -1.323E-05  7.539E-03  6.408E-15  1.577E+00  1.577E+00
0.800E-03 1.513E+01 -1.314E-09  7.596E-03  5.832E-15  1.580E+00  1.580E+00
0.160E-02 1.581E+01 -6.559E-10  7.773E-03  5.353E-15  1.587E+00  1.587E+00
0.240E-02 1.708E+01 -4.379E-10  8.092E-03  4.947E-15  1.598E+00  1.598E+00
0.320E-02 1.916E+01 -3.295E-10  8.592E-03  4.598E-15  1.612E+00  1.612E+00
0.400E-02 2.254E+01 -2.647E-10  9.351E-03  4.295E-15  1.627E+00  1.627E+00
0.480E-02 2.772E+01  8.180E-01  9.079E-03  8.448E-04  1.642E+00  1.642E+00
0.560E-02 3.367E+01  9.686E+00  8.691E-03  2.064E-03  2.112E+00  1.231E+00
0.640E-02 4.523E+01  3.613E+01  1.082E-02  2.943E-03  1.197E+00  2.173E+00
0.720E-02 8.736E+01  1.481E+02  1.714E-02  4.750E-03  5.409E-01  2.895E+00
0.760E-02 1.783E+02  4.313E+02  2.873E-02  7.617E-03 -2.099E-01  3.647E+00
0.792E-02 5.302E+02  1.644E+03  1.280E-01  2.518E-02 -7.337E-01  4.167E+00

PSI(DEG) = HOLE1 TO ECCENTRICITY VECTOR IN WHIRL DIRECTION
```

Table 3-4

Dimensionalized Circular Orbit Coefficients

SQUEEZE FILM DAMPER ANALYSIS

FLEXURE FLEXIBILITY= 0.0
SHAFT FLEXIBILITY= 0.0

EPS	ALPHA	F(S)	F(R)	GAMMA	F	BETA(1)	BETA(2)	SIGMA(1)	SIGMA(2)	T(1)	T(2)
0.100	0.0	**********									
0.100	0.100	0.4957D-01	-0.4306D-11	0.9000D+02	0.4957D-01	-0.8686D-11	-0.8686D-11	-0.5707D+10	-0.5707D+10	-0.8686D-10	-0.8686D-10
0.100	0.200	0.4957D-01	-0.4306D-11	0.9000D+02	0.4957D-01	0.1732D+00	-0.1732D+00	0.2862D+00	-0.2862D+00	0.8660D+00	-0.8660D+00
0.100	0.300	0.4957D-01	-0.4306D-11	0.9000D+02	0.4957D-01	0.2828D+00	-0.2828D+00	0.1753D+00	-0.1753D+00	0.9428D+00	-0.9428D+00
0.100	0.400	0.4957D-01	-0.4306D-11	0.9000D+02	0.4957D-01	0.3873D+00	-0.3873D+00	0.1280D+00	-0.1280D+00	0.9682D+00	-0.9682D+00
0.100	0.500	0.4957D-01	-0.4306D-11	0.9000D+02	0.4957D-01	0.4899D+00	-0.4899D+00	0.1012D+00	-0.1012D+00	0.9798D+00	-0.9798D+00
0.100	0.600	0.4957D-01	-0.4306D-11	0.9000D+02	0.4957D-01	0.5916D+00	-0.5916D+00	0.8379D-01	-0.8379D-01	0.9860D+00	-0.9860D+00
0.100	0.700	0.4957D-01	-0.4306D-11	0.9000D+02	0.4957D-01	0.6928D+00	-0.6928D+00	0.7155D-01	-0.7155D-01	0.9897D+00	-0.9897D+00
0.100	0.800	0.4957D-01	-0.4306D-11	0.9000D+02	0.4957D-01	0.7937D+00	-0.7937D+00	0.6245D-01	-0.6245D-01	0.9922D+00	-0.9922D+00
0.100	0.900	0.4957D-01	-0.4306D-11	0.9000D+02	0.4957D-01	0.8944D+00	-0.8944D+00	0.5542D-01	-0.5542D-01	0.9938D+00	-0.9938D+00
0.200	0.0	**********									
0.200	0.100	**********									
0.200	0.200	0.1036D+00	-0.4299D-11	0.9000D+02	0.1036D+00	-0.8295D-11	-0.8295D-11	-0.1249D+11	-0.1249D+11	-0.4147D-10	-0.4147D-10
0.200	0.300	0.1036D+00	-0.4299D-11	0.9000D+02	0.1036D+00	0.2236D+00	-0.2236D+00	0.4635D+00	-0.4635D+00	0.7454D+00	-0.7454D+00
0.200	0.400	0.1036D+00	-0.4299D-11	0.9000D+02	0.1036D+00	0.3464D+00	-0.3464D+00	0.2992D+00	-0.2992D+00	0.8660D+00	-0.8660D+00
0.200	0.500	0.1036D+00	-0.4299D-11	0.9000D+02	0.1036D+00	0.4583D+00	-0.4583D+00	0.2262D+00	-0.2262D+00	0.9165D+00	-0.9165D+00
0.200	0.600	0.1036D+00	-0.4299D-11	0.9000D+02	0.1036D+00	0.5657D+00	-0.5657D+00	0.1832D+00	-0.1832D+00	0.9428D+00	-0.9428D+00
0.200	0.700	0.1036D+00	-0.4299D-11	0.9000D+02	0.1036D+00	0.6708D+00	-0.6708D+00	0.1545D+00	-0.1545D+00	0.9583D+00	-0.9583D+00
0.200	0.800	0.1036D+00	-0.4299D-11	0.9000D+02	0.1036D+00	0.7746D+00	-0.7746D+00	0.1338D+00	-0.1338D+00	0.9682D+00	-0.9682D+00
0.200	0.900	0.1036D+00	-0.4299D-11	0.9000D+02	0.1036D+00	0.8775D+00	-0.8775D+00	0.1181D+00	-0.1181D+00	0.9750D+00	-0.9750D+00
0.300	0.0	**********									
0.300	0.100	**********									
0.300	0.200	**********									
0.300	0.300	0.1679D+00	-0.4305D-11	0.9000D+02	0.1679D+00	-0.7691D-11	-0.7691D-11	-0.2183D+11	-0.2183D+11	-0.2564D-10	-0.2564D-10
0.300	0.400	0.1679D+00	-0.4305D-11	0.9000D+02	0.1679D+00	0.2646D+00	-0.2646D+00	0.6347D+00	-0.6347D+00	0.6614D+00	-0.6614D+00
0.300	0.500	0.1679D+00	-0.4305D-11	0.9000D+02	0.1679D+00	0.4000D+00	-0.4000D+00	0.4198D+00	-0.4198D+00	0.8000D+00	-0.8000D+00
0.300	0.600	0.1679D+00	-0.4305D-11	0.9000D+02	0.1679D+00	0.5196D+00	-0.5196D+00	0.3232D+00	-0.3232D+00	0.8660D+00	-0.8660D+00
0.300	0.700	0.1679D+00	-0.4305D-11	0.9000D+02	0.1679D+00	0.6325D+00	-0.6325D+00	0.2655D+00	-0.2655D+00	0.9035D+00	-0.9035D+00
0.300	0.800	0.1679D+00	-0.4305D-11	0.9000D+02	0.1679D+00	0.7416D+00	-0.7416D+00	0.2264D+00	-0.2264D+00	0.9270D+00	-0.9270D+00
0.300	0.900	0.1679D+00	-0.4305D-11	0.9000D+02	0.1679D+00	0.8485D+00	-0.8485D+00	0.1979D+00	-0.1979D+00	0.9428D+00	-0.9428D+00
0.400	0.0	**********									
0.400	0.100	**********									
0.400	0.200	**********									
0.400	0.300	**********									
0.400	0.400	0.2512D+00	-0.4318D-11	0.9000D+02	0.2512D+00	-0.6877D-11	-0.6877D-11	-0.3653D+11	-0.3653D+11	-0.1719D-10	-0.1719D-10
0.400	0.500	0.2512D+00	-0.4318D-11	0.9000D+02	0.2512D+00	0.3000D+00	-0.3000D+00	0.8373D+00	-0.8373D+00	0.6000D+00	-0.6000D+00
0.400	0.600	0.2512D+00	-0.4318D-11	0.9000D+02	0.2512D+00	0.4472D+00	-0.4472D+00	0.5617D+00	-0.5617D+00	0.7454D+00	-0.7454D+00
0.400	0.700	0.2512D+00	-0.4318D-11	0.9000D+02	0.2512D+00	0.5745D+00	-0.5745D+00	0.4373D+00	-0.4373D+00	0.8207D+00	-0.8207D+00
0.400	0.800	0.2512D+00	-0.4318D-11	0.9000D+02	0.2512D+00	0.6928D+00	-0.6928D+00	0.3626D+00	-0.3626D+00	0.8660D+00	-0.8660D+00
0.400	0.900	0.2512D+00	-0.4318D-11	0.9000D+02	0.2512D+00	0.8062D+00	-0.8062D+00	0.3116D+00	-0.3116D+00	0.8958D+00	-0.8958D+00
0.500	0.0	**********									
0.500	0.100	**********									
0.500	0.200	**********									
0.500	0.300	**********									
0.500	0.400	**********									
0.500	0.500	0.3693D+00	-0.4337D-11	0.9000D+02	0.3693D+00	-0.5872D-11	-0.5872D-11	-0.6290D+11	-0.6290D+11	-0.1174D-10	-0.1174D-10
0.500	0.600	0.3693D+00	-0.4337D-11	0.9000D+02	0.3693D+00	0.3317D+00	-0.3317D+00	0.1114D+01	-0.1114D+01	0.5528D+00	-0.5528D+00
0.500	0.700	0.3693D+00	-0.4337D-11	0.9000D+02	0.3693D+00	0.4899D+00	-0.4899D+00	0.7539D+00	-0.7539D+00	0.6999D+00	-0.6999D+00
0.500	0.800	0.3693D+00	-0.4337D-11	0.9000D+02	0.3693D+00	0.6245D+00	-0.6245D+00	0.5914D+00	-0.5914D+00	0.7806D+00	-0.7806D+00
0.500	0.900	0.3693D+00	-0.4337D-11	0.9000D+02	0.3693D+00	0.7483D+00	-0.7483D+00	0.4935D+00	-0.4935D+00	0.8315D+00	-0.8315D+00

Table 3-5a Jump Analysis Output

0.600	0.0	**********									
0.600	0.100	**********									
0.600	0.200	**********									
0.600	0.300	**********									
0.600	0.400	**********									
0.600	0.500	**********									
0.600	0.600	0.5450D+00	0.1608D-01	0.8831D+02	0.5453D+00	0.3539D-01	-0.3452D-15	0.1541D+02	-0.1579D+16	0.5899D-01	-0.5753D-15
0.600	0.700	0.5450D+00	0.1608D-01	0.8831D+02	0.5453D+00	0.3787D+00	-0.3433D+00	0.1440D+01	-0.1588D+01	0.5410D+00	-0.4904D+00
0.600	0.800	0.5450D+00	0.1608D-01	0.8831D+02	0.5453D+00	0.5471D+00	-0.5117D+00	0.9965D+00	-0.1065D+01	0.6839D+00	-0.6397D+00
0.600	0.900	0.5450D+00	0.1608D-01	0.8831D+02	0.5453D+00	0.6888D+00	-0.6534D+00	0.7917D+00	-0.8345D+00	0.7653D+00	-0.7260D+00
0.700	0.0	**********									
0.700	0.100	**********									
0.700	0.200	**********									
0.700	0.300	**********									
0.700	0.400	**********									
0.700	0.500	**********									
0.700	0.600	**********									
0.700	0.700	0.7722D+00	0.2222D+00	0.7395D+02	0.8036D+00	0.3871D+00	0.0	0.2076D+01	0.0	0.5530D+00	0.0
0.700	0.800	0.7722D+00	0.2222D+00	0.7395D+02	0.8036D+00	0.6265D+00	-0.2394D+00	0.1283D+01	-0.3356D+01	0.7831D+00	-0.2993D+00
0.700	0.900	0.7722D+00	0.2222D+00	0.7395D+02	0.8036D+00	0.7914D+00	-0.4043D+00	0.1015D+01	-0.1987D+01	0.8793D+00	-0.4493D+00
0.800	0.0	**********									
0.800	0.100	**********									
0.800	0.200	**********									
0.800	0.300	**********									
0.800	0.400	**********									
0.800	0.500	**********									
0.800	0.600	**********									
0.800	0.700	0.1186D+01	0.9470D+00	0.5138D+02	0.1517D+01	0.8143D+00	0.1842D+00	0.1863D+01	0.8238D+01	0.1163D+01	0.2631D+00
0.800	0.800	0.1186D+01	0.9470D+00	0.5138D+02	0.1517D+01	0.9985D+00	0.1388D-16	0.1520D+01	0.1093D+18	0.1248D+01	0.1735D-16
0.800	0.900	0.1186D+01	0.9470D+00	0.5138D+02	0.1517D+01	0.1147D+01	-0.1482D+00	0.1323D+01	-0.1024D+02	0.1274D+01	-0.1647D+00
0.900	0.0	**********									
0.900	0.100	**********									
0.900	0.200	**********									
0.900	0.300	**********									
0.900	0.400	**********									
0.900	0.500	0.2576D+01	0.4367D+01	0.3054D+02	0.5070D+01	0.9772D+00	0.5731D+00	0.5188D+01	0.8847D+01	0.1954D+01	0.1146D+01
0.900	0.600	0.2576D+01	0.4367D+01	0.3054D+02	0.5070D+01	0.1164D+01	0.3868D+00	0.4357D+01	0.1311D+02	0.1939D+01	0.6446D+00
0.900	0.700	0.2576D+01	0.4367D+01	0.3054D+02	0.5070D+01	0.1305D+01	0.2452D+00	0.3885D+01	0.2068D+02	0.1864D+01	0.3503D+00
0.900	0.800	0.2576D+01	0.4367D+01	0.3054D+02	0.5070D+01	0.1432D+01	0.1188D+00	0.3542D+01	0.4269D+02	0.1789D+01	0.1484D+00
0.900	0.900	0.2576D+01	0.4367D+01	0.3054D+02	0.5070D+01	0.1550D+01	0.2776D-16	0.3270D+01	0.1827D+18	0.1723D+01	0.3084D-16

Table 3-5b

Jump Analysis Output

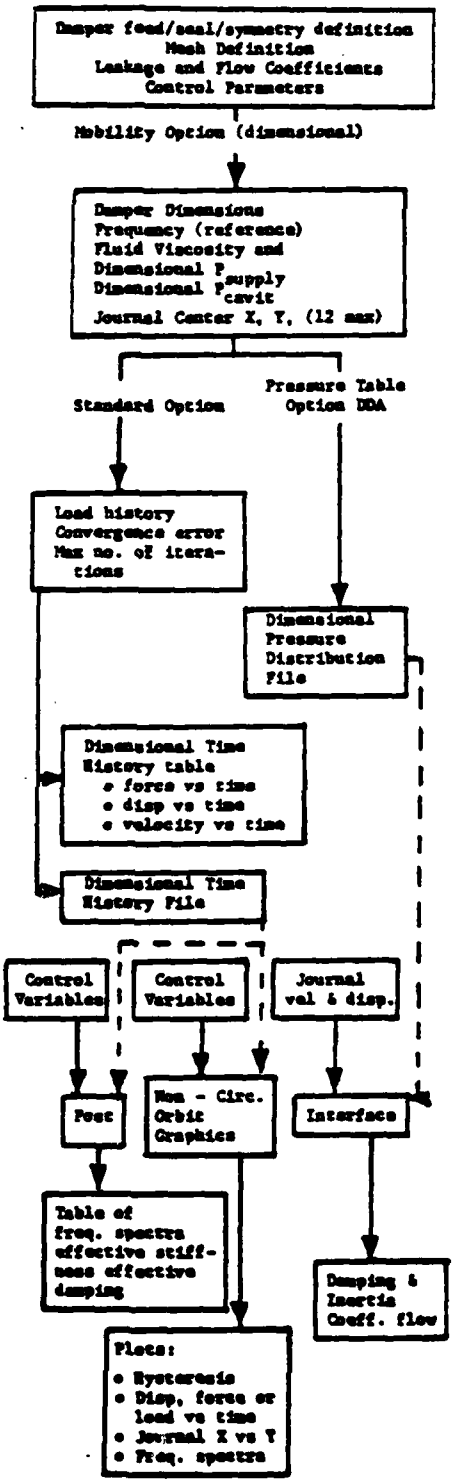

Figure 3-7 Mobility Calculation Flowchart

```
INPUT DATA LISTING
PROGRAM   PN812                          02/16/82  15:21:25


 USE THIS FORM IF (NXY.LT.0) ***
*********************************************************************************
 CARD1                          TITLE
 CASE 1 - SEALED DAMPER : MOBILITY CALCULATION AT 8000. RPM
---------------------------------------------------------------------------------
 CARD2      INTEGER CONTROLS
  M N   NDIM  INERT  NXY   INP  IUNITS  ICIRC  MCONST
   24  9  0    0     -5     1     0       0      1
---------------------------------------------------------------------------------
 CARD3B       BEARING DIMENSIONS
  DIAM  BLG  CLRC  VISC  DENS  FREQ
  5.0  1.0  .008 1.0000E-6 7.90E-5  133.33
---------------------------------------------------------------------------------
 CARD4        BEARING DESCRIPTION  OPTIONS
  MSL MFD MHF NFS
   1   0   1   0
---------------------------------------------------------------------------------
  CARD9                                (SUBMIT IF MSL=1)
  CG1       CG2
  2.0       2.0


---------------------------------------------------------------------------------
  CARD 10                     LUBRICANT INFORMATION
  PSP     PCV
  20.   -14.70


---------------------------------------------------------------------------------
 CARD 11A   (8E10.3)                  X-COORDINATE OF JOURNAL CENTER
  TXY(I)
  .00001 .001   .004   .006   .0079


---------------------------------------------------------------------------------
 CARD 11B   (8E10.3)                  Y-COORDINATE OF JOURNAL CENTER
  TYZ(I)
   .0     .0     .0     .0     .0
---------------------------------------------------------------------------------
 CARD 13     (1615)                        USE FOR: MOBILITY ONLY
   NTST    MXIT    ITOP     NSTEP    IDIG
  240      25       3         0       0


---------------------------------------------------------------------------------
 CARD  14     (8E10.3)                      USE FOR: MOBILITY ONLY
  XZ     YZ     XV     YV     CVER
 .0001  -.002  0.     0.       .0001


---------------------------------------------------------------------------------
 CARD 17                                    TIME-HISTORY DATA
    TIME   DELT   WXINIT   WYINIT   UNBAL   PHI
    0.    .0001    25.      0.     8.5E-5    270.
 CASE 1 - SEALED DAMPER : MOBILITY CALCULATION AT 8000. RPM
  02/16/82
  24     9     0     0    -5     1     0     1
0.2000+00 0.5000+01 0.1000+01 0.8000-02 0.1000-05 0.1330+03 0.7900-04
   1     0     1     0
0.0         0.0
```

Table 3-6a Input Data for Mobility Calculation

```
 CASE 1 - SEALED DAMPER : MOBILITY AT 8000. RPM
   02/16/82
   24    9    0    0   -5    1    0    1
0.2000+00 0.5000+01 0.1000+01 0.8000-02 0.1000-05 0.133D+03 0.7900-04
    1    0    1    0
0.0       0.0
0.1000-04 0.1000-02 0.4000-02 0.6000-02 0.7900-02 0.0       0.0       0.0
0.0       0.0       0.0       0.0       0.0       0.0       0.0       0.0
0.0       0.0       0.0       0.0       0.0       0.0       0.0       0.0
0.0       0.0       0.0       0.0       0.0       0.0       0.0       0.0
0.0       0.0       0.0       0.0       0.0       0.0       0.0       0.0
    0    0
0.2000+01 0.2000+01
0.2000+02-0.1470+02
0.1530+01 0.2810+01 0.2040-01-0.1500-01
  240   25    3    0
```

0.0	2.500000D+01	5.96533D+01	1.53051D+00	2.81077D+00	1.00000D-04	-2.00000D-03	-2.50000D+01	-5.96533D+01	1
1.000000-04	2.000850+01	5.94441D+01	1.31818D+00	3.11307D+00	2.53051D-04	-1.71892D-03	-2.00085D+01	-5.94441D+01	2
2.000000-04	1.505190+01	5.88180D+01	1.05603D+00	3.37836D+00	3.84870D-04	-1.40762D-03	-1.50519D+01	-5.88180D+01	3
3.000000-04	1.016520+01	5.77793D+01	7.47520D-01	3.56239D+00	4.90473D-04	-1.06978D-03	-1.01652D+01	-5.77793D+01	4
4.000000-04	5.382490+00	5.63353D+01	4.13983D-01	3.63234D+00	5.65225D-04	-7.13541D-04	-5.38249D+00	-5.63353D+01	5
5.000000-04	7.373910-01	5.44962D+01	7.12877D-02	3.60666D+00	6.06623D-04	-3.50307D-04	-7.37391D-01	-5.44962D+01	6
6.000000-04	-3.737540+00	5.22749D+01	-2.48440D-01	3.48554D+00	6.13752D-04	1.03589D-05	3.73754D+00	-5.22749D+01	7
7.000000-04	-8.010900+00	4.96870D+01	-5.43607D-01	3.29804D+00	5.88908D-04	3.58913D-04	8.01090D+00	-4.96870D+01	8
8.000000-04	-1.205270+01	4.67505D+01	-8.29822D-01	3.04140D+00	5.34547D-04	6.88716D-04	1.20527D+01	-4.67505D+01	9
9.000000-04	-1.583470+01	4.34861D+01	-1.07982D+00	2.73579D+00	4.51565D-04	9.92856D-04	1.58347D+01	-4.34861D+01	10
1.000000-03	-1.933820+01	3.99168D+01	-1.26876D+00	2.52467D+00	3.43583D-04	1.26644D-03	1.93302D+01	-3.99168D+01	11
1.100000-03	-2.251480+01	3.60674D+01	-1.40006D+00	2.41701D+00	2.16707D-04	1.51890D-03	2.25148D+01	-3.60674D+01	12
1.200000-03	-2.536610+01	3.19651D+01	-1.61881D+00	2.39029D+00	7.27012D-05	1.76060D-03	2.53661D+01	-3.19651D+01	13
1.300000-03	-2.786420+01	2.76386D+01	-1.81544D+00	2.42298D+00	-8.91794D-05	1.99963D-03	2.78642D+01	-2.763[illegible]	14
1.400000-03	-2.999150+01	2.31182D+01	-2.02502D+00	2.45040D+00	-2.70723D-04	2.24193D-03	2.99915D+01	-2.31[illegible]	15
1.500000-03	-3.173310+01	1.84357D+01	-2.19685D+00	2.47847D+00	-4.73225D-04	2.48697D-03	3.17331D+01	-1.843[illegible]	16
1.600000-03	-3.307670+01	1.36238D+01	-2.23159D+00	1.70576D+00	-6.92910D-04	2.71482D-03	3.30767D+01	-1.36238D+01	17
1.700000-03	-3.401300+01	8.71643D+00	-2.14220D+00	9.81279D-01	-9.16069D-04	2.88539D-03	3.40130D+01	-8.71643D+00	18
1.800000-03	-3.453540+01	3.74791D+00	-2.03285D+00	4.06931D-01	-1.13029D-03	2.98352D-03	3.45354D+01	-3.74791D+00	19
1.900000-03	-3.464030+01	-1.24691D+00	-1.93799D+00	-1.52245D-02	-1.33357D-03	3.02421D-03	3.46403D+01	1.24691D+00	20
2.000000-03	-3.432680+01	-6.23298D+00	-1.85484D+00	-3.45048D-01	-1.52737D-03	3.02269D-03	3.43268D+01	6.23298D+00	21
2.100000-03	-3.359720+01	-1.11753D+01	-1.77647D+00	-6.20952D-01	-1.71286D-03	2.98819D-03	3.35972D+01	1.11753D+01	22
2.200000-03	-3.245660+01	-1.60393D+01	-1.69731D+00	-8.56183D-01	-1.89050D-03	2.92609D-03	3.24566D+01	1.60393D+01	23
2.300000-03	-3.091300+01	-2.07908D+01	-1.61795D+00	-1.06072D+00	-2.06024D-03	2.84047D-03	3.09130D+01	2.07908D+01	24
2.400000-03	-2.897720+01	-2.53964D+01	-1.53351D+00	-1.24823D+00	-2.22203D-03	2.73440D-03	2.89772D+01	2.53964D+01	25
2.500000-03	-2.666280+01	-2.98239D+01	-1.43973D+00	-1.42991D+00	-2.37538D-03	2.60958D-03	2.66628D+01	2.98239D+01	26
2.600000-03	-2.398610+01	-3.40423D+01	-1.33498D+00	-1.60719D+00	-2.51935D-03	2.46659D-03	2.39861D+01	3.40423D+01	27
2.700000-03	-2.096580+01	-3.80218D+01	-1.22218D+00	-1.77761D+00	-2.65285D-03	2.30587D-03	2.09658D+01	3.80218D+01	28
2.800000-03	-1.762310+01	-4.17347D+01	-1.10257D+00	-1.94131D+00	-2.77507D-03	2.12811D-03	1.76231D+01	4.17347D+01	29
2.900000-03	-1.398140+01	-4.51549D+01	-9.71757D-01	-2.09998D+00	-2.88533D-03	1.93398D-03	1.39814D+01	4.51549D+01	30
3.000000-03	-1.006640+01	-4.82583D+01	-8.26906D-01	-2.25411D+00	-2.98250D-03	1.72398D-03	1.00664D+01	4.82583D+01	31
3.100000-03	-5.905330+00	-5.10233D+01	-6.67405D-01	-2.40398D+00	-3.06519D-03	1.49857D-03	5.90533D+00	5.10233D+01	32
3.200000-03	-1.527530+00	-5.34304D+01	-4.92553D-01	-2.54880D+00	-3.13193D-03	1.25817D-03	1.52753D+00	5.34304D+01	33
3.300000-03	3.036320+00	-5.54627D+01	-3.01818D-01	-2.68757D+00	-3.18119D-03	1.00329D-03	-3.03632D+00	5.54627D+01	34
3.400000-03	7.754240+00	-5.71060D+01	-9.44659D-02	-2.81913D+00	-3.21137D-03	7.34533D-04	-7.75424D+00	5.71060D+01	35
3.500000-03	1.259310+01	-5.83488D+01	1.31189D-01	-2.94188D+00	-3.22082D-03	4.52620D-04	-1.25931D+01	5.83488D+01	36
3.600000-03	1.751900+01	-5.91823D+01	3.76365D-01	-3.05349D+00	-3.20770D-03	1.58433D-04	-1.75190D+01	5.91823D+01	37
3.700000-03	2.249740+01	-5.96008D+01	6.41244D-01	-3.15034D+00	-3.17006D-03	-1.46916D-04	-2.24974D+01	5.96008D+01	38
3.800000-03	2.749330+01	-5.96012D+01	9.26024D-01	-3.22848D+00	-3.10594D-03	-4.61950D-04	-2.74933D+01	5.96012D+01	39
3.900000-03	3.247170+01	-5.91835D+01	1.23126D+00	-3.28263D+00	-3.01334D-03	-7.84798D-04	-3.24717D+01	5.91835D+01	40
4.000000-03	3.739770+01	-5.83508D+01	1.55341D+00	-3.30697D+00	-2.89021D-03	-1.11306D-03	-3.73977D+01	5.83508D+01	41
4.100000-03	4.223680+01	-5.71087D+01	1.86666D+00	-3.31264D+00	-2.73487D-03	-1.44376D-03	-4.22368D+01	5.71087D+01	42
4.200000-03	4.695500+01	-5.54662D+01	2.18268D+00	-3.28595D+00	-2.54820D-03	-1.77502D-03	-4.69550D+01	5.54662D+01	43
4.300000-03	5.151910+01	-5.34345D+01	2.50608D+00	-3.20558D+00	-2.32994D-03	-2.10362D-03	-5.15191D+01	5.34345D+01	44
4.400000-03	5.589730+01	-5.10281D+01	2.82185D+00	-3.05966D+00	-2.07933D-03	-2.42418D-03	-5.58973D+01	5.10281D+01	45
4.500000-03	6.005880+01	-4.82638D+01	3.11534D+00	-2.83450D+00	-1.79714D-03	-2.73014D-03	-6.00588D+01	4.82638D+01	46
4.600000-03	6.397430+01	-4.51610D+01	3.35463D+00	-2.54193D+00	-1.48561D-03	-3.01359D-03	-6.39743D+01	4.51610D+01	47
4.700000-03	6.761650+01	-4.17414D+01	3.53261D+00	-2.17991D+00	-1.15015D-03	-3.26779D-03	-6.76165D+01	4.17414D+01	48
4.800000-03	7.095980+01	-3.80291D+01	3.64213D+00	-1.76497D+00	-7.96884D-04	-3.48578D-03	-7.09598D+01	3.80291D+01	49
4.900000-03	7.398080+01	-3.40500D+01	3.68009D+00	-1.33478D+00	-4.32670D-04	-3.66227D-03	-7.39808D+01	3.40500D+01	50

Table 3-6b Output (First Page) from Mobility Calculation

Plots of this output obtained by running the NON-CIRCULAR ORBIT GRAPHICS program are shown in Figures 3-8. Figure 3-8a shows the damper journal orbit within its housing for several cycles of motion. Figures 3-8b and 3-8c are plots of displacement and force along the Y-axis as functions of time, while Figure 3-8d is a hysteresis plot along the Y-axis (force as a function of displacement).

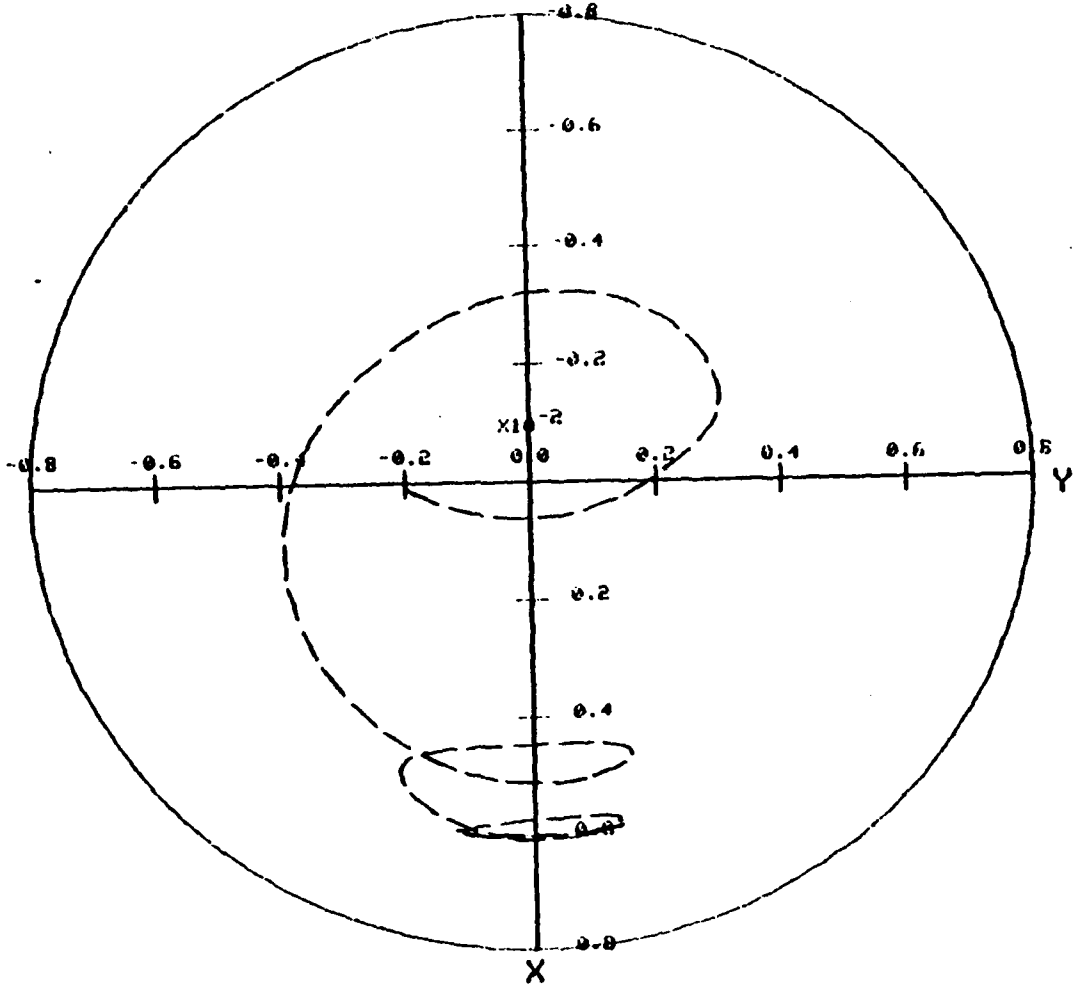

CASE 1 - SEALED DAMPER : MOBILITY CALCULATION AT 8000. RPM

Figure 3-8a Orbit Plot for Damper

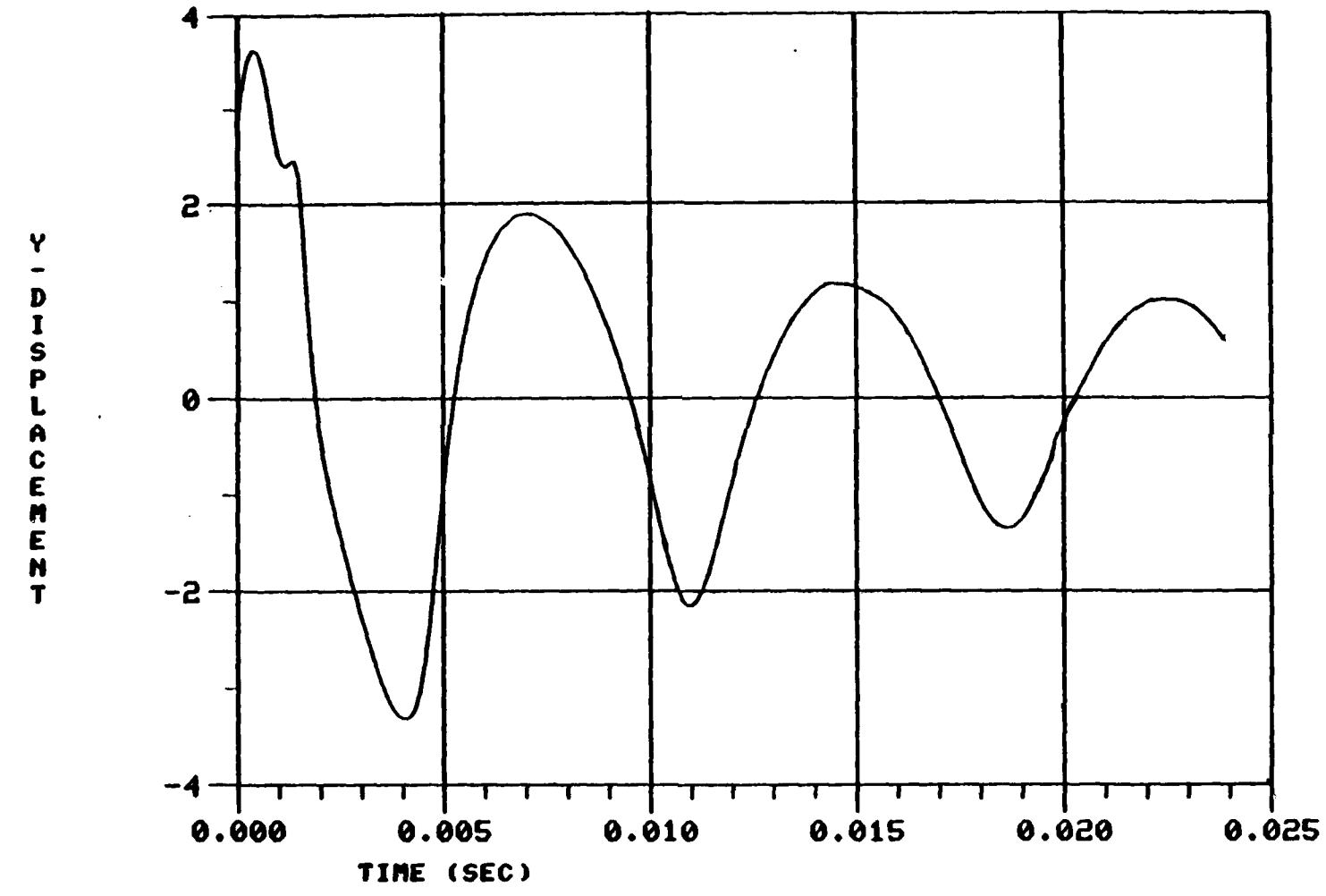

Figure 3-8b Y - Axis Displacement as a Function of Time

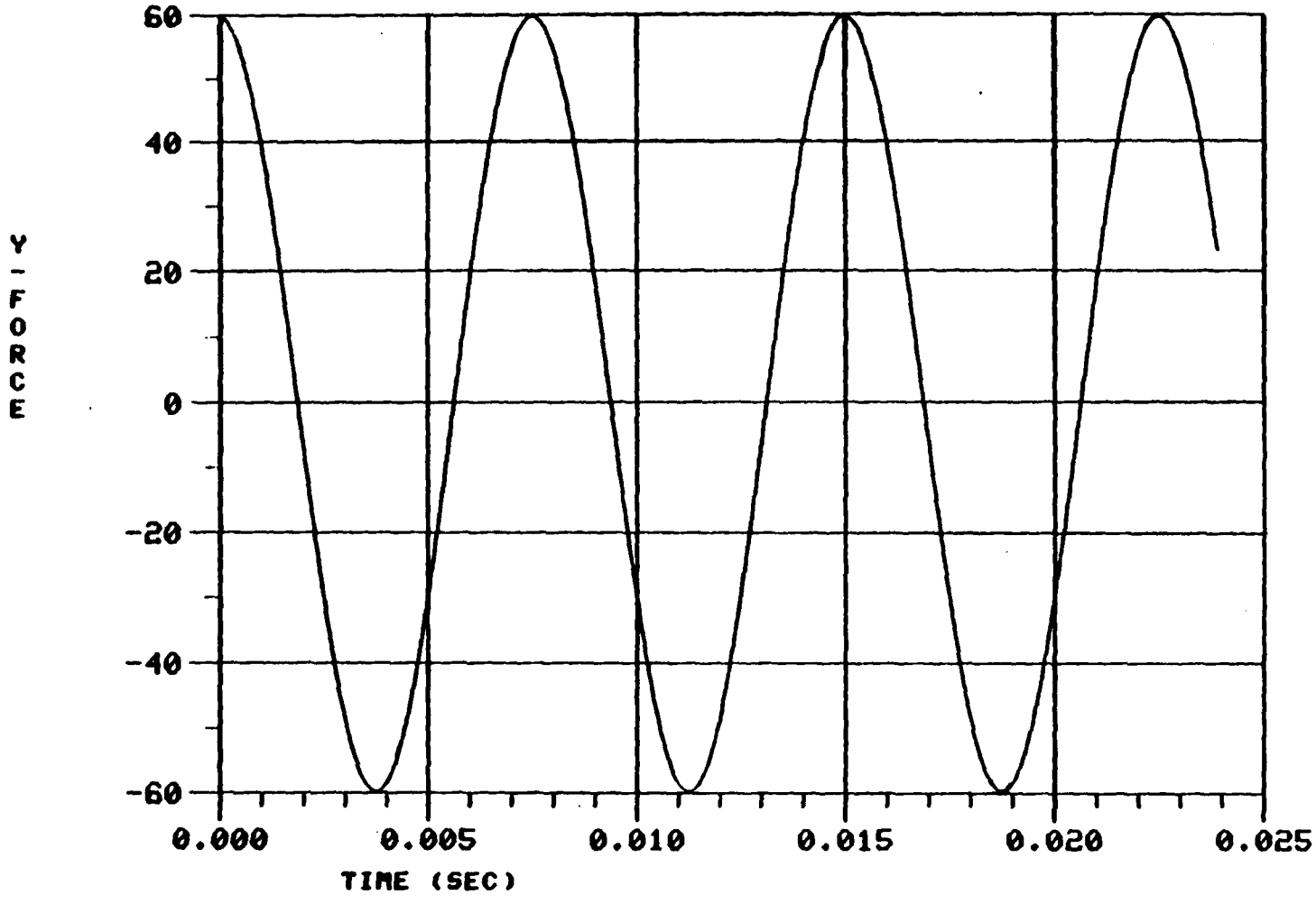

CASE 1 - SEALED DAMPER : MOBILITY AT 8000. RPM

Figure 3-8c Y - Axis Force as a Function of Time

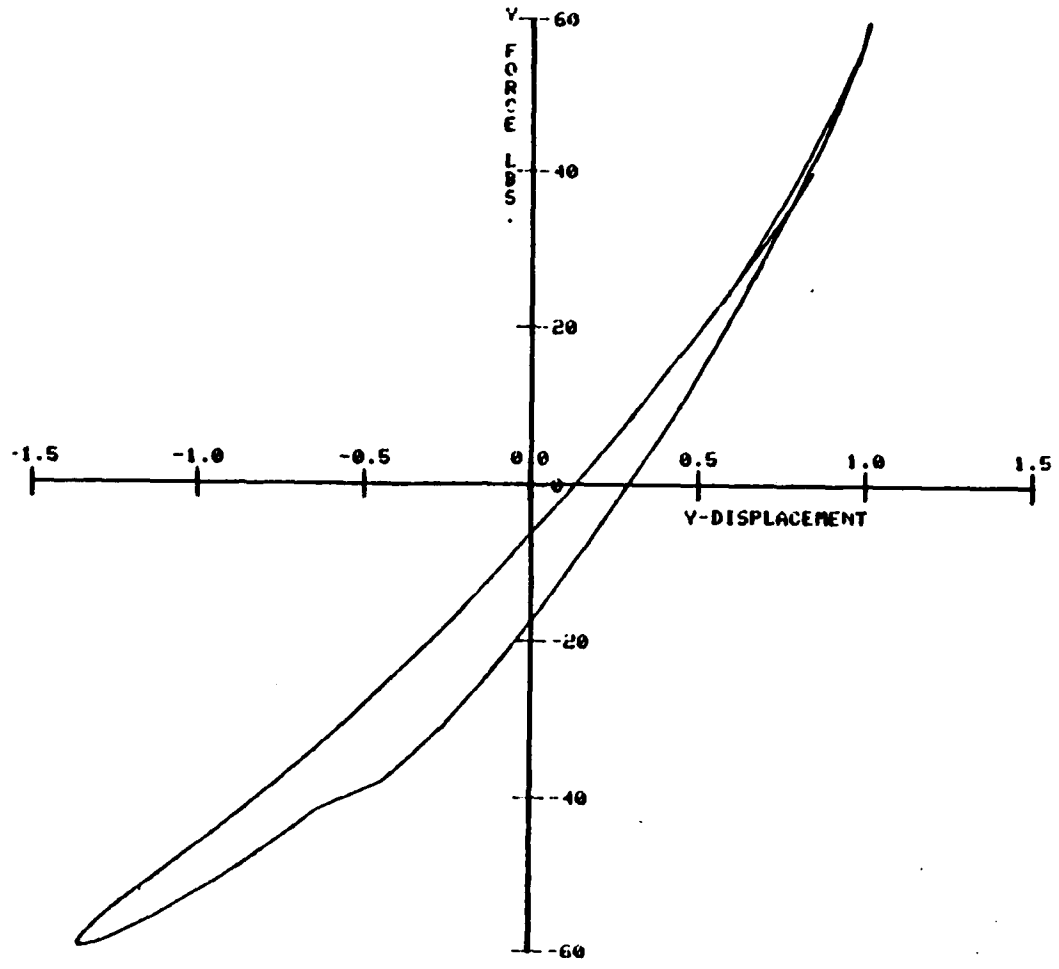

CASE 1 - SEALED DAMPER : HYSTERESIS - DISPLACEMENT - Y AT 8000. RPM

Figure 3-8d Hysteresis Plot - Displacement vs Force Along Y Axis

SECTION IV

INTEGRATION OF COMPONENT ANALYSIS TOOLS

An essential feature of the application of a damper component analysis tool in the design of engine dampers is its integration with rotordynamics analysis software. Therefore, a key aspect of this program has been to develop a coupled rotor system/damper component analysis capability. This capability was developed through the combination of an existing rotordynamic analysis program by Detroit Diesel Allison (DDA) with the damper component analysis software developed by MTI.

This and the following section describe the interface between the system and component programs. Descriptions of the solution algorithms used in the rotor system analysis program are presented to the extent that treatment of the interface logic can be readily understood. A sample problem is shown to illustrate the input and output of the analysis program. It is not the intent of this report to discuss the merits of each analysis and its applicability to coupled design. Rather, the intent is to provide the reader a description of the interface with the coupled calculations.

1. Overall Integration Philosophy

DDA's rotor dynamic analysis program, BB60, is coupled to the MTI damper analysis as shown in Figure 4-1. The overall philosophy is as follows:

1. Calculate the damper component output in non-dimensional form and store in files. Up to 4 dampers may be calculated with 2 files created for each. The 1st file contains a table of damping coefficients as a function of eccentricity ratio e/c. This file is used for single plane calculations where circular orbits are expected. The 2nd file contains a table of velocity and supply pressure distributions which are also a function of e/c. This file is used for 2 or 3 plane calculations where non-circular orbits are expected.

2. Generate dimensional damper forces. The rotor dynamic analysis, BB60, uses the damper component tables to generate modal forces. Input to BB60 includes the rotor mass/elastic data and dimensional damper information. Damper size, oil properties, and oil film radial clearance are used to calculate a dimensional force. The damper file number, damper location and system connection information is also given in BB60 input to locate the appropriate table and to apply the modal forces at the proper location.

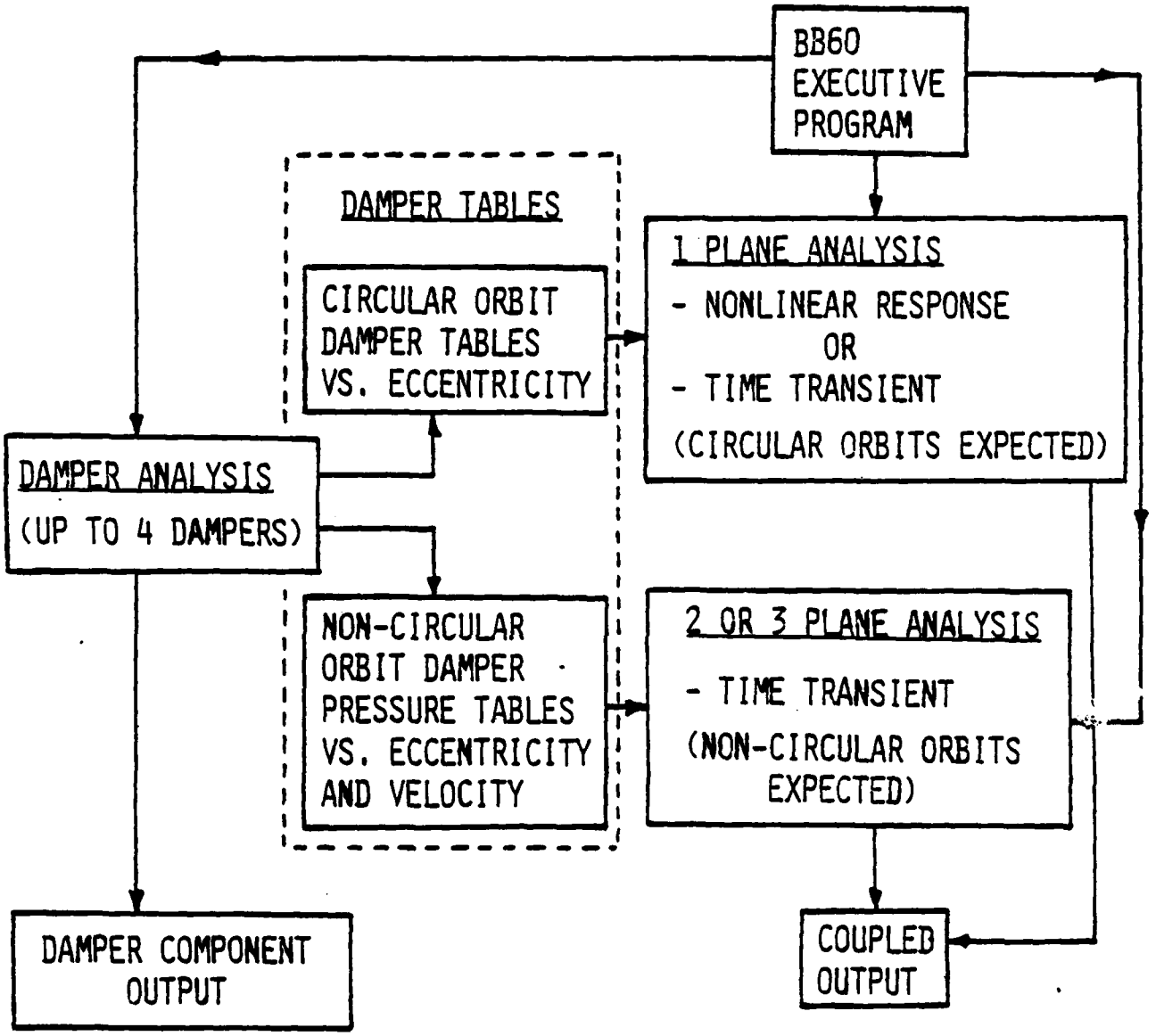

Figure 4-1 Overall Integration Philosopny

3. Calculate rotor/damper response. The damper motion is unknown in general and must be determined by an iteration scheme so that the damper calculated motion matches that used to determine its force. For the time transient analysis the force is determined from the previous time step damper motion. Details are discussed in the rotor/damper interface section of this report. In all calculations the damper forces are interpolated from the circular orbit coefficients for the single plane analysis and from the pressure tables for the 2 or 3 plane analysis.

The damper component analysis and the BB60 analysis may be executed separately or together. The damper component analysis may be executed in its dimensional or non-dimensional form. Coupling the damper to BB60 in its non-dimensional form allows a one time calculation of the damper model and saves the dimensional quantities for BB60 input where they may be used parametrically. These inputs include:

1. Damper location in terms of engine station, system connection, and damper file number.
2. Damper diameter and radial damper clearance.
3. Oil viscosity and density.
4. Supply pressure.

The goal of this integration philosophy was to provide for the most direct and simplest coding. The input of dimensional damper data in BB60 allows for rapid parametric studies that would be required in any design analysis.

A description of the creation of BB60 damper execution for the non-linear squeeze film dampers is given in Figure 4-2. It shows how information concerning the squeeze film dampers enters the BB60 analysis.

2. Rotor Dynamic Analysis Tool

A general description of the DDA rotor dynamic analysis program (BB60) is presented to establish the computing capabilities and briefly describe the solution technique used.

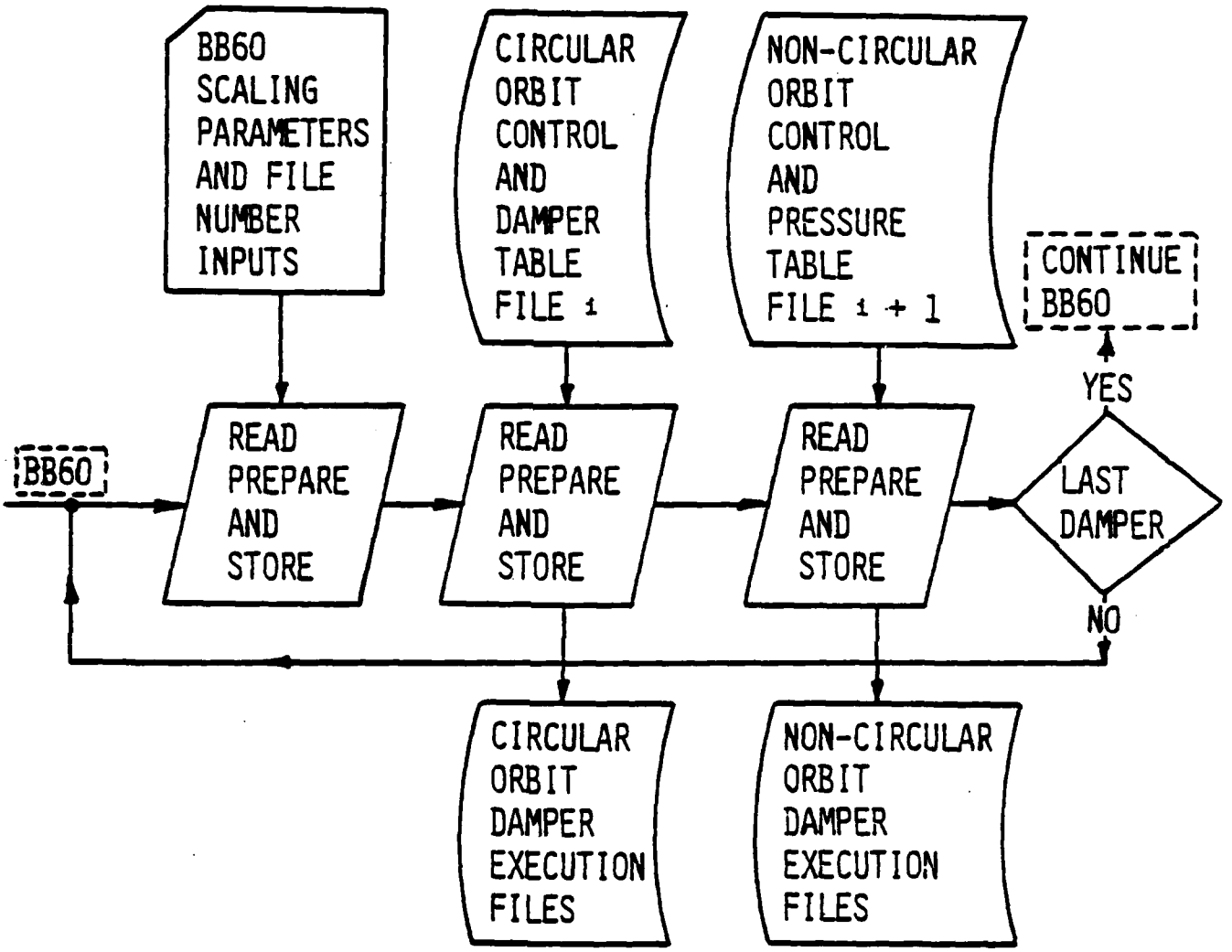

Figure 4-2 Creation of BB60 damper files.

BB60 SCALING PARAMETER LIST

- DAMPER NUMBER
- CLEARANCE
- VISCOSITY
- DENSITY
- DIAMETER
- FILE NUMBER

CIRCULAR ORBIT

NON-CIRCULAR ORBIT

CONTROL DATA

- NORMALIZATION TRIGGER
- LAND/DIAMETER (L/D)

- NUMBER OF AXIAL STATIONS
- NUMBER OF CIRCUMFERENTIAL STATIONS
- FEEDER HOLES/END GROOVES/?
- CAVITATION PRESSURE
- SYMMETRIC/NOT SYMMETRIC
- NUMBER OF ECCENTRICITIES
- INTEGRATION PARAMETERS
- TABLE OF INCREMENTAL SINE AND COSINE VALUES

TABLE DATA

DAMPER TABLES

- INDEX NUMBER
- BXY
- BXX
- CXY] INERTIA
- CXX] CONTRIBUTIONS
- ECCENTRICITY RATIO

PRESSURE DISTRIBUTION TABLES

- AXIAL AND CIRCUMFERENTIAL VELOCITY PRESSURES
- SUPPLY PRESSURE
- ECCENTRICITY RATIO

Figure 4-2 (continued). Creation of BB60 damper files.

Program Capabilities

DDA has developed a computer program for the analysis of coupled rotor/case dynamic systems. This program is routinely used to compute the critical speeds and dynamic response characteristics of an engine and/or component rig with as many as eight major systems (i.e., rotors and casings). Beam element representations for the cone, cylinder, and beam structures are normally used, although provisions are made for externally supplying shell and platelike flexibilities to the analysis. Gyroscopic effects are included for multiple rotor systems with co-rotational and counter-rotational shafts. Non-linear effects can be included in the dynamic response calculations. The program has been structured to be very user oriented. Inputs are simply generated from layout or detail drawings in the form of inside and outside diameters as a function of axial position. Masses and stiffnesses of the structural elements are computed internally. Output data are in the form of tabular frequencies, mode shapes, and responses as well as machine-generated plots. The output can also be routed to microfiche if desired. The program is written in Fortran IV and machine language for the IBM 370 system.

The basic program structure uses lumped parameter analyses for rotor and casing structures. Masses and inertias can be computed internally or input separately. A flexibility matrix between connected masses is computed, using beam and/or tapered cone equations. Local flexibilities are accounted for separately; that is, computed or tested externally and input as a flexibility matrix. Nonbeamlike structures are accommodated by the input of a modal description of the 1D modes of that structure which have been determined from a finite element model. This means that only the center-line deflection is considered. Stiffness coupling elements between substructures may be either linear or nonlinear.

The undamped critical speeds of linear systems and the damped linear and/or nonlinear steady-state response to rotor unbalances are computed by the rotor analysis program. Transient solutions are determined for various ground and engine shocks as well as response to a suddenly applied unbalance, such as blade loss.

Other capabilities of the analysis tool include:

- Damped natural frequencies
- Resonances at constant rotor speeds
- Whirl flutter stability
- Loads due to misalignment of redundant bearing arrangements
- System deflections resulting from discrete forces, moments, and loads due to gravity.

The rotor dynamics program is also used to compute stall-induced rotor/case response characteristics. The case-to-rotor relative displacement is calculated for a force on the rotor and equal but opposite force on the case, where the force rotates at a speed subsynchronous to the rotor speed. Again, the normal case definition is beamlike but 1D shell modes can be accommodated with a modal input description.

Solution Technique

The prediction of rotor dynamic characteristics is performed in BB60 using a modal synthesis technique [3, 4][1] as shown in Figure 4-3.

Step 1 - The input data describing the simulation are read. These data include the description for each substructure (rotors and case) and the interconnecting mount characteristics (stiffness and damping). Calculation mode selections are read.

Step 2 - Mass and flexibility matrices are computed for each substructure and, assuming the end mass stations to be simply supported (pinned), the uncoupled modes (natural frequencies and associated mode shapes) are computed without gyroscopic effects (zero rpm). These pinned-pinned modes are used in later calculations to form the coupled modes.

---

1 Numbers in brackets refer to references at the end of this report.

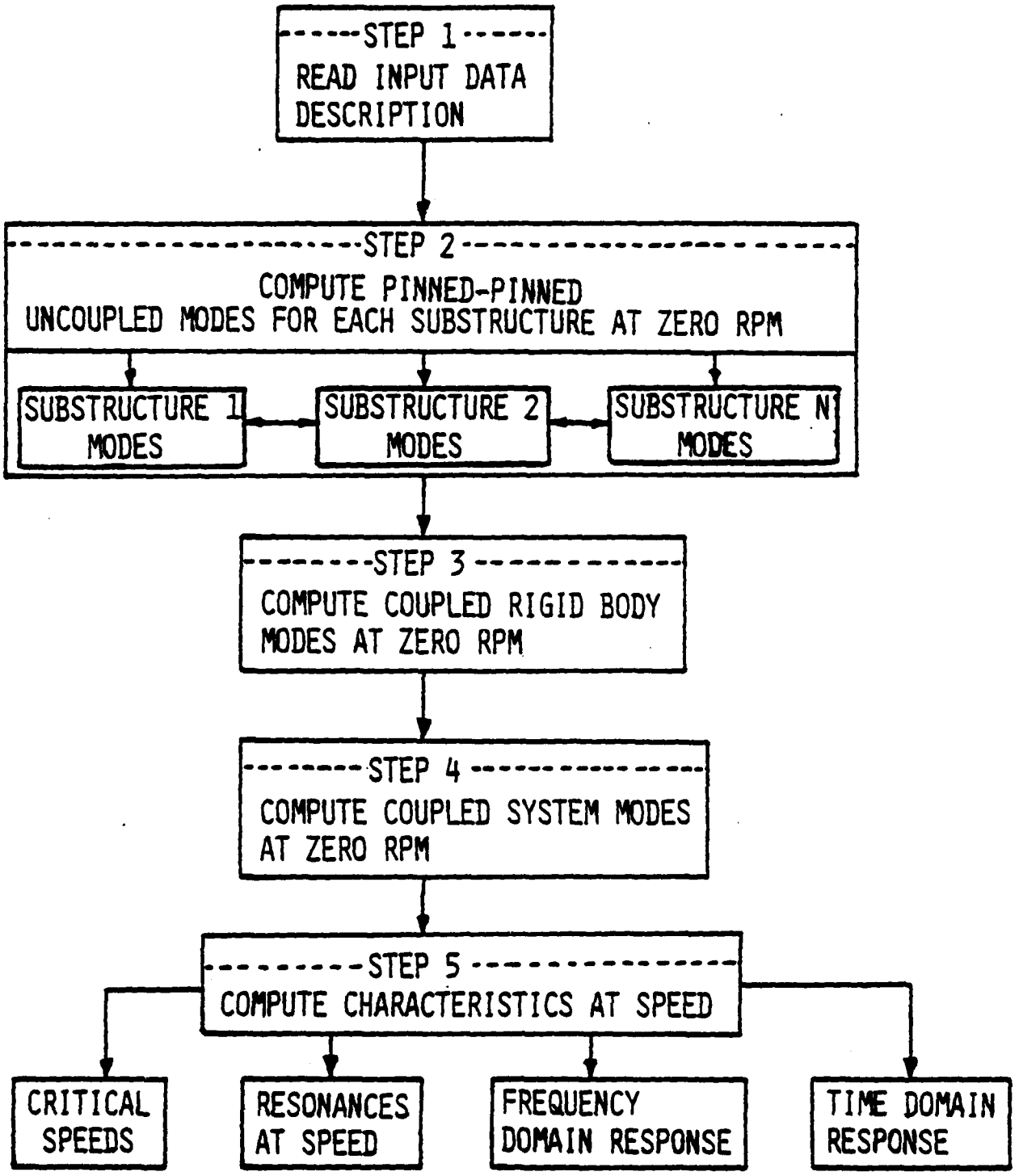

Figure 4-3 Flow Chart Depicting 8860 Calculation Procedure

Step 3 - The coupled rigid body modes are computed without gyroscopics effects by assuming the substructures to be infinitely stiff and joined to each other through the linear stiffness elements. Nonlinearities are ignored at this point in the procedure.

Step 4 - The coupled system modes are computed without gyroscopics effects. The previously computed substructure uncoupled pinned-pinned modes and the coupled rigid body modes are used as degrees of freedom in this calculation. The resulting coupled system modes become the basis for all subsequent calculations.

Step 5 - Any of a large number of calculations are possible. Among those are the ones associated with including the effects of squeeze film dampers. Specifically they are:

- Frequency domain response
- Time domain response
- Log decrement (damped natural frequency)

The damper effects are included in the nonlinear response calculations as modal forces. They are included in the damped natural frequency calculation as complex stiffness and viscous damping coefficients. This treatment is discussed further in Section V.

This discussion was presented to provide a general description of the rotor dynamic analysis computer program used at DDA. The models are developed using a lumped mass, beam element formulation. Solutions are performed using a modal synthesis approach and nonlinear effects, such as supplied by squeeze film dampers, are included in the response calculations as modal forces.

3. Damper Component Analysis Tool

The damper component analysis tool used in forming the integrated rotor/damper analysis program was developed by MTI and was delivered to DDA for coupling with the rotordynamics code. A brief description of this tool is

presented to: 1) indicate the type of data which must be assimilated in the rotor dynamics program and 2) establish some of the equations and terminology used in the integration of the programs.

General Description

The squeeze film damper analysis is centered on a calculation of the response of the film to an imposed velocity at a particular location. A finite difference solution of the Reynolds equation is used which provides algebraic difference equations linking pressure values at each point of a rectangular mesh on the developed damper surface. The analysis is sufficiently generalized to facilitate both circular and noncircular orbit calculations.

The squeeze film fluid pressure distribution, in its most general form, is dependent on the bearing journal velocity and acceleration components, the squeeze film thickness, cavitation and supply pressure, the physical properties of the film fluid, and the bearing geometry. The Reynolds equation for the squeeze film pressure distribution is written in terms of pressure coefficients of velocity and acceleration. This provides a form of the component pressures which are nondimensionalized and tabulated as a function of journal eccentricity. Subsequent damping and inertia coefficient calculations, which are functions of velocity and acceleration, make use of the tabulated pressure coefficients, thereby avoiding the need to re-solve the Reynolds equation.

A simplification to circular orbit, is used when applicable, to further reduce the number of calculations required during a rotor response analysis. By utilizing the relationship between velocity, acceleration, and journal eccentricity, a table of damping and inertia coefficients can be generated as a function of journal eccentricity.

The comprehensive squeeze film damper analysis accounts for the following effects:

- Fluid film cavitation is treated using the π or half-film approach where any computed subambient pressures are set to ambient, thus defining the cavitation boundary.

- Fluid inertia effects are accounted for by adjusting the Reynolds solution. These effects result in a linear correction to the viscous damping term.
- Fluid supply conditions are determined by designating pressure to be equal to inlet pressure over the region of the supply hole or groove.
- Flow is determined by integrating around the boundary of interest. The local flow is calculated, using the computed pressure gradient, viscosity, and film thickness.
- The damper length is accounted for.
- As an implicit part of the Reynolds equation solution, the following are accounted for:
  - Finite orbit size or eccentricity
  - Damper clearance and diameter
  - Fluid viscous effects.

The squeeze film damper analysis uses a fixed Cartesian x-y coordinate system with origin at the bearing center, as shown in Figure 4-4. In this system the journal center has the coordinates x and y, the velocities dx/dt and dy/dt, and the accelerations d^2x/dt^2 and d^2y/dt^2. Points in the lubricant film are located by the axial coordinate z, measured from the centerplane, and by the circumferential angle θ, measured from the negative x-axis.

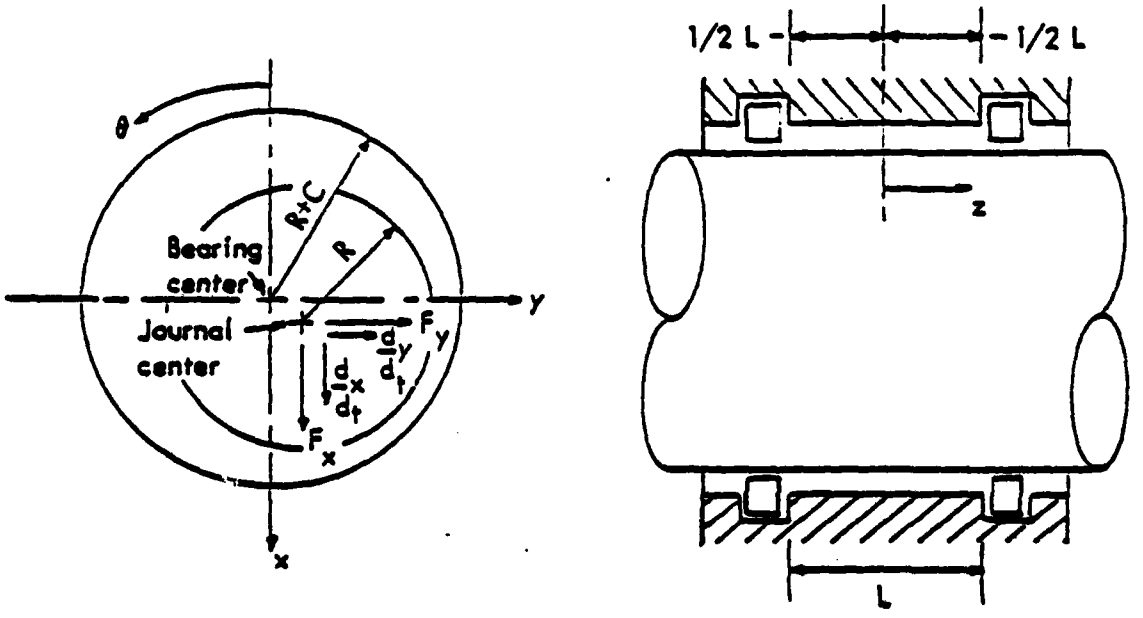

Figure 4-4 Squeeze film damper model. TE-80-123

The squeeze film damper outer cylinder supports a non-rotating bushing on an oil film. The bearing dimensions and lubricant properties are:

R = 1/2D = squeeze film inner radius, (m*)

L = land length, (m)

C = radial film clearance when centered, (m)

μ = lubricant viscosity, ($N.s/m^2$)

ρ = lubricant density, (kg/m^3)

x, y = bushing center coordinates (m)

θ = circumferential coordinate angle, measured from negative x-axis (radians)

z = axial coordinate, (m)

$h = C + x\cos\omega\tau + y\sin\omega\tau$ = local film thickness, (m)

τ = time, (sec)

q_k = flow from k'th feeding hole, (m^3/s)

f = reference** frequency, (Hz)

$\Omega = 2\pi f$ = reference** angular frequency, (rad/sec)

p = film pressure, (N/m^2)

Rotor Response Calculations

Within the squeeze film analysis, four damping coefficients (B_{xx}, B_{xy}, B_{yx}, and B_{yy}) and four inertia coefficients (C_{xx}, C_{xy}, C_{yx}, and C_{yy}) are determined, at constant supply pressure, for a given damper motion. The instantaneous forces exerted by the damper during orbit are

$$F_x = -B_{xx}\dot{X} - B_{xy}\dot{Y} - C_{xx}\ddot{X} - C_{xy}\ddot{Y}$$

$$F_y = -B_{yx}\dot{X} - B_{yy}\dot{Y} - C_{yx}\ddot{X} - C_{yy}\ddot{Y} \qquad (4\text{-}1)$$

---

* The units shown are metric. Equivalent English units also apply.

** A reference frequency is used to reduce intermediate pressure tables to non-dimensional form.

Linear Analysis with Circular Orbit

In the case of linear circular orbit

$$B_{yy} = B_{xx};\ B_{yx} = -B_{xy};\ C_{yy} = C_{xx};\ C_{xy} = -C_{yx} \qquad (4\text{-}2)$$

These damping inertia coefficients are used directly in the DDA linearized rotor dynamics analysis in which the journal orbit is treated as circular and at fixed radius.

Nonlinear Analysis with Circular Orbit

The circular orbit coefficient tables are used in DDA rotor dynamics analyses to carry out nonlinear steady-state rotor response calculations in the frequency domain. For these calculations the journal orbit radius is allowed to vary with response displacement, thereby introducing variable damping and inertia coefficients. Thus, the instantaneous forces, as defined by equation (4-1), also vary with response displacement.

Within the DDA rotor dynamics analysis, nonlinear circular orbit calculations, using the squeeze film damper analysis, are carried out iteratively. An initial response value of radial deflection is computed. Using this deflection, the damping and inertia coefficients are determined. These coefficients are used to form the real space forces on the rotor as defined by equation (4-1). A Newton-Raphson technique is used to solve for the next iteration until the solution converges. This is fully described in the Rotor/Damper interface section. If the calculated deflection exceeds the damper clearance the unbalance force is reduced and then increased incrementally with convergence at each step. A solution is attained when the unbalance reaches its original value.

Nonlinear Analysis with Noncircular Orbit

The DDA rotor dynamics analysis uses the table of Reynolds pressure coefficients of velocity and acceleration when the nature of the problem demands that noncircular orbits be considered. In cases such as the time history of nonsynchronous response to unbalance, the journal orbit is noncircular and the journal center velocity and acceleration components are not directly a

function of radial displacement. The damping and inertia coefficients are calculated based on pressure coefficients interpolated using the Reynolds pressure coefficient table. Thus, the forces defined in equation (4-1) are calculated for each rotor state (δ, $\dot{X}$, $\dot{Y}$, $\ddot{X}$, $\ddot{Y}$) in a given time step. Within each time step these forces are equilibrated, and the orbital trajectory is determined using a predictor-corrector technique.

SECTION V

ROTOR/DAMPER INTERFACE

Squeeze film dampers interface with the rotor dynamic analysis program in the following calculations:

- Linear
  - Undamped critical speeds - (Define need for squeeze film damping)
  - Log decrement - (Define squeeze film damping required for maximum modal damping)
  - Frequency domain response - (Define required squeeze film damper motion)
- Nonlinear
  - Frequency domain response - (Define overall unbalance response)
  - Time domain response - (Define suddenly applied load effects and 2 plane non-circular steady state response)

The linear calculations are performed using circular orbit, linearized coefficients. The non-linear calculations are performed using either circular orbit forces, computed from the coefficients, or non-circular orbit forces, computed from the velocity and acceleration pressure distribution tables. Each of these areas of calculation is discussed.

1. Linear Calculations

Squeeze film dampers are inherently non-linear devices as can be seen in the damper force plot of Figure 5-1. This characteristic was computed for circular whirl of a 4.5-inch diameter bearing with a length-to-diameter (L/D) ratio of 0.11 and a radial clearance C of 0.005 inches. The tangential (damping) force is relatively linear for an eccentricity ratio (e/C), between 0.0 and 0.6. For eccentricity ratios larger than 0.6 the damping increases rapidly. The radial (stiffness) force component is substantially lower than the tangential force through an eccentricity ratio of about 0.5. However, it is linear only through about 0.4. The radial force also has a stiffening characteristic for higher eccentricity ratios. Although the damper is clearly non-linear, certain information related to critical speeds,

AD-A129 021 DAMPER COMPONENT ANALYSIS AND INTEGRATION WITH ROTOR-DYNAMICS PROGRAM(U) MECHANICAL TECHNOLOGY INC LATHAM N Y J A TECZA ET AL. NOV 82 MTI-82TR61

UNCLASSIFIED AFWAL-TR-82-2112 F33615-79-C-2050 F/G 9/5 NL

2/2

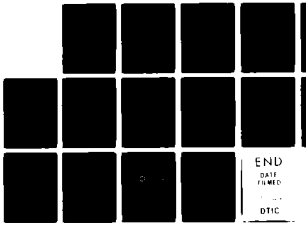

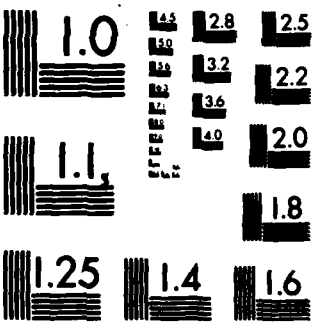

MICROCOPY RESOLUTION TEST CHART
NATIONAL BUREAU OF STANDARDS-1963-A

response to unbalance, and logarithmic decrement can be determined for quick screening purposes using effective stiffness and damping coefficients.

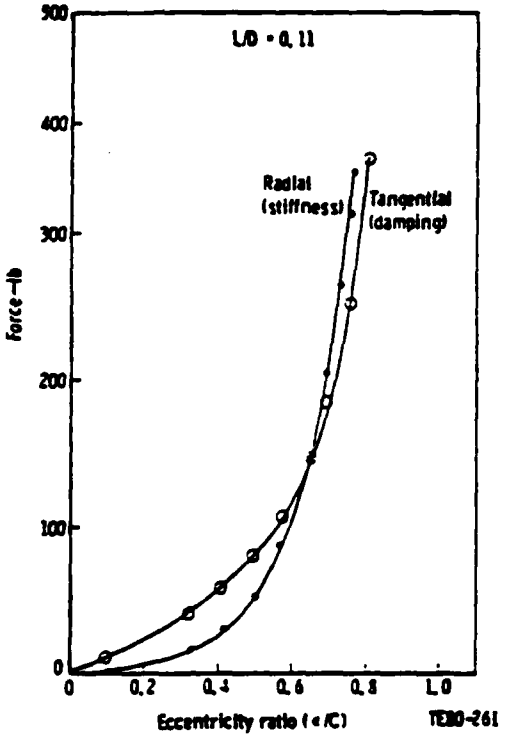

Figure 5-1. Squeeze film damper forces for circular whirl.

The damper component computer program, SQZDMP, described in earlier sections of this report, can produce stiffness and damping information in several forms. Circular orbit coefficients, computed as a ratio of tangential and radial force to tangential velocity for purely circular whirl are presented. These are the direct damping (B_{xx}) and cross-coupling damping (B_{xy}) coefficients. They are used in the following equation for the tangential and radial forces.

$$F_t = B_{xx} e \dot{\phi}$$

$$F_r = B_{xy} e \dot{\phi} \qquad (5\text{-}1)$$

where

F_t - tangential force (damping)

F_r - radial force (stiffness)

e - radial eccentricity (deflection)

$\dot{\phi}$ - whirl velocity

If an eccentricity, e and whirl speed, are assumed, then for circular whirl

$$F_t = B_{xx} e \dot{\phi} = (B_{xx} e) \dot{\phi}$$

$$F_r = B_{xy} e \dot{\phi} = (B_{xy} e) \dot{\phi} \qquad (5\text{-}2)$$

or

$$K_D = (1 + ig)K$$

$$K = B_{xy} \dot{\phi} \qquad (5\text{-}3)$$

$$g = B_{xx}/B_{xy}$$

where

K_D - dynamic stiffness coefficient (lb/in.)

K - spring stiffness coefficient (lb/in.)

g - structural damping coefficient

This allows the treatment of a damper as a dynamic stiffness element with linear radial stiffness and structural damping for an assumed circular orbit eccentricity and speed. This simplifies the numercial calculations and is only valid for linear steady state response calculations.

Another approach treats the damper as both a stiffness and a viscous damping element. Again, assuming a circular orbit eccentricity of e and a whirl speed of $\dot{\phi}$.

$$F_t = (B_{xx} e) \dot{\phi}$$

$$F_r = (B_{xy} e) \dot{\phi} \qquad (5\text{-}4)$$

or

$$K = B_{xy}\,\dot{\phi}$$

$$C = B_{xx} \qquad (5\text{-}5)$$

where

K = spring stiffness coefficient (lb/in.)

C = viscous damping coefficient (lb sec/in.)

When the whirling motion can no longer be considered as a centered, circular orbit, the problem is more complicated. However, there still is a need to evaluate the damper on a basis much simpler than becoming involved in a time history analysis. Therefore, provisions have been made in the damper component analysis to compute effective stiffness and damping values for non-circular orbits. These have been computed from a hysteresis loop relationship between force and displacement in orthogonal directions as indicated in Figure 5-2. The effective linear stiffness in the X direction, K_x, is the slope of the line joining points of maximum and minimum displacement. The effective linear damping coefficient is determined from the area enclosed by the hysteresis loop and the relationship indicated. This will produce a viscous damping coefficient, B_x. Similar effective linear coefficients are computed for the Y direction, K_y and B_y. These may be used in an asymmetric linear calculation or averaged for an assumed circular analysis. Structural damping coefficients may be obtained from the viscous coefficients by the relationship.

$$g_x = B_x\,\dot{\phi}/K_x$$

$$g_y = B_x\,\dot{\phi}/K_y \qquad (5\text{-}6)$$

where $\dot{\phi}$ is the whirl speed in rad/sec.

Each of these approaches to determining damper stiffness and damping coefficients is assimilated by computer program BB60 in open loop fashion (i.e. there is no computerized interface with these calculations). However, the ability to evaluate damping elements with these characteristics exists and are briefly described.

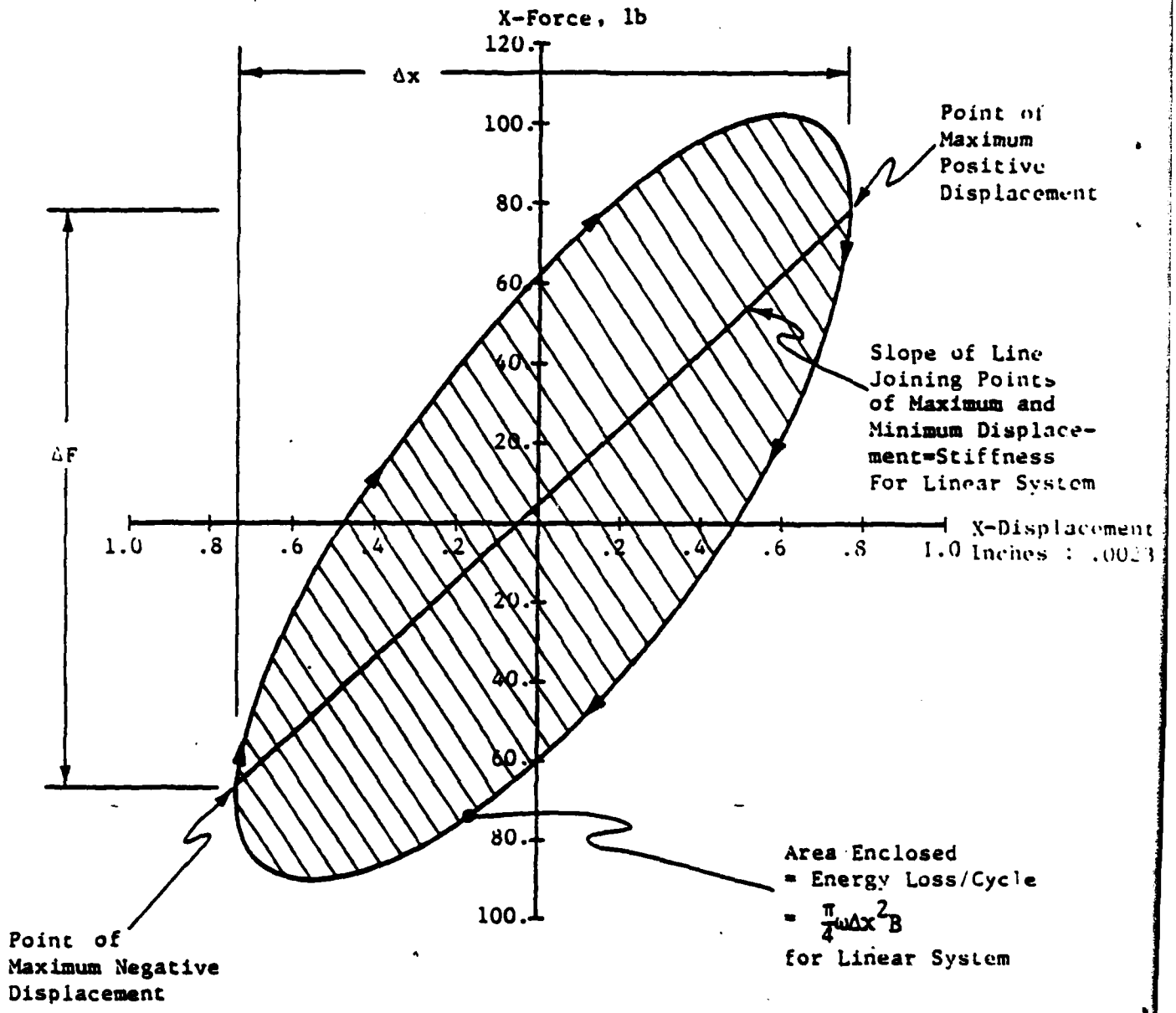

Figure 5-2. Typical hysteresis loop with definitions of quantities used for calculation of stiffness and damping

Undamped Critical Speeds

As previously stated in Section 4.0, all rotordynamics calculations are performed using a set of coupled system modes at zero speed as the basic degrees of freedom. These modes were generated from the modal synthesis of substructure pinned-pinned modes and coupled rigid body modes. The rigid body modes consider the systems to be rigid and coupled by interconnecting stiffnesses. A dynamic matrix is formed with gyroscopic effects included in the mass matrix. This is done by setting a speed ratio. This is the ratio of the undamped mode frequency to the system rotor speed. The degrees of freedom are the linear complete engine modes. The critical speeds and mode shapes are calculated for the rotor operating at specified ratios to the critical speeds. For a single-rotor engine, the speed ratio would be 1.0. A two-rotor system would have two sets of critical speeds. For example, an engine with a counterrotating rotor with rated rotor speeds of 10,000 and 7,500 rpm would have speed ratios sets of (1.0, -0.75) and (-1.33, 1.0). The first set of modes are excited by the first rotor, and the second set of modes are excited by the second rotor. The analysis is performed in modal space, and the results are converted to real space before output. Frequency-speed maps can be generated with this calculation procedure by performing the calculation at various speed ratios. The calculation will allow the estimate of damper effects on critical speeds and mode shapes as a first order evaluation.

Logarithmic Decrement

The logarithmic decrement (log dec) calculation is used to determine the mount damping required for maximum modal damping. The damped modal natural frequencies and associated log dec may be plotted as a root locus with mount damping varied. This information is used to select the amount of desirable squeeze film damping.

This calculation is specifically used to determine the effect of direct and indirect damping on mode damping and frequencies. Two options are available for log dec calculations. The first accepts a direct viscous damping input and calculates log dec. The second accepts a damper eccentricity and interpolates

for both direct and indirect damping. Input of damper eccentricity is included on the squeeze film damper input card to BB60. The method for calculation is the same in both cases and is given below.

The log dec calculation involves the solution of the following modal differential equations.

$$[M](\ddot{h}) + [C](\dot{h}) + [K](h) + [I_G](\dot{h}) = (o) \qquad (5\text{-}7)$$

where

$[M]$ = modal mass matrix

$[K]$ = complex stiffness matrix substructure with mount structural damping

$[C]$ = viscous damping matrix in modal degrees of freedom

$[I_G]$ = gyroscopic inertia matrix

Ω = rotor speed

(h) = vector of modal participations

Each modal degree of freedom has associated with it a normalized deflected mode shape. The coupled modes will include participation of all uncoupled modes. The complex vector (h) will be the participation vector of the uncoupled modes.

The solution of the coupled modal differential equation is obtained by letting $h = h_o e^{\lambda t}$.

where

λ - complex eigenvalues = $r + iw$

r - modal damping

w - damped natural frequency

The characteristic equation becomes:

$$\left|\lambda^2[M] + \lambda[[C] + [I_G] + [K]]\right| = 0 \qquad (5\text{-}8)$$

The energy dissipation for the mounts will be transformed from local to modal degrees of freedom to be included in the modal damping matrix

$$[C] = [\beta]^T [C_{SF}] [\beta] \tag{5-9}$$

where $[C_{SF}]$ - squeeze film damping matrix in local degrees of freedom (X)

$X = [\beta](h)$, $[\beta]$ - is the transformation matrix

The log dec will be calculated for each mode as: $\delta = -\frac{r}{w}$ where $w \neq 0$ and is in RAD/SEC.

Steady State Response

The results of this analysis are the forced deflections at each of the mass station due to an imposed unbalance distribution. With the optimum mount damping input, the resulting response at the mount is that expected for the damper or dampers. To keep the damping in the linear range the target squeeze film radial clearance is set to 1.7 times the 1/2 peak-to-peak response.

The input damping is included as part of the viscous damping matrix or as an imaginary stiffness component. For steady state response the damping may be included using either approach. In BB60 it is included as an imaginary stiffness ratio (g) or as a viscous damper (c).

The equation solved is written as follows:

$$[M] \langle \ddot{q} \rangle + [C] \langle \dot{q} \rangle + [K] \langle q \rangle = \langle F \rangle \tag{5-10}$$

where M is the mass matrix with gyroscopic terms included as previously discussed.

$[C]$ is the damping matrix

$[K]$ is the complex stiffness matrix

$\langle q \rangle$ is the displacement degrees of freedom

$\langle F \rangle$ is the forcing function due to rotating unbalance

The zero frequency undamped mode shapes are calculated using the real part of the stiffness matrix $[K]$ and the mass matrix $[M]$ without gyroscopic terms. The transformation from displacement to undamped zero frequency modal degrees of freedom $\{h\}$ is:

$$\{q\} = [P]\{h\} \tag{5-11}$$

$\{h\}$ - will be referred to as the modal displacement participation factors in the remaining discussion.

The dynamic matrix may be written as follows:

$$[D] \equiv [K] + \Omega[C]\, i - \Omega^2 [M] \tag{5-12}$$

where Ω is the rotor speed at which the unbalance occurs.

$[D]\{q\} = \{F\}$ can be written for modal degrees of freedom as:

$$[P]^T[D][P]\{h\} = [P]^T\{F\} \tag{5-13}$$

This reduces the computational complexity.

2. Nonlinear Calculations

The linear calculations just described are useful in screening damper designs and allow the elimination of damper variables and configurations which are unsatisfactory. It provides an analysis which can be used to "get in the neighborhood" of a solution. Nonlinear analyses must then be conducted to further quantify the effects of squeeze film dampers on the rotor dynamic behavior of a rotor system. The damper component software, described in earlier sections, has been combined with the rotor dynamic software, described in Section IV, to provide coupled evaluations of dampers in gas turbine engines. The resulting coupled response analyses in the frequency and time domain are discussed.

Steady State Response

This routine calculates steady state, circular orbit response for specific squeeze film designs and is used to make damper refinements.

The coupled rotor/damper analysis for frequency domain response is performed with the squeeze film damper forces included as external forcing functions which are dependent on mount displacement. Therefore, the solution is iterative. The squeeze film damper forces are a function of absolute displacement and are resolved into radial and tangential components for use in BB60. The complex dynamic matrix that was calculated for the linear response problem is now expanded for real and imaginary response components. The reason for this will be shown later.

$$[DD]\{h\} = [P]^T[D][P]\{h\} = [P]^T\{F\} = \{Q\}$$

$$[DD] = [DD_R] + [DD_I]\,i$$
$$\{h\} = \{h_R\} + \{h_I\}\,i \qquad (5\text{-}14)$$
$$\{Q\} = \{Q_R\} + \{Q_I\}\,i$$

$$[DD_R]\{h_R\} - [DD_I]\{h_I\} = \{Q_R\}$$
$$[DD_I]\{h_R\} + [DD_R]\{h_I\} = \{Q_I\} \qquad (5\text{-}15)$$

The generalized force vectors for the nonlinear response calculation includes the squeeze film reaction forces f ($[q]$). These forces are stored in tables of the radial and tangential forces versus displacement eccentricity ($[q]/C$), where C is the squeeze film clearance. The radial $f_R([q])$ and the tangential $f_T([q])$ forces are rotated into BB60's real displacement coordinates by the following equations: $F([q]) = f_R([q]) + if_T([q])$

$$\mathrm{Re}(B([q])) = f_R([q])\frac{\mathrm{Req}}{[q]} - f_T([q])\frac{\mathrm{Imq}}{[q]} \qquad (5\text{-}16)$$

and

$$\mathrm{Im}(B([q])) = f_R([q])\frac{\mathrm{Imq}}{[q]} + f_T([q])\frac{\mathrm{Req}}{[q]}$$
$$\{Q_R^P\} = \{Q_R\} - [P^T]\{\mathrm{ReB}([q])\} \qquad (5\text{-}17)$$
$$\{Q_I^P\} = \{Q_I\} - [P^T]\{\mathrm{ImB}([q])\}$$

$\{Q_R^P\}$ and $\{Q_I^P\}$ replace $\{Q_R\}$ and $\{Q_I\}$

on right hand side of equations.

Since the squeeze film forces are iteratively determined from the relative displacement of the journal, the equation will not exactly balance and a residual force $\{f_\Delta([q])\}$ may be calculated

$$\{f_\Delta([q])\}_R = [DD_R]\{h_R\} - [DD_I]\{h_I\} + [P^T]\{ReB([q])\} - \{Q_R\}$$

$$\{f_\Delta([q])\}_I = [DD_I]\{h_R\} + [DD_R]\{h_I\} + [P^T]\{ImB([q])\} - \{Q_I\} \qquad (5\text{-}18)$$

To converge the residual forces to zero a Newton Raphson iteration is used

$$\Delta\{q_i\} = -\frac{\partial\{q_i\}}{\partial\{f_\Delta(|q_i|)\}}, \qquad \{q_{i+1}\} = \{q_i\} + \Delta\{q_i\}$$

$$\{f_\Delta([q])\} = \begin{Bmatrix} f_\Delta(|q|)R \\ f_\Delta(|q|)I \end{Bmatrix} \qquad [DD]_T = \left[\begin{array}{c|c} [DD_R] & -[DD_I] \\ \hline [DD_I] & [DD_R] \end{array}\right] \qquad (5\text{-}19)$$

$$\frac{\partial\{f_\Delta(|q|)\}}{\partial\{q\}} = [DD]_T + \underbrace{[P]^T[J(B(|q|))][P]}_{\text{Sum over all non-linear mounts}}$$

where

$$[J(B(|q|))] = \left[\begin{array}{c|c} \frac{\partial ReB}{\partial Req} & \frac{\partial ReB}{\partial Imq} \\ \hline \frac{\partial Imb}{\partial Req} & \frac{\partial ImB}{\partial Imq} \end{array}\right] \qquad (5\text{-}20)$$

$$\frac{\partial ReB(q)}{\partial Req} = \frac{1}{|q|^2}\left\{\frac{\partial f_R}{\partial|q|}(Req)^2 + f_R\left[|q| - \frac{(Req)^2}{|q|}\right] - (Req)(Imq)\left[\frac{\partial f_T}{\partial|q|} - \frac{f_T}{|q|}\right]\right\} \qquad (5\text{-}21)$$

Req = Real part of q
Imq = Imaginary part of q

$$\frac{\partial ReB(q)}{\partial Imq} = \frac{1}{|q|^2}\left\{(Req)\ (Imq)\ \left[\frac{\partial f_R}{\partial |q|} - \frac{f_R}{|q|}\right] - \frac{\partial f_I}{\partial |q|}\ (Imq)^2 - f_T\left[|q| - \frac{(Imq)^2}{|q|}\right]\right\} \tag{5-22}$$

$$\frac{\partial ImB(q)}{\partial Req} = \frac{1}{|q|^2}\left\{(Req)\ (Imq)\ \left[\frac{\partial f_R}{\partial |q|} - \frac{f_R}{|q|}\right] + \frac{\partial f_T}{\partial |q|} + f_T\left[|q| - \frac{(Req)^2}{|q|}\right]\right\} \tag{5-23}$$

$$\frac{\partial ImB(q)}{\partial Imq} = \frac{1}{|q|^2}\left\{(Imq)^2\ \frac{\partial f_R}{\partial |q|} + f_R\left[|q| - \frac{(Imq)^2}{|q|}\right] + (Req)\ (Imq)\left[\frac{\partial f_T}{\partial |q|}\left[\frac{\partial f_T}{\partial |q|} - \frac{f_T}{|q|}\right]\right]\right\} \tag{5-24}$$

The terms do not satisfy the Cauchy-Riemann conditions for analytic complex functions. This means that

$$\frac{\partial ReB(|q|)}{\partial Req} \neq \frac{\partial Im(B(|q|))}{\partial Imq} \tag{5-25}$$

and

$$\frac{\partial ReB(|q|)}{\partial Imq} \neq \frac{-\partial ImB(|q|)}{\partial Req}$$

Consequently, the matrix $[DD]$ was expanded into real and imaginary parts.

The iteration is begun by assuming the squeeze film forces to be zero and calculating the displacement of the mount. If the displacement is less than the damper clearance the derivatives $\frac{dB_{xx}}{de}$ and $\frac{dB_{xx}}{de}$ are calculated from a spline fit of the tabular data in the vicinity of the calculated displacement $[q]$. The eccentricity e is equal to $[q]/C$.

If the damper clearance c is exceeded, then the unbalance forces $\{F\}$ are reduced and then incremented upward to reach the original unbalance. The final values of the state variables are used as starting values for the next iteration.

The radial and tangential forces f_R and f_T used in the iteration are calculated as follows:

$$f_R = - Bxx\Omega\ q\ + Cxy\Omega^2\ q$$
$$f_T = - Bxy\Omega\ q\ + Cyy\Omega^2\ q \qquad (5\text{-}26)$$

This analysis assumed circular orbits so that f_R and f_T are steady rotating forces.

The radial and tangential force derivatives are given below:

$$\frac{df_R}{d|q|} = \left(\frac{f_R}{|e|} - \frac{dB_{xx}}{d|e|} - \Omega|q| + \frac{dC_{xy}}{d|e|} - \Omega^2|q|\right)\frac{1}{c}$$
$$\frac{df_T}{d|q|} = \left(\frac{f_T}{|e|} - \frac{dB_{xy}}{d|e|} - \Omega|q| + \frac{dC_{yy}}{d|e|} - \Omega^2|q|\right)\frac{1}{c} \qquad (5\text{-}27)$$

They are written with the clearance (c) factored out.

The coordinate system used for the rotor dynamic analysis is left-handed and is right-handed for the damper component analysis. Figure 5-3 compares the two coordinate systems. Figure 5-4 gives an overview of the non-linear steady state calculation.

Time Domain Response

So far the discussion has covered the case of coupled rotor/damper analyses having orbits with circular symmetry. The general case of damper motion is noncircular and non-centered in the damper clearance space. The proper approach to evaluating this condition is to use a time domain solution so that the non-circular orbit can be tracked as a function of time and noncircular state variables and damper forces can be computed. DDA has modified it's existing rotor dynamic transient analysis to incorporate the effects of a squeeze damper for both circular and non-circular whirl. The following is a discussion of the DDA time domain response calculation followed by discussions of the circular orbit and non-circular orbit interfaces.

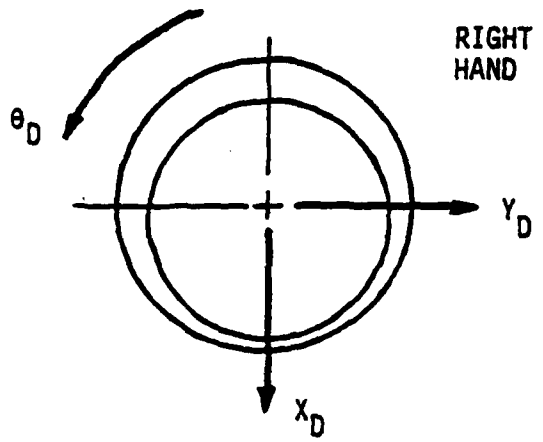

a) Damper Component Coordinate System

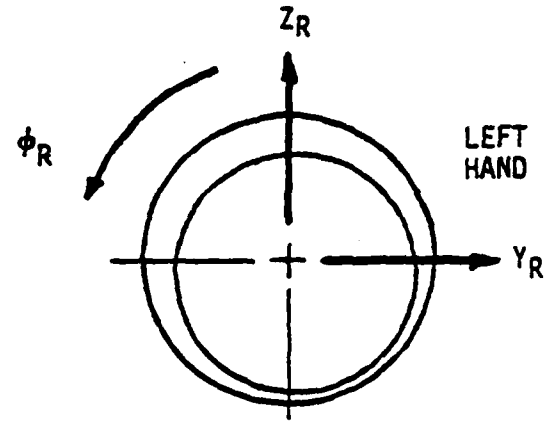

b) Rotor Dynamic (8860) Coordinate System

	Damper Component	Rotor Dynamic
Rotor to Damper	X_D	$-Y_R$
	X_D	$-Y_R$
	X_D	$-Y_R$
	Y_D	Z_R
	Y_D	Z_R
	Y_D	Z_R
Damper to Rotor	F_{XD}	F_T
	$-F_{YD}$	F_R

c) Coordinate Transformations

Figure 5-3. Comparison of Component and System Coordinate Systems.

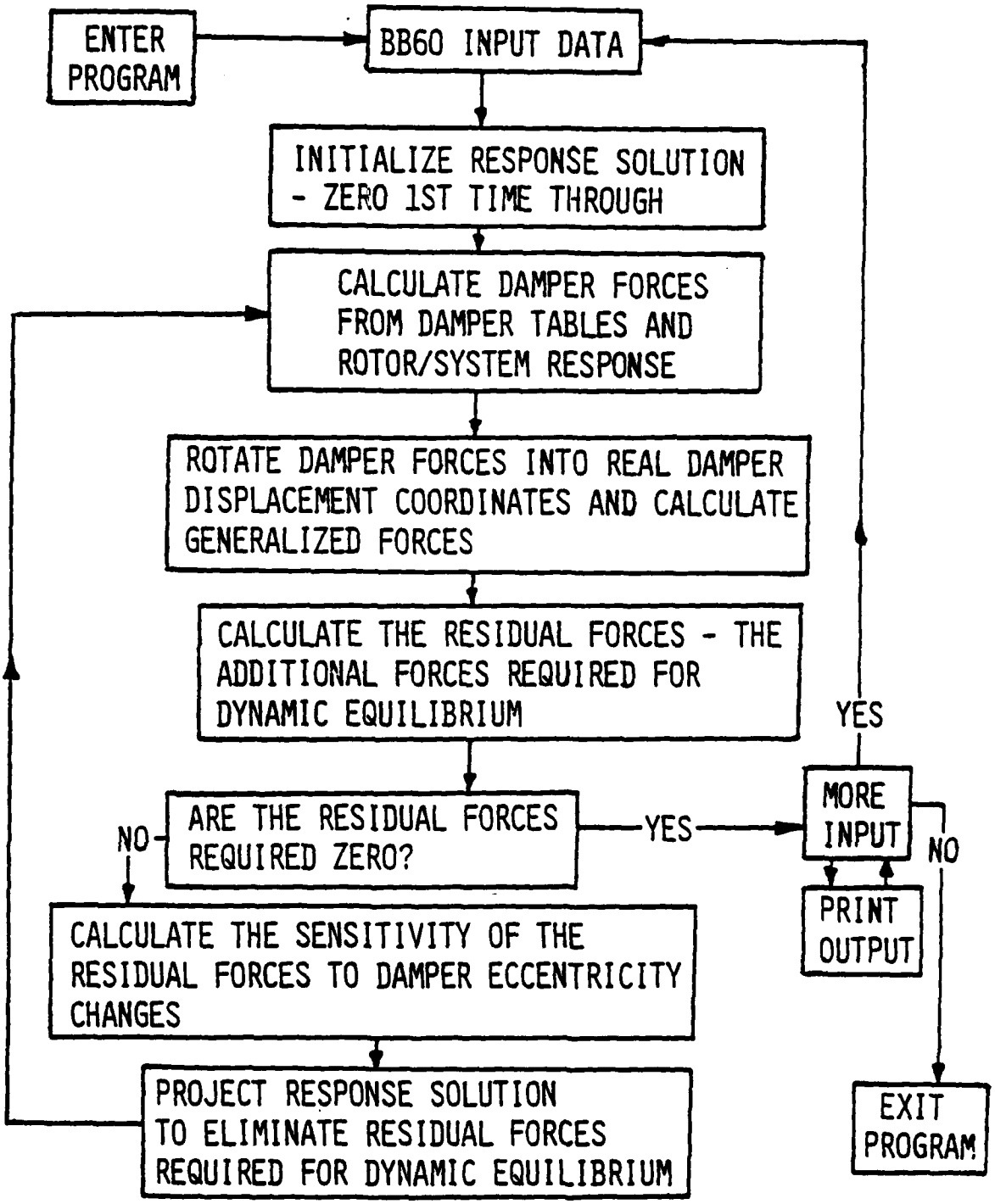

Figure 5-4 Overview of non-linear steady state response calculation

Response Calculation

This analysis calculates the response of the engine to various shock excitation such as

- Initial velocity (a drop)
- Half sine displacement
- Rectangular displacement
- Series displacement
- Versine displacement
- Half sine acceleration
- Rectangular acceleration
- Series acceleration
- Versine acceleration
- Suddenly applied unbalance

The displacement shocks are displacements of the ground while the acceleration shocks are applied to the engine. The series shock input is a fourth order polynominal. The option of most initial interest for rotor dynamics is the time response to suddenly applied unbalances. It is with this option that evaluations will be made as to the coupled effect of squeeze film dampers on rotor dynamic behavior during conditions of blade loss. If the transient solution is allowed to decay, the steady state solution results. This method, which considers the effects of gravity, is a more accurate model of rotor/damper systems which have offset noncircular orbits. An additional feature also allows the evaluation of the rotor/damper system using circular orbit coefficients. The solution is capable of analyzing either linear or nonlinear systems.

The calculation is performed in modal space with a time marching integration. A predictor-corrector method with a variable time step is used. The basic equations are:

$$\left.\begin{aligned} \{\dot{X}\} &= \{\ddot{X}\}_{i-1} + \Delta t\left[1.5\{\ddot{X}\}_{i-1} - .5\{\ddot{X}\}_{i-2}\right] \\ \{X\} &= \{X\}_{i-1} + .5\,\Delta t\left[\{\dot{X}\}_{i-1} + \{\dot{X}\}_{i}\right] \end{aligned}\right\} \text{Predictor } \{\ddot{X}\}_i = [M]^{-1}\{F\}_i$$

$$\{F\} = \{F_L\}\cos\frac{t}{2\pi n} + \{F_v\}\sin\frac{t}{2\pi n} - [K]\{X\} + \{F_a\} - [S]\{\dot{X}\} + \{L_N\} \qquad (5\text{-}28)$$

$$\left.\begin{aligned} \{\dot{X}\}_i &= \{\dot{X}\}_{i-1} + \Delta t\left[\frac{5}{8}\{\ddot{X}\}_{i-1} - \frac{1}{16}\{\ddot{X}\}_{i-2} + \frac{7}{16}\{\ddot{X}\}_{i}\right] \\ \{X\}_i &= \{X\}_{i-1} + \Delta t\left[\frac{5}{8}\{\dot{X}\}_{i-1} - \frac{1}{16}\{\dot{X}\}_{i-2} + \frac{7}{16}\{\dot{X}\}_{i}\right] \end{aligned}\right\} \text{Corrector}$$

where

$\{F\}$ is the modal force vector

$\{F_L\}$ is the modal lateral force due to unbalance

$\{F_V\}$ is the modal vertical force due to unbalance

$\{X\}$ is the modal displacement

$[K]$ is the diagonal modal stiffness matrix

$\{F_a\}$ is the modal force due to acceleration

$[S]$ is the damping gyroscopic matrix

$\{L_n\}$ is the modal forces due to nonlinearities

This is calculated at each step from the displacements and nonlinear mounts.

$[M]$ is the diagonal modal mass matrix

The interface between this calculation in the rotor dynamic program and the damper component program is made through the modal force vector L_N. The damper reactions at each increment of time are treated as modal forces. The modal forces need to be re-evaluated at each of these increments in terms of the real space state variables (i.e. vertical and lateral displacement, velocity, and acceleration). This is described in the section called Non-Linear Steady State Response Calculation in some detail along with the dynamic matrix equation. The state variables are passed to interpolation routines, one for circular orbit (1 plane) and another for noncircular orbit

(2 plane). Again the calling state variables are transformed to account for differences in the coordinate system as seen in Figure 5-3. The state variables are defined as:

Damper Variables	Rotor Variables
X_D	$-Y_R$
X_D	$-Y_R$
X_D	$-Z_R$
Y_D	Z_R
Y_D	Z_R
Y_D	Y_R

With this transformation the forces returned from the interpolation routines for rotor program use are $-F_{YR}$ and F_{ZR}. As in the circular orbit, nonlinear, steady state calculation, the real space forces are transformed to modal forces L_N by the equation

$$\{L_N\} = [f]\{F_{RE}\} \tag{5-29}$$

where, as before

$[f]$ - matrix of mode shapes
$\{F_{RE}\}$ - real space complex force vector

This process is repeated at each time step in the simulation.

Circular Orbit Interface

The interface with the circular orbit option of the time domain response calculation is made through a call to the interpolation subroutine FIND in the same manner described for the circular orbit, steady state analysis. FIND interpolates the circular orbit, normalized coefficient tables. The coefficients are converted to real dimensions and the F_{XD} and F_{YD} forces are computed using equation (5-29). As before, the forces which are returned to the calling routine in BB60 are opposing motion along the Z_R and Y_R orthogonal axes and are respectively, $-F_{YR}$ and F_{ZR}. The only difference

between this interface and the interface with the steady state, circular orbit calculation is that nonzero values of the rotor X_D velocity and Y_D acceleration are used. The important aspect of this interface relates to the difference in the rotor dynamic and damper component coordinate systems. As a result, two coordinate transformations are required. The rotor dynamic state variables must be transformed to the damper component coordinate system prior to calling subroutine FIND. This permits the calculations to occur in the damper analysis in its programmed coordinates. However, upon the return of forces to the rotor dynamic analysis, the forces must be transformed from the damper coordinate system to that of the rotor. This procedure is indicated in Figure 5-4. Figure 5-5 gives an overview of the non-linear time transient analysis.

Noncircular Orbit Interface

The interface with the noncircular orbit option of the time domain response calculation is made through a call to the interpolation subroutine FORCE. Values called to the subroutine from the damper analysis are values of the state variables which have been transformed to account for differences in the damper and rotor coordinate systems (Figure 5-3). Within the subroutine the damper forces F_{XD} and F_{YD} of the damper component analysis are computed from stored pressure data. These data assume the bearing to have axisymmetric geometry so that the only parameter is eccentricity e. The stored data refer to a rotating coordinate system and are used to compute the rotating damper forces. These are then transformed to the fixed X_D-Y_D coordinate system. The values of F_{XD} and F_{YD} are then returned to the calling routine as $-F_{YR}$ and F_{ZR} respectively for BB60 use.

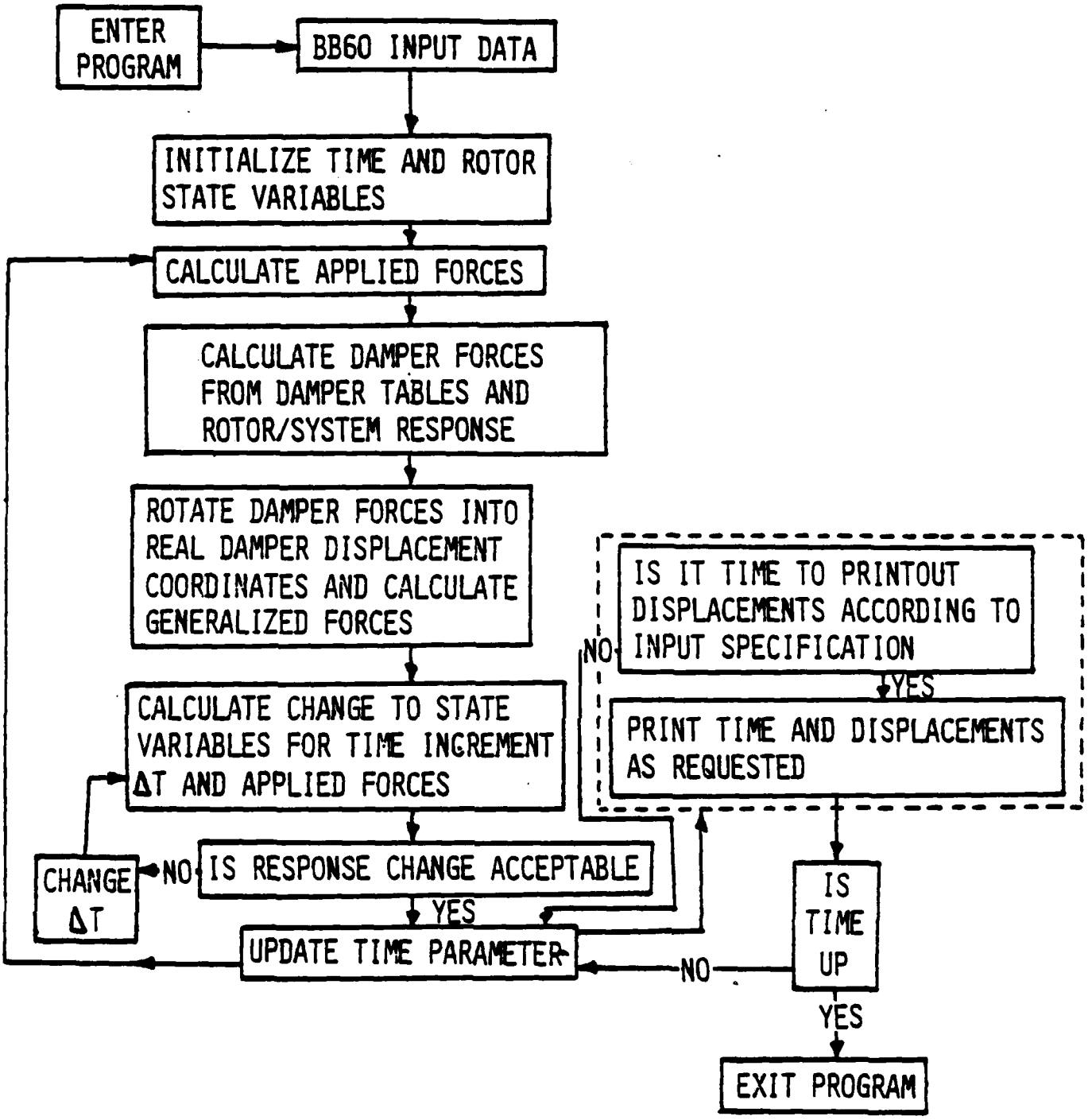

Figure 5-5 Overview of non-linear time transient analysis

SECTION VI

SAMPLE ROTORDYNAMICS PROBLEM

The analytical tools that have been described are demonstrated here for a typical jet engine. A system geometric representation is given in Figure 6-1 which shows the O.D. and I.D. plotted versus engine station for the rotor and case. This information is used to develop the engine stiffness model. Masses and inertias are lumped at locations along the rotor to represent the compressor and turbine stages. Masses are also distributed along the case. The rotor is mounted to the case at engine stations 0.0 and 65.70. The case is also mounted to ground at stations 0.0 and 65.70. The aft rotor mount has a 150,000 lb/in. isolator in series with the bearing. The forward mount is in series with a squeeze film damper. A 100,000 lb/in. isolator is in parallel with the damper. The damper film is 10.34 inches in diameter and its width is 2.59 inches. The oil is fed through unsealed ends.

The sample analyses shown here include calculations of:

- Critical Speeds
- Log Dec
- Response to Unbalance (Steady State)
  - Normal
  - Abusive
- Time Transient (Shock Loading)
  - Small Unbalance (Normal)
  - Blade Loss (Abusive)

The critical speeds and mode shapes for this sample problem are shown in Figure 6-2 for a front rotor to case stiffnesses of 500,000 and 100,000 lb/in. These plots may be made automatically when requested in the rotor dynamic input.

Figure 6-3 shows the damped eigenvalues for the typical jet engine with front compressor mount viscous damping varied. The parallel stiffness is held constant at 100,000 lbs/in. This shows the effect of direct damping only.

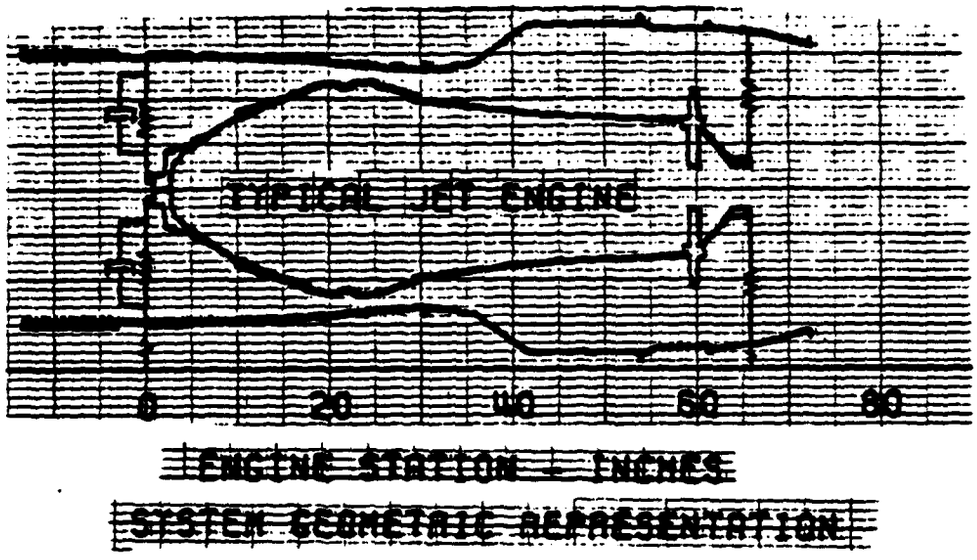

ROTOR (COMPRESSOR AND TURBINE)

WEIGHT = 810 LBS

C.G. = 37.4 IN

PITCHING INERTIA ABOUT C.G. = 1172 LB-SEC^2/IN

MOUNTED FRONT - 100,000 LBS/IN ISOLATOR + SQUEEZE FILM DAMPER

BACK - 150,000 LBS/IN ISOLATOR

1ST PINNED MODE = 9,900 CPM

CASE

WEIGHT = 1687 LBS

C.G. = 29.8 IN

PITCHING INERTIA ABOUT C.G. = 3528 LB-SEC^2/IN

MOUNTS FRONT - 200,000 LBS/IN

BACK - 50,000 LBS/IN

1ST PINNED MODE = 7,370 CPM

Figure 6-1 Sample problem input description

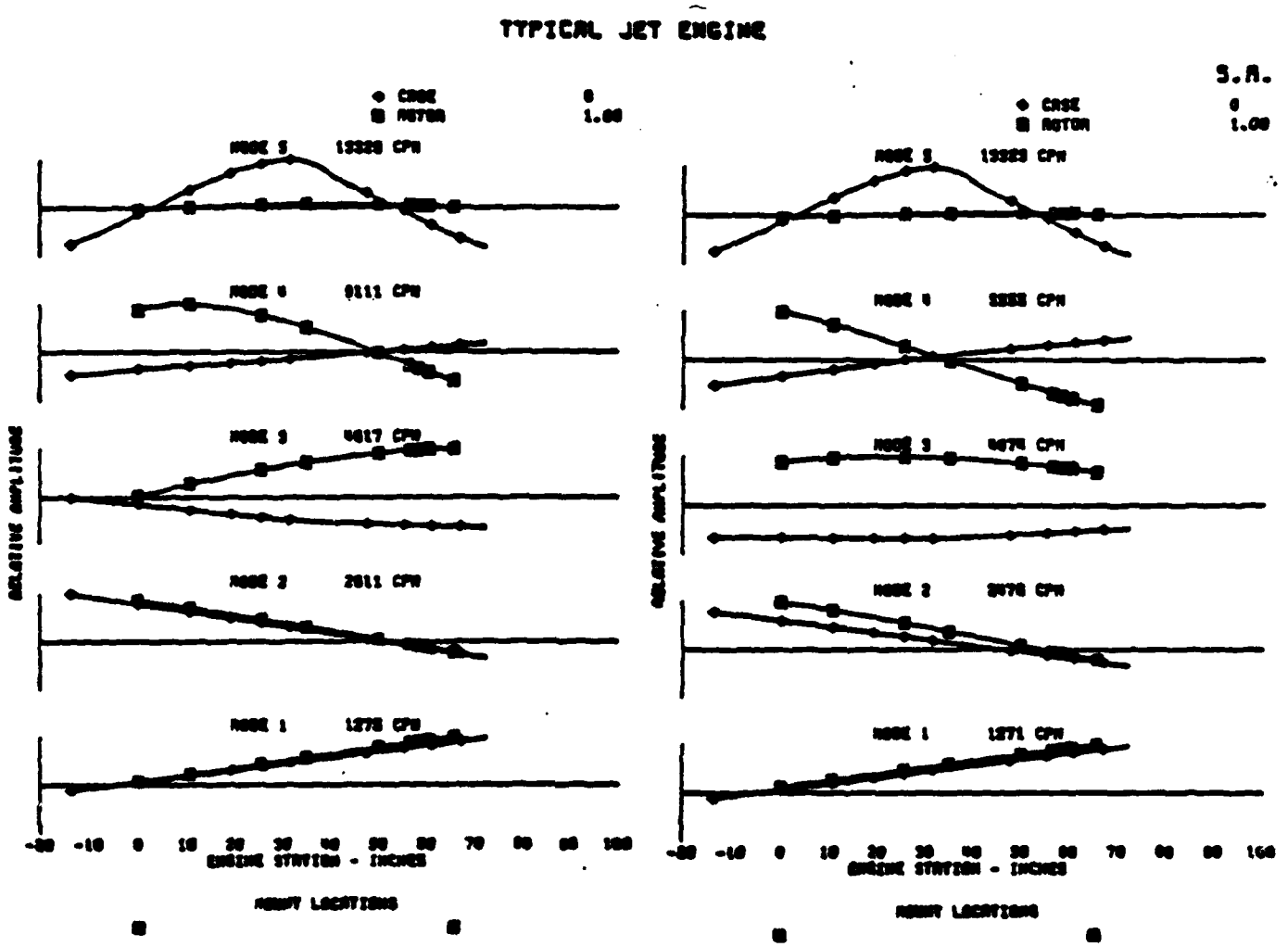

STA 0.0 500,000 LBS/IN

STA 0.0 100,00 LBS/IN

Figure 6-2 Critical speeds and mode shapes

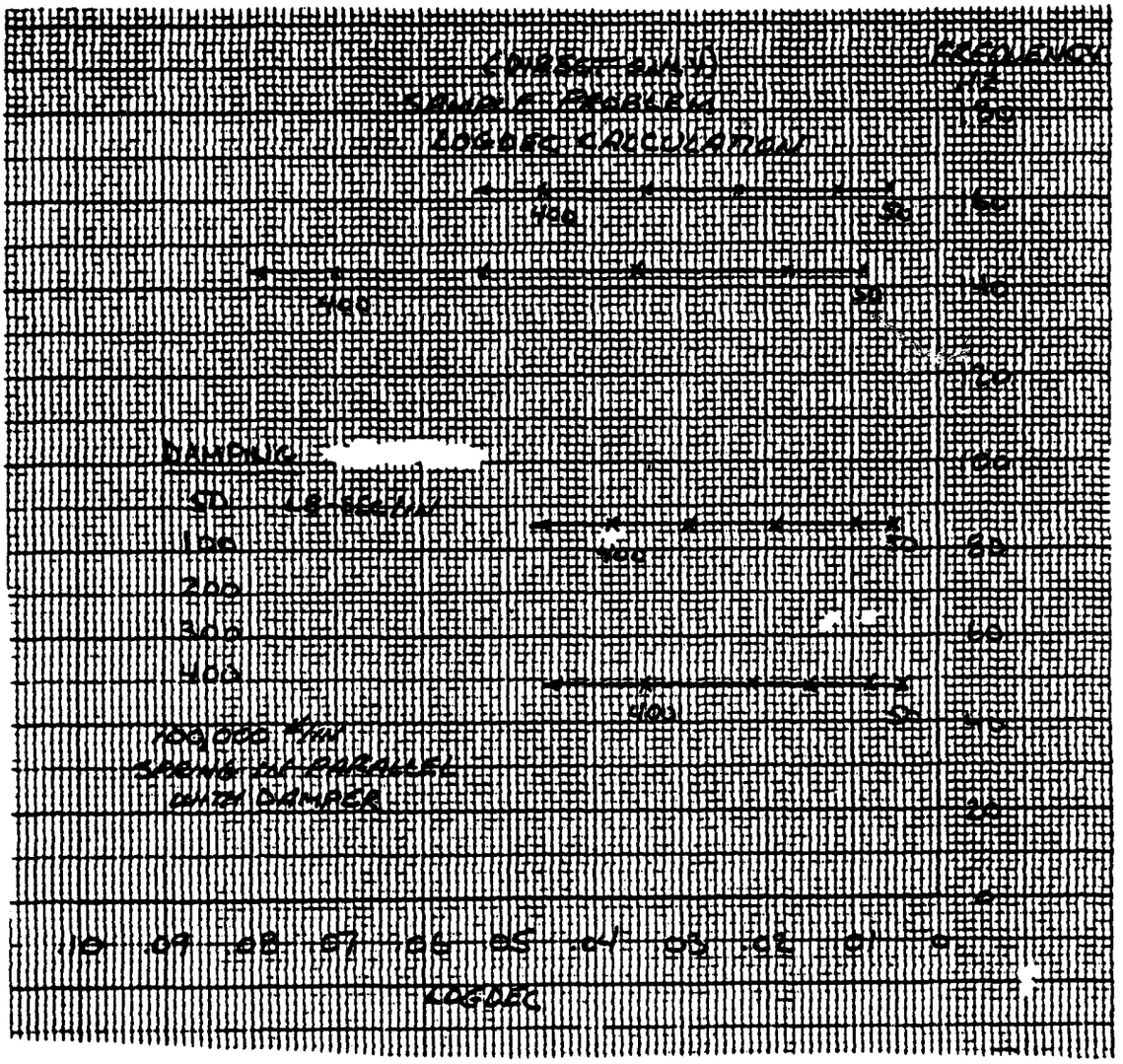

Figure 6-3

Sample Problem for Log Dec Calculation, Direct Damping Varied

Figure 6-4 shows the damped eigenvalues with both direct and indirect viscous damping varied. The variable is the squeeze film damper eccentricity.

The log dec calculation just demonstrated would be used to help size and understand the operation of the squeeze film damper.

The steady state response is shown in Figures 6-5 and 6-6 for a normal unbalance of 2 ounce inches and for a blade loss with 19.5 in/lbs unbalance 2.28 inches aft of the damper. Automatic plotting of response vs. speed is available if requested. The rotor time transient response, for abusive unbalance, at the squeeze film damper is shown in Figure 6-7 for a damper with a clearance of 7 mils. The transient analysis uses circular orbit coefficients. The case response at the squeeze film is also given. The case is responding mostly at its two lowest rigid body frequencies of 20 Hz and 40 Hz. Figure 6-8 shows the transient response for a normal unbalance. These analyses just demonstrated would be typically used to design a squeeze film damper.

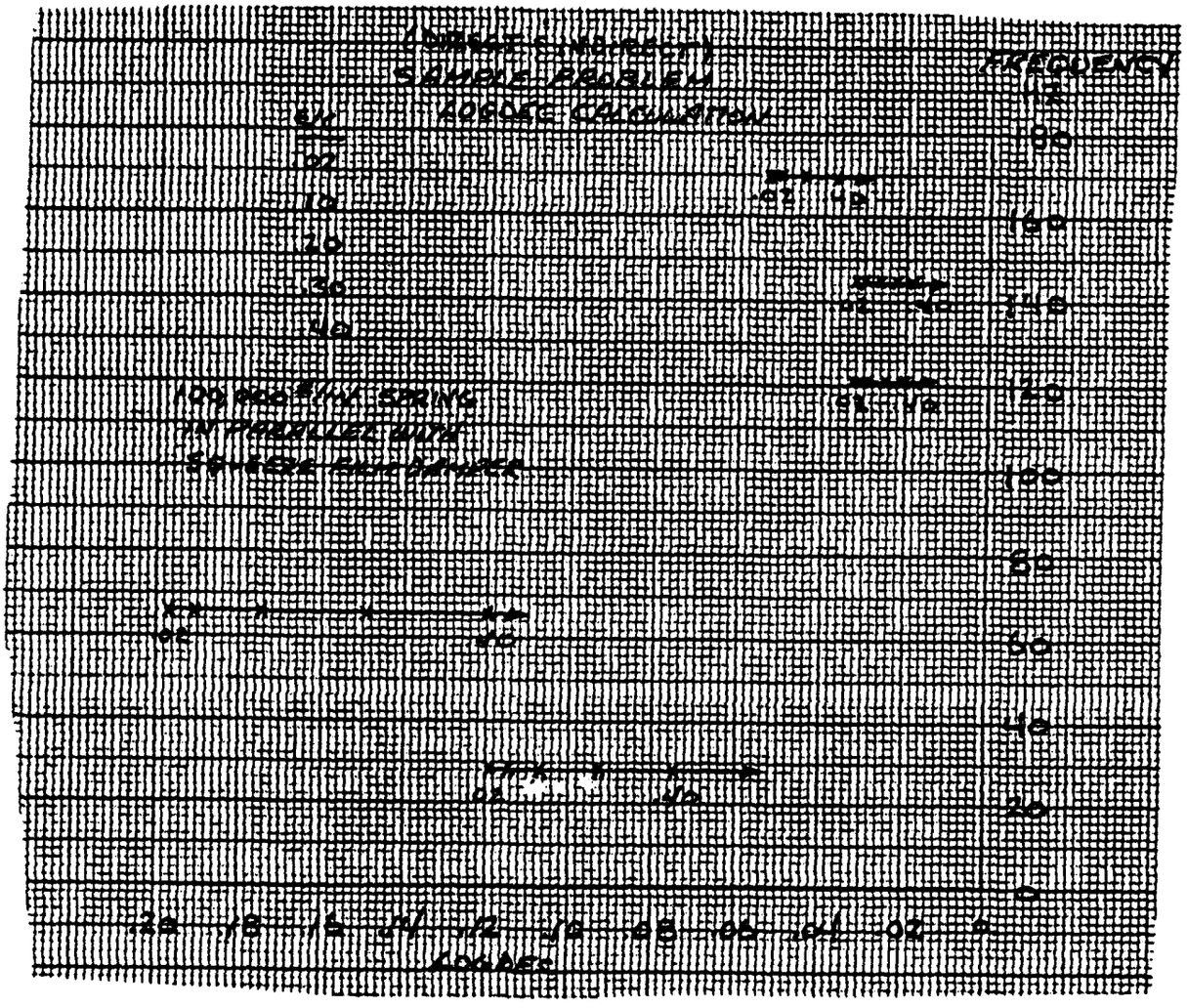

Figure 6-4

Sample Problem for Log Dec Calculation, Direct and Indirect Damping Varied

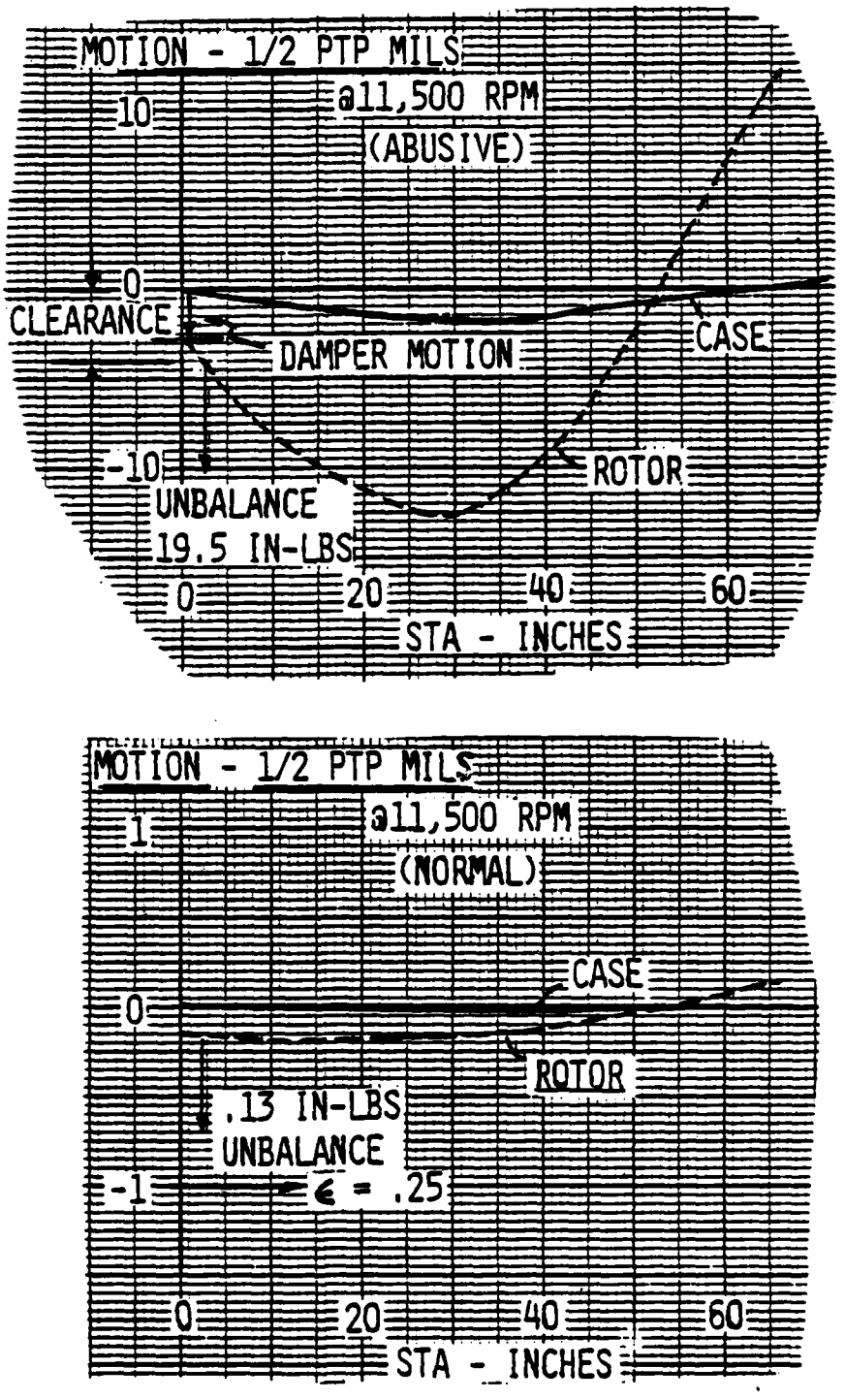

Figure 6-5 Steady State Response vs. Station

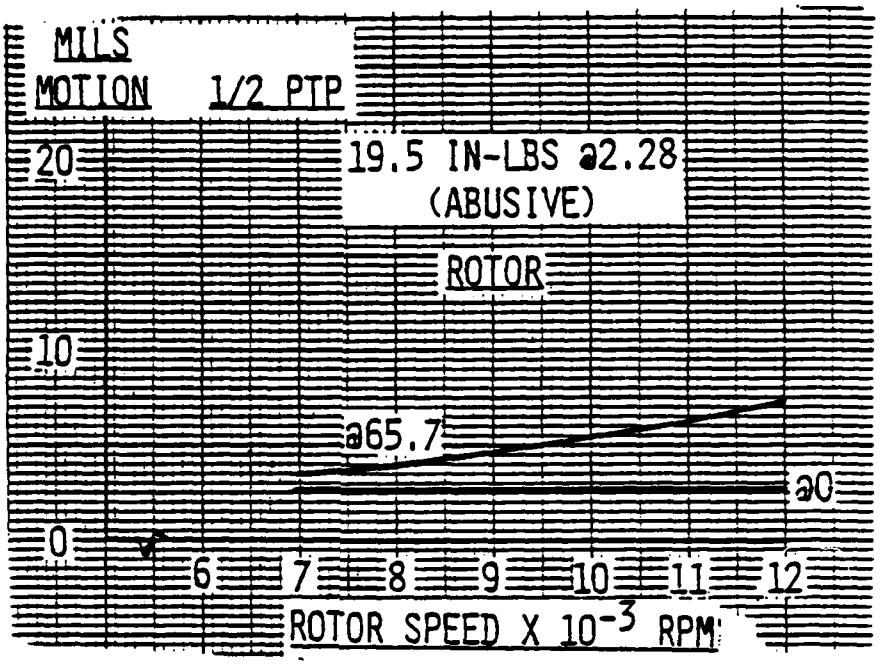

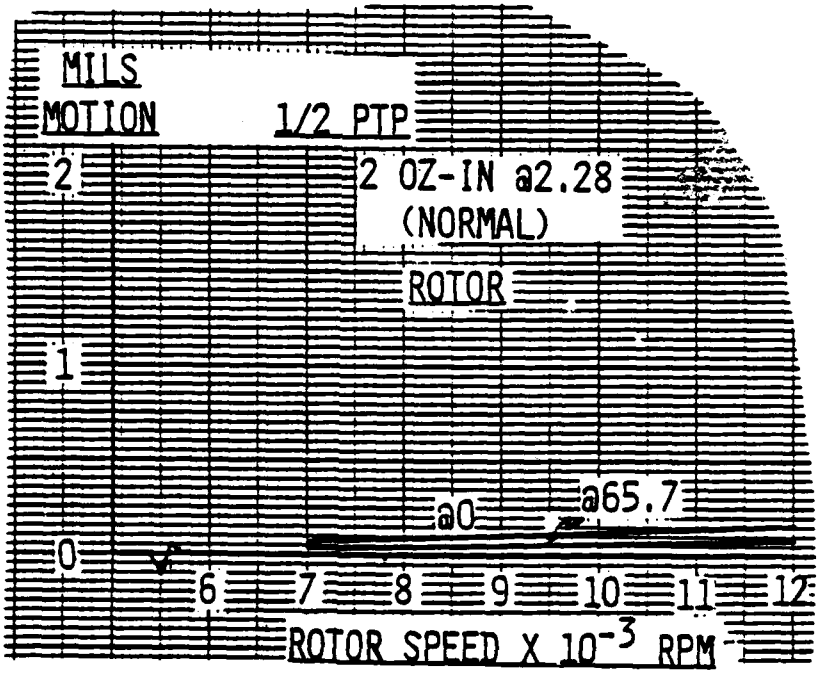

Figure 6-6 Steady State Response vs. Speed

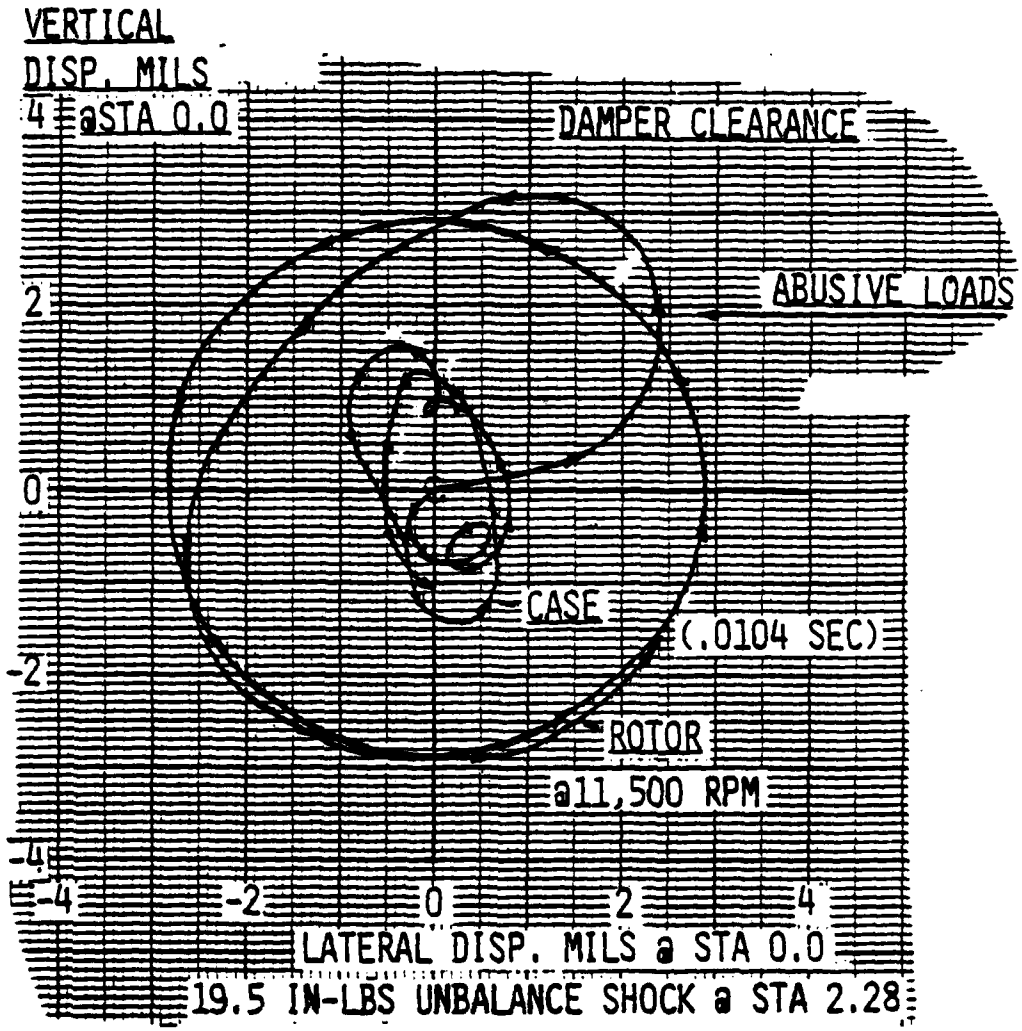

Figure 6-7 Time Transient Response to Abusive Unbalance

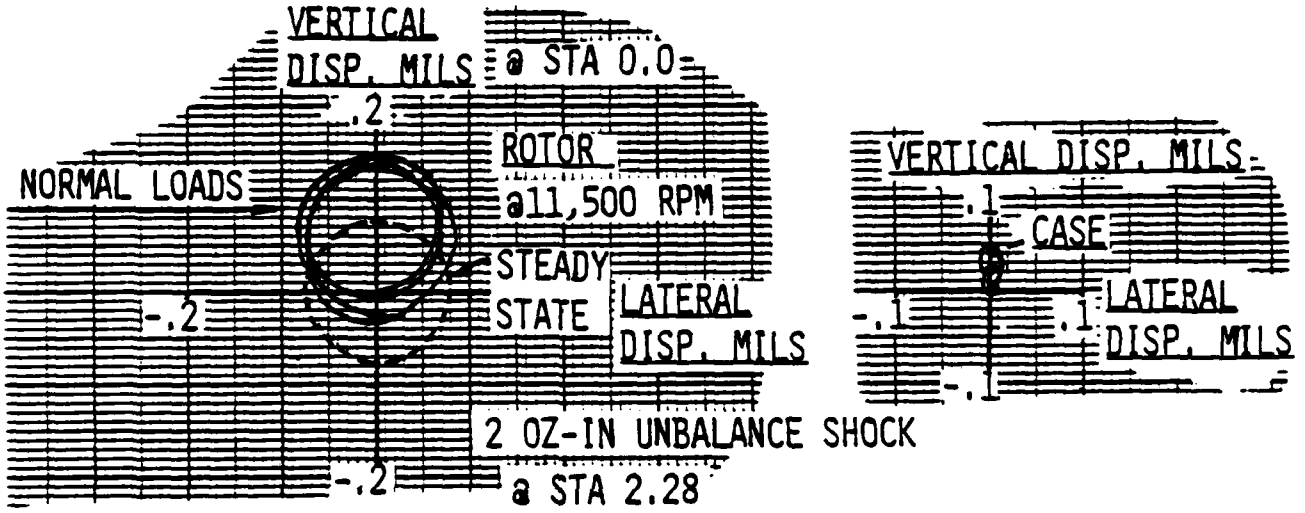

Figure 6-8 Time Transient Response for Normal Loads

REFERENCES

1. Reinhardt, E. and Lund, J.W., "The Influence of Fluid Inertia on the Dynamic Properties of Journal Bearings," Trans. ASME, JOC7, pp 159-167.

2. White, D.C., "The Dynamics of a Rigid Rotor Supported on Squeeze Film Bearings," Conference on Vibrations of Rotating Systems, London, Proceedings IMechE, Feb. 14-15, 1972.

3. Scanlan, R. H. and Rosenbaum, R., "Aircraft Vibration and Flutter", The Macmillan Company, New York, 1951.

4. Przemieniecki, J. S., Theory of Matrix Structural Analysis, McGraw-Hill, New York, 1968.

*USGPO: 1983-659-062-919